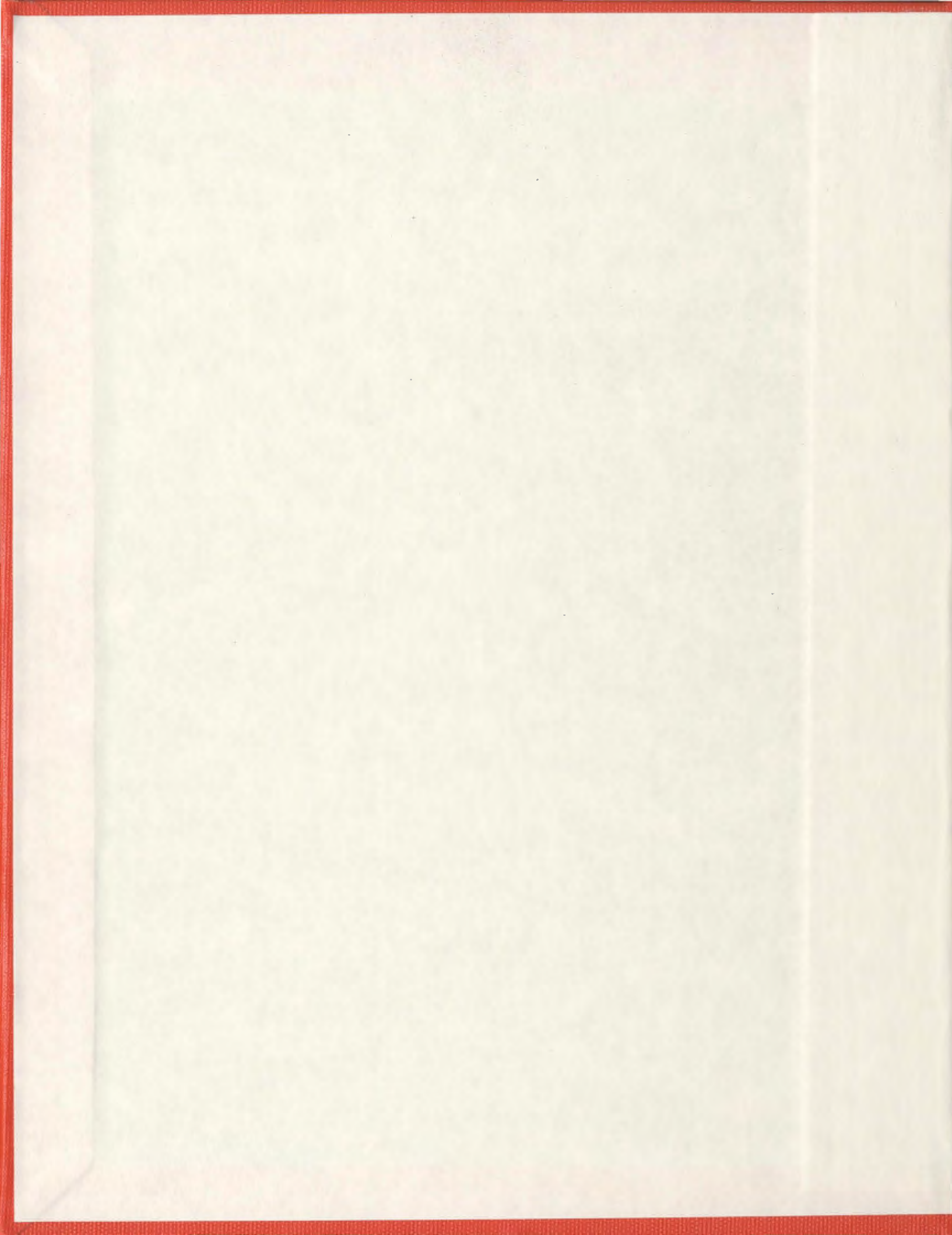


PRESSURE RIDGE ICE GOUGE MORPHOLOGY AND
THE DEVELOPMENT OF A REPRESENTATIVE
PHYSICAL ICE KEEL MODEL FOR THE
BEAUFORT SEA

TIMOTHY L. G. PARK



PRESSURE RIDGE ICE GOUGE MORPHOLOGY AND THE DEVELOPMENT OF A
REPRESENTATIVE PHYSICAL ICE KEEL MODEL FOR THE BEAUFORT SEA

By

© Timothy L. G. Park, P.Eng.

A thesis submitted to the
School of Graduate Studies
in partial fulfilment of the
requirements for the degree of
Master of Engineering

Faculty of Engineering & Applied Science
Memorial University of Newfoundland

July 2012

St. John's

Newfoundland & Labrador

Canada

ABSTRACT

Ice gouge experiments have been conducted by numerous authors since the early 1970s. A common theme in nearly all experiments is the use of an idealized prismatic wedge shape model to represent the keel of an iceberg or pressure ridge. In the case of icebergs, it is well known that keel morphology is highly variable. However, for pressure ridge ice keels a common morphology has been recognized. An in-depth study of extreme gouge features in five multi-beam bathymetric datasets, from the Beaufort Sea, has led to the development of a three-dimensional representative model of an ice keel. A qualitative 1g scale model test comparing the representative three-dimensional model to a traditional prismatic wedge was conducted using Beaufort Sea clay. The experiment used a model pipeline to compare the loads from a representative keel to that of an idealized prismatic wedge. The three-dimensional representative model resulted in a lower force/deflection on the pipeline when compared to the traditional prismatic wedge shape model. However, the shape of the representative model keel resulted in proportionately higher stresses being transmitted through the soil than the simple prismatic model.

ACKNOWLEDGEMENT

I would like to thank my thesis supervisor, Dr. Ryan Phillips at C-CORE, for first introducing me to the subject of pressure ridge ice gouge morphology, and scale model testing. I would like to thank Dr. Laurie Davis, for bringing me in on the many ice gouge projects while at Fugro Geosurveys Inc. I would like to thank my friend, Dr. Chris Woodworth-Lynas, for his knowledge and help in putting together my thesis; our gouge related conversations were quite entertaining and inspiring. To Dr. Michael Hinchey, thank you for your support in designing and building the ice gouge experiments, your course was invaluable in advancing my work. To my friend, Kenton Pike, for our discussions and collaboration on the ice gouge subject. To Tony King at C-CORE, thank you for all your help and advice. I would like to thank Kevin MacKillop and Steve Blasco of the Geological Survey of Canada (GSC) for their help and insight into the gouge problem, and to the GSC in general for agreeing to let me use the results from the extreme gouge catalogue to further my research. I would like to thank Dr. Jeff Dingler, at BP, for agreeing to let me use the Beaufort Sea soil samples in my experiment.

To my supervisor at Fugro Geosurveys Inc., Jørn Landva, thank you for giving me the time and support for finishing my coursework, and thesis.

Most of all, I would like to thank my wife, Mary, for supporting me through this whole experience.

TABLE OF CONTENTS

ABSTRACT	i
ACKNOWLEDGEMENT	ii
TABLE OF CONTENTS	iii
LIST OF TABLES	v
LIST OF FIGURES	v
1.0 INTRODUCTION	1
1.1 General	1
1.2 Background	3
1.2.1 <i>Significance of the Beaufort Sea</i>	3
1.2.2 <i>Challenge to Offshore Pipeline Development in the Beaufort Sea</i>	5
1.2.3 <i>A Brief History of Ice Keel Models Used in Gouge Experiments</i>	7
1.3 Current Work	12
1.3.1 <i>Justification of Study</i>	12
1.3.2 <i>Purpose of this Thesis</i>	14
1.3.3 <i>Thesis Outline</i>	15
2.0 FACTORS AFFECTING ICE GOUGE MORPHOLOGY	16
2.1 General	16
2.2 Gouge Factors	17
2.2.1 <i>Ice Ridge Morphology</i>	17
2.2.2 <i>Soil Characteristics</i>	23
2.2.3 <i>Extreme Wind Events</i>	29
2.2.4 <i>Ice Zonation</i>	31
2.3 Discussion	38
3.0 EXTREME GOUGE MORPHOLOGY STUDY	39
3.1 Introduction	39
3.2 Methodology	43
3.2.1 <i>Overview</i>	43
3.2.2 <i>Raster Data</i>	44
3.2.3 <i>ArcMap</i>	45
3.2.4 <i>ArcScene</i>	49
3.3 Gouge 1 Study	50
3.3.1 <i>Overview</i>	50
3.3.2 <i>Gouge 1 - Leg A</i>	53
3.3.3 <i>Gouge 1 - Direction Change 1</i>	55
3.3.4 <i>Gouge 1 - Leg B</i>	59
3.3.5 <i>Gouge 1 - Leg C</i>	62
3.3.6 <i>Gouge 1 - Termination Mound</i>	64
3.4 Gouge 2 Study	67
3.4.1 <i>Overview</i>	67
3.4.2 <i>Gouge 2 - Direction Change 1</i>	70
3.4.3 <i>Gouge 2 - Leg A</i>	72

3.4.4	<i>Gouge 2 - Direction Change 2</i>	74
3.5	Gouge 3 Study	77
3.5.1	<i>Overview</i>	77
3.5.2	<i>Gouge 3 - Transition Zone 1</i>	80
3.5.3	<i>Gouge 3 - Transition Zone 2</i>	81
3.5.4	<i>Gouge 3 - Transition Zone 3</i>	84
3.5.5	<i>Gouge 3 - Termination Point</i>	85
3.6	Gouge 4 Study	88
3.6.1	<i>Overview</i>	88
3.6.2	<i>Gouge 4 - Transition Zone 1</i>	91
3.6.3	<i>Gouge 4 - Direction Change 1</i>	92
3.6.4	<i>Gouge 4 - Transition Zone 2</i>	94
3.6.5	<i>Gouge 4 - Rotation Point</i>	96
3.7	Gouge 5 Study	98
3.7.1	<i>Overview</i>	98
3.7.3	<i>Gouge 5 - Direction Change</i>	103
3.8	Gouge Study Summary	106
3.8.1	<i>Gouge Behavior Summary</i>	106
3.8.2	<i>Gouge Morphology Summary</i>	110
4.0	EXTREME GOUGE CATALOGUE REVIEW	114
4.1	Introduction	114
4.2	Extreme Gouge Plot	115
4.3	Discussion	116
5.0	GOUGE MORPHOLOGY EXPERIMENT	117
5.1	Introduction	117
5.2	Experiment Design and Setup	118
5.2.1	<i>Model Ice Keel Design</i>	118
5.2.2	<i>The Gouge Tank and Test Bed</i>	121
5.2.3	<i>Drive and Drive Assembly</i>	122
5.2.4	<i>The Model Pipeline Load Cell</i>	124
5.2.5	<i>Data Acquisition System</i>	126
5.2.6	<i>Experiment Methodology</i>	128
5.3	Experimental Results	130
6.0	SUMMARY, CONCLUSIONS, AND RECOMMENDATIONS	137
6.1	Summary	137
6.2	Conclusions	138
6.2.1	<i>Conclusions on Keel Morphology and Experimental Results</i>	138
6.2.2	<i>Conclusions on Factors Affecting Gouge Morphology</i>	139
6.3	Recommendations	141
6.3.1	<i>Recommendations Regarding Keel Morphology and Experimentation</i>	141
6.3.2	<i>Recommendations Regarding the Study of Gouge Factors</i>	142
7.0	BIBLIOGRAPHY	143
	APPENDIX A – EXPERIMENTAL RESULTS	147

LIST OF TABLES

Table 1: Geotechnical Description of Geologic Model (modified from O'Connor and Blasco, 1980)	24
Table 2: Gouge 1 - Leg B- Profile Parameters.....	60
Table 3: Gouge 2 – Leg A – Profile Parameters	73
Table 4: Overall Gouge Summary	110
Table 5: Individual Keel Summary	111
Table 6: 30 Degree Idealized Wedge Experimental Results.....	130
Table 7: 3D Representative Model Keel Experiment Results	130
Table 8: 30 Degree Wedge - Projected Pressure.....	132
Table 9: 3D Representative Keel - Projected Pressure	132
Table 10: Projected Pressure Comparison	133

LIST OF FIGURES

Figure 1: Mackenzie Gas Project –2030 Hypothetical Scenario (GOC, 2009)	4
Figure 2: Palmers Concept of Pipeline Burial Zones (Palmer, 1997).....	5
Figure 3: Chari's Ice keel Models (a) "Idealized" and (b) "Rounded Toe")	8
Figure 4: Green's Ice Keel Models.....	9
Figure 5: Prasad's Keel Models	9
Figure 6: Been <i>et al.</i> (1990) Pressure Ridge Ice Gouge Model	10
Figure 7: Ice Keel Models Used by Ivanovic <i>et al.</i> (2011).....	11
Figure 8: Idealized First-Year Ridge (Timco and Burden, 1997).....	18
Figure 9: Idealized Multi-Year Ridge (Timco and Burden, 1997)	18
Figure 10: Keel Width Vs. Keel Depth for First Year Ridges (Timco and Burden, 1997)	18
Figure 11: Structure of a Multi-Year Keel (Kovacs <i>et al.</i> , 1973)	20
Figure 12: Proposed Three Stages of Gouge Based On Ice Sheet Flexure.....	21
Figure 13: Three Phase Gouge (Blasco <i>et al.</i> , 2007)	22
Figure 14: Beaufort Sea Surficial Sediment Map	23
Figure 15: Multi-beam Image of Heavily Gouged Sea-bottom	26
Figure 16: The effect of soil type on Gouge Depth (C-CORE, 2000).....	28
Figure 17: Stamukhi Process Illustration.....	32
Figure 18: Stamukhi in the Arctic.....	32
Figure 19: Shelf Break (Hequette <i>et al.</i> , 1995)	33
Figure 20: Ice Zonation (Hequette <i>et al.</i> , 1995).....	35
Figure 21: Ice Zonation Variations (Reimnitz <i>et al.</i> , 1979).....	35
Figure 22: Pressure Ridge Keel Morphology in the Northumberland Strait (Obert and Brown, 2011)	36
Figure 23: Extreme Gouge Locations	40

Figure 24: Example of a Raster File	44
Figure 25: Screenshot from ArcMap (a) Color elevation legend (b) Interpolate Line (c) Profile Graph.....	45
Figure 26: Profile Vertical to Horizontal Scale difference (a) 1:12 (b) 1:1	46
Figure 27: Raster Slope Algorithm (Modified from ArcGIS 10 help page).....	47
Figure 28: Example of Slope Raster Overlay	48
Figure 29: Gouge 1 Study Area	50
Figure 30: Gouge 1 – Elevation Profile	52
Figure 31: Gouge 1 - Leg A - Overview.....	53
Figure 32: Gouge 1 - Leg A - Relative Finger Elevation.....	54
Figure 33: Gouge 1 - Direction Change 1 Overview	56
Figure 34: Direction Change 1 Slope Overlay.....	58
Figure 35: Leg B – Overview	59
Figure 36: Gouge 1 – Leg B – Additional Keel Finger	61
Figure 37: Gouge 1 – Leg B – Direction Change Slope Raster Overlay	61
Figure 38: Gouge 1 - Leg C - Sudden Elevation Change	62
Figure 39: Gouge 1 - Leg C - Before and After Elevation Change Profile	63
Figure 40: Gouge 1 - Termination Mound Overview.....	64
Figure 41: Gouge 1 - Termination Mound Slope Raster Overlay.....	65
Figure 42: Gouge 1 - Rendered Image- Termination Mound Gouge Interference	66
Figure 43: Gouge 2 - Study Area Overview	67
Figure 44: Gouge 2 - Elevation Profile.....	69
Figure 45: Gouge 2 - Direction Change 1 Overview.....	70
Figure 46: Gouge 2 - Leg A – Profile Comparison.....	72
Figure 47: Gouge 2 - Keel Being Sheared	73
Figure 48: Gouge 2 - Direction Change 2.....	74
Figure 49: Gouge 2 - Direction Change 2 - Slope Overlay	76
Figure 50: Gouge 3 - Overview	77
Figure 51: Gouge 3 - Elevation Profile.....	79
Figure 52: Gouge 3 - Transition Zone 1	80
Figure 53: Gouge 3 - Transition Zone 2	81
Figure 54: Gouge 3 - Transition Zone 2 – West Berm Slope Raster Overlay	82
Figure 55: Gouge 3 - Transition Zone 2 – Side Slope Raster Overlay	83
Figure 56: Gouge 3 - Transition Zone 3	84
Figure 57: Gouge 3 – Transition Zone 3 – Slope Raster Overlay.....	85
Figure 58: Gouge 3 - Termination	86
Figure 59: Gouge 3 - Termination - Slope Raster Overlay.....	87
Figure 60: Gouge 4 - Study Area.....	88
Figure 61: Gouge 4 - Elevation Profile.....	90
Figure 62: Gouge 4 - Transition Zone 1	91
Figure 63: Gouge 4 - Direction Change 1.....	92
Figure 64: Gouge 4 - Direction Change 1 - Slope Raster Overlay	93
Figure 65: Gouge 4 - Transition Zone 2	94
Figure 66: Gouge 4 - Transition Zone 2 - Slope Raster Overlay.....	95

Figure 67: Gouge 4 - Termination	96
Figure 68: Gouge 5 - Overview	98
Figure 69: Gouge 5 - Elevation Profile.....	100
Figure 70: Gouge 5 - Inception Area	101
Figure 71: Gouge 5 - Direction Change.....	103
Figure 72: Gouge 5 - Direction Change with Slope Data	105
Figure 73: Superimposed Keel Curvature Profiles	112
Figure 74: Extreme Gouge Depth versus Width.....	115
Figure 75: 30 Degree Prismatic Wedge Experiment Model.....	118
Figure 76: 3D Representative Model Keel	119
Figure 77: Design of Representative Keel	120
Figure 78: Comparison of Discretization to Gouge Profiles at turning point and termination berms.	120
Figure 79: Experimental Tank	121
Figure 80: Movement Assembly Attached to Scour Tank.....	123
Figure 81: Pipeline Load Cell	124
Figure 82: Data Acquisition System	126
Figure 83: Representative Keel Vs. 30 Degree Prismatic Wedge - Resultant Loads	131
Figure 84: Difference in peak load times for lateral and vertical load on the 30° wedge keel model	134

1.0 INTRODUCTION

1.1 General

Pressure ridge ice gouging is perhaps the most prolific threat to subsea structures on the Beaufort Sea shelf. The concept of an ice keel system is daunting; a massive ice structure stretching from the water surface to possibly 20 to 30 meters below sea level, tearing several meters deep into the seabed, leaving a gouge up to 5 m deep and 50 m wide. Unlike icebergs, a pressure ridge can be supported by an integral ice sheet, possibly hundreds of kilometres in surface area, allowing it to harness a disproportionately high amount of wind energy, making it a virtual juggernaut to the seafloor, and anything residing on it. However, the Beaufort Sea houses a vast amount of riches in the form of hydrocarbons in the form of oil and gas. The key to obtaining these riches is for engineers to address the pressure ridge ice gouge problem.

The pressure ridge ice gouge problem is complex. The capabilities of pressure ridge ice are somewhat of an enigma. Gouging occurs annually, however, it is often not directly observed. In most cases, the only clue to the capabilities of ice pressure ridges are by viewing the aftermath of a gouging event, through bathymetric imagery. In this case, the only option for engineers is to back calculate the forces required to create the resulting gouge. In terms of geotechnical engineering, ice gouging is not a classical problem; it is a unique phenomenon worthy of its own study.

The first step in studying a new phenomenon of such magnitude as ice gouge is to create a physical scale model test. Scale model testing in the field of ice gouge has been underway since the mid-1970s. As in most problems, when there is a lack of information available, certain assumptions are made. For the ice gouge phenomenon, one such assumption is that the shape of the ice keel can be idealized as a simple prismatic structure. In multiple physical scale model experiments, the effect of changing morphology has been documented to result in a significant variation from the effects of an idealized shape. However, there has been little done to take this observation further and explore the effects of a representative 3D keel model. This is partly due to the lack of verifiable evidence that there is even a reasonable 3D shape that can be described as being representative. In the case of icebergs the randomness of morphology is well documented, however, in the case of pressure ridge ice keels, an in-depth morphological study may prove that this is not necessarily the case.

1.2 Background

1.2.1 Significance of the Beaufort Sea

One of the reasons interest in the Beaufort Sea exists is due to the proposal of the Mackenzie Gas Project. First proposed in the early 1970s, the purpose of the Mackenzie Gas Project is to develop a pipeline network, to transport natural gas over 1200 km from the Beaufort Sea, through the Mackenzie Valley, to tie into existing pipeline infrastructure in Alberta, Canada. The approval for this project was delayed due to political requirement to assess social, economic, and environmental factors involved in such a large project (Wikipedia, Mackenzie Gas Project). On, 10 March 2011, the Mackenzie Gas Project was given Federal approval to commence (NEB, 2011).

The proposed initial stages of the Mackenzie Gas Project are for the development of onshore gas fields, and construction of a pipeline network. The proposed future development would see the development of an offshore pipeline network (Figure 1). With the development of an offshore pipeline network, the estimated maximum daily production rate of natural gas that will flow from this project is approximately 1.8 billion cubic feet per day (GOC, 2009).

1.2.2 Challenge to Offshore Pipeline Development in the Beaufort Sea

One of the main challenges to the development of offshore pipeline networks is from the annual presence of gouging ice pressure ridges. Direct observations of gouging pressure ridges are rare, in most cases the only evidence that these events occur is by the gouges that remain in the seabed. The force required to make a gouge is estimated to reach several thousand tonnes, and if the gouging ice mass should make direct contact with a pipeline, the pipeline would inevitably be damaged severely (Palmer, 2011). In addition to this, stress can be induced in soils below the gouge depth, potentially damaging the pipeline without being in direct contact. Palmer (1997) illustrates the pipeline burial problem in Figure 2, below. In this figure, zone 1 is the region of direct contact between the pipeline and ice keel. Zone 2, represents an area where the loads on a pipeline are the result of stress transferred through the soil, and zone 3 represents the depth at which the transferred forces are no longer significant to cause damage to a pipeline.

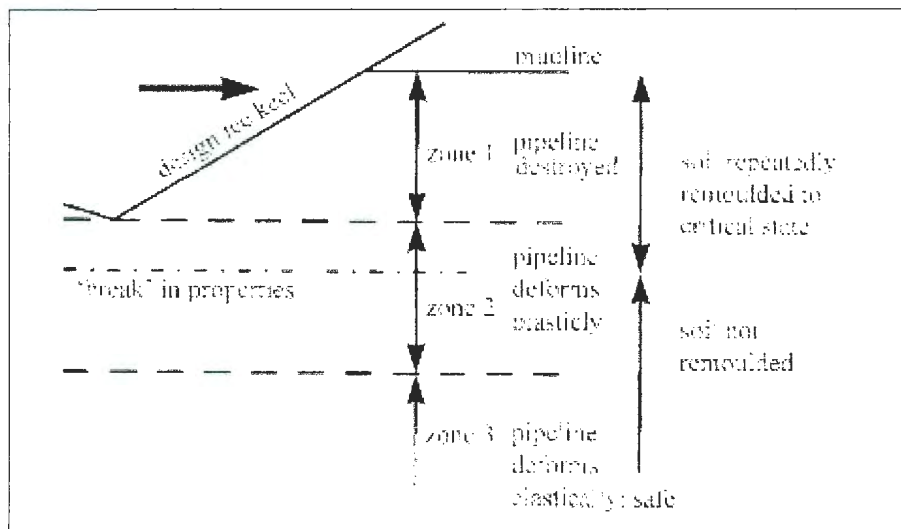


Figure 2: Palmers Concept of Pipeline Burial Zones (Palmer, 1997)

The issue of pressure ridge ice gouging in the Beaufort Sea results in two fundamental questions when considering pipeline design:

- 1- How deep must a pipeline be buried in order to avoid a direct impact with an ice keel, and;
- 2- How much deeper must it be buried to avoid excessive force transmitted through the soil.

The solution to the first question has typically been determined statistically. Based on analysis of bathymetric data, a probabilistic design gouge is determined. Such studies have been conducted by King (2002) and Younan *et al.* (2007). Attempting to answer the second question requires the development of a new geotechnical sub-discipline.

Most classical geotechnical studies such as bearing capacity and retaining wall theory focus on small vertical or lateral movement, but the ice gouge phenomenon combines simultaneous large lateral and vertical deformation. Thus, it is unclear how accurate an estimate a pipe burial depth would be when trying to estimate gouge forces using these classical methods. In situations involving a unique phenomenon, such as pressure ridge ice gouging, physical scale model tests are required in order to obtain accurate realistic estimate of the environmental loads. In ice gouging scale model testing, the development of an ice keel model is the primary challenge.

1.2.3 A Brief History of Ice Keel Models Used in Gouge Experiments

The common methodology employed in gouge scale model testing is the use of simple prismatic shapes to represent an ice keel. In the case of icebergs, the randomness and variation of iceberg morphology requires the use of a simple model to be representative (Chari, 1975). Simple model shapes are also used when trying to develop numerical models, as the main objective is to develop contact equations, simple geometry allows for easier input and understanding of governing equations.

The main variable between experimental programs has been the selection of the attack angle of the keel. The attack angle (for the purposes of this thesis) is the angle measured between the forward face of the keel model and a level seabed. However, further studies showed that shape has an effect on the total soil resistance in scale model experiments (Green 1984 and Prasad 1985).

Chari (1975) conducted one of the first ice gouge scale model experiments. His selection of ice keel model was a simple rectangular Plexiglas block. The justification for this shape was that iceberg shapes are random and thus no one shape could be considered representative, however, one shape was sought which could provide a reasonable estimate. The majority of Chari's experiments were conducted in dry sand using an idealized model, which was essentially a rectangular prism, see Figure 3a. Chari also evaluated a number of different face shapes to assess the significance of shape as a factor; one such model was with a rounded toe (Figure 3b). His conclusion was that the shape

effect did not produce a significant variation from the idealized model but recommended future study into the shape affect.

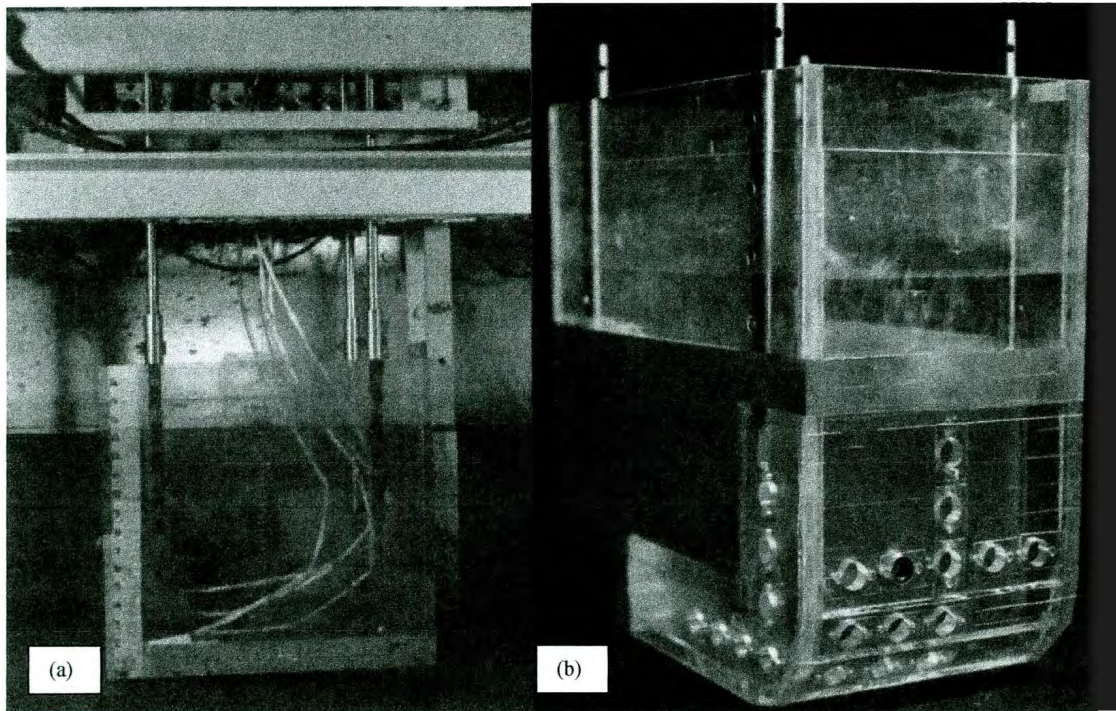


Figure 3: Chari's Ice keel Models (a) "Idealized" and (b) "Rounded Toe")

Green (1984) and Prasad (1985) continued the work of Chari, also using dry sand. Green used a larger keel model made from aluminum to represent Chari's idealized keel; he also included a model pipeline in his experiments to measure the pressure induced on a pipeline below the gouge depth. Green (1984) experimented with varying ice keel shapes (Figure 4) and concluded that the shape of the ice keel model was a significant factor in gouge model experiments. He noted, by changing the frontal face of the gouge model by 30 degrees, the soil resistance was increased by approximately 35 %. Green recommended that further work be conducted into the effects of different shapes in gouge studies.

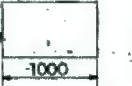
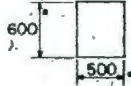
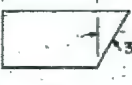
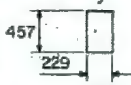
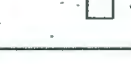
DESIGNATION	DESCRIPTION	PROFILE (mm)	FRONT VIEW (mm)
L1	RECTANGULAR BLOCK		
L2	RECTANGULAR BLOCK WITH 30° INCLINED FRONT FACE		
L3	FLAT PLATE		
S1	RECTANGULAR BLOCK		
S2	RECTANGULAR BLOCK WITH 30° INCLINED FRONT FACE		
S3	FLAT PLATE		

Figure 4: Green's Ice Keel Models

Prasad (1985) used additional keel model shapes in his work, as can be seen in Figure 5. He concluded that experiments using different shapes could result in variations in soil resistance of +30 %, to -50 %, from previous analytical models. Prasad also noted that more work was required on model keel shapes, in particular with curved surfaces. Prasad also mentions the potential inaccuracies in using a prismatic model, when actual keels in nature may be curved in two or three planes.

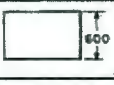
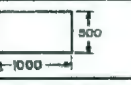
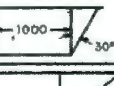
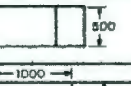
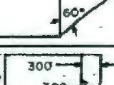
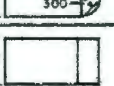
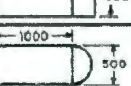
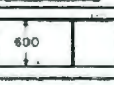
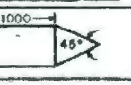
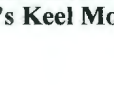
REFERENCE	DESCRIPTION	SIDE VIEW (mm)	TOP VIEW (mm)
M1	RECTANGULAR PRISM		
M2	RECTANGULAR PRISM WITH 30° INCLINED PROFILE		
M3	RECTANGULAR PRISM WITH 60° INCLINED PROFILE		
M4	RECTANGULAR PRISM WITH CURVED PROFILE		
M5	RECTANGULAR PRISM WITH CYLINDRICAL FRONT SHAPE		
M6	RECTANGULAR PRISM WITH WEDGE TYPE FRONT FACE		

Figure 5: Prasad's Keel Models

Been *et al.* (1990), developed a model specifically for pressure ridge ice gouging. The type of model that was used was also an idealized simple shape. Notably, one of the assumptions used in the development of their model was that an ice keel is considered very wide and thus 3D effects are considered negligible (Figure 6).

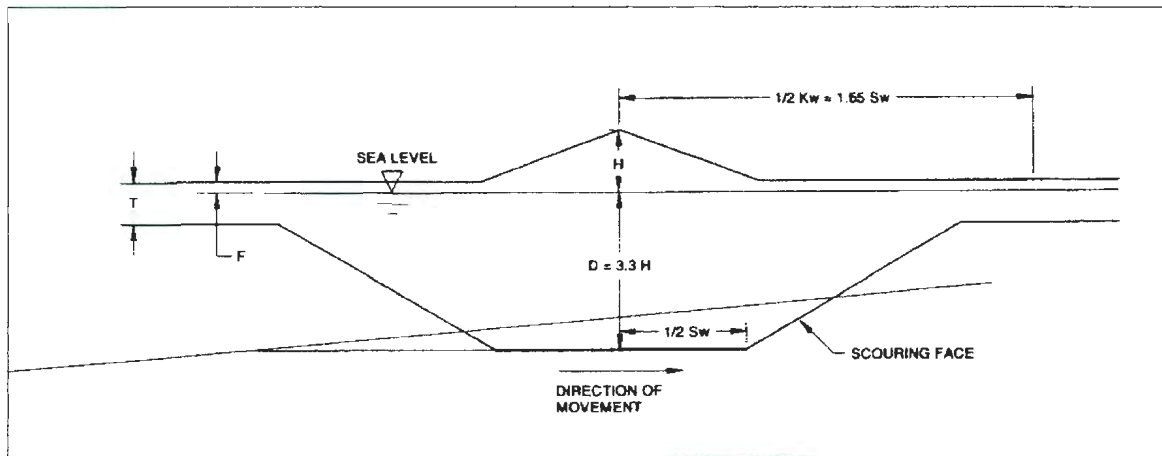


Figure 6: Been *et al.* (1990) Pressure Ridge Ice Gouge Model

The Pressure Ridge Ice Scour Experiment (PRISE) undertaken by C-CORE from 1993 to 1995 also used prismatic models in consolidated, saturated cohesive clays in a geotechnical centrifuge. Two different models were used, one with a 30 degree attack angle and the other with a 15 degree attack angle. Unique to these models is that they were parallelepipeds, considered to be more realistic than traditional models used by Chari (1975), Green (1984) and Prasad (1985) and a number of other authors (C-CORE, 1999).

A set of experiments was conducted by Ivanovic *et al.* (2011) that also used simple prismatic models similar to those used by Green (1984) and Prasad (1985) (Figure 7).

However, curved surfaces and multiple attack angles were also used. Ivanovic *et al.* (2011) drew two main conclusions made from their experiments. The first was that by reducing the attack angle, the forces on the ice keel model are significantly affected. The second was that a curved face may actually cause less damage to a buried pipeline than an idealized keel with a sharp edge.

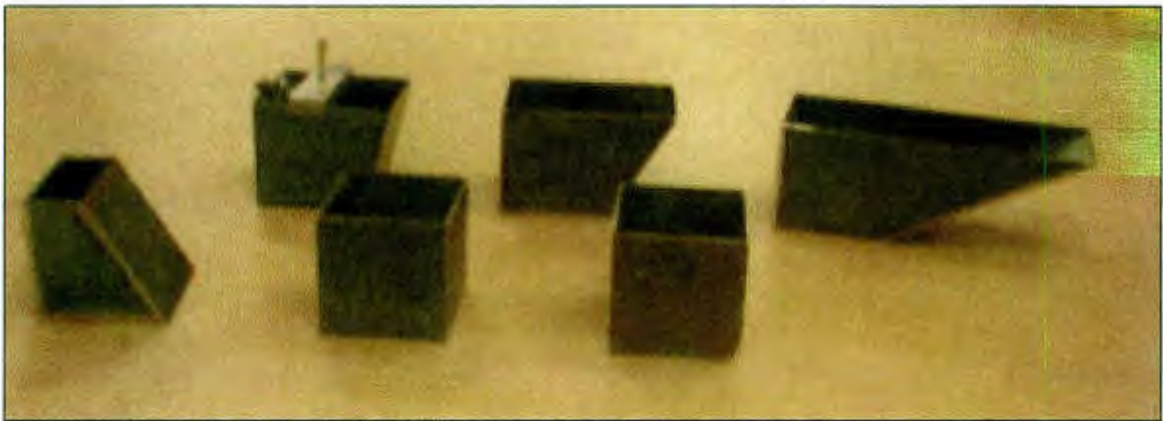


Figure 7: Ice Keel Models Used by Ivanovic *et al.* (2011)

There are numerous recent works conducted by other authors, Barrette (2011) summarises a number of studies, both using physical scale model test, and statistical models. The theme that is prevalent through the majority of studies is to use a simple prismatic wedge model to represent an ice keel.

1.3 Current Work

1.3.1 Justification of Study

The simplification of keel models is common place in ice gouge scale modelling. This is largely due to the unpredictable shapes that can be found in icebergs and pressure ridges. The concept of an idealized ice keel model is regarded as the most practical method of dealing with the variability in keel morphology. However, experiments in which the keel model shape was varied, or curvature used, have shown significantly varied results from idealized models. In every case the authors have recommended further testing into the shape effect, and in some cases acknowledge the potential effects of multi-planar curvature on gouging forces. These observations suggest that the idealization of ice keel models has oversimplified the problem, and that the effects of varying keel shape should be investigated.

It has been recognized that icebergs have drastically varying keel morphologies (Chari, 1975); however studies conducted by, Timco and Burden (1997), into pressure ridge shape seems to indicate a common morphology. This may be due to an “archetypal terrestrial deformation process”, as noted by Bowen and Topham (1994) in their study of the morphology of first year pressure ridges. Simply put, because pressure ridges form in a similar manner, this results in similar ice keel morphologies.

Arguably, common ice keel morphology implies that gouging keels may have a common morphology as well. In the case of the gouging portion of individual keels, the common

morphology could also be three-dimensional. However, as seen from Been *et al.* (1990), three dimensional affects are often assumed negligible, and thus ignored.

The assumption of using an idealized prismatic model has been the industry standard since the beginning of ice gouge physical scale model experimentation, but if there is a common 3D morphology among gouging pressure ridge ice keels then this shape must be identified. At the very least, the assumption of using prismatic models should be validated against a shape which is considered to be representative.

1.3.2 Purpose of this Thesis

The primary purpose of this thesis is to ascertain if a morphologically representative 3D pressure ridge ice keel model does exist, and if such a model does produce significant variation from the use of a simple prismatic model. A secondary objective of this thesis is to identify any physical limitations, or behavioural tendencies, which could be used to advance the understanding of the physical properties of gouging ice pressure ridges.

Based on an in-depth morphological study, this thesis shows that a common 3D morphology, specific to ice pressure ridges, in the Beaufort Sea does in fact exist. In addition, it can be shown experimentally that a representative 3D shape results in significant variation to gouge forces when compared to an idealized shape.

By demonstrating that the 3D shape of an ice keel produces significant variation in forces from traditional idealized models, it is argued that future experimental studies should attempt to incorporate the use of such shapes. By using ice keel models that are representative of those that occur in nature, the results from experiments can be considered more accurate and thus closer to a true solution.

1.3.3 Thesis Outline

The research for this thesis was conducted in three phases. The first phase consisted of studying, and becoming familiar with factors associated with the pressure ridge ice gouge problem; specifically, the factors which can be observed in gouge morphology study. This study is covered in the following section (Section 2) of this thesis.

The second research phase consisted of using ArcGIS software in the analysis of extreme gouges. Multi-beam bathymetric data was thoroughly studied in order to obtain morphologic characteristics of extreme gouge ice keels. In addition the general characteristics of the gouges were studied to identify factors associated with gouging. This is covered in Section 3 of this thesis. A brief study of an extreme gouge catalogue compiled by the Geological Survey of Canada and Canadian Seabed Research Ltd. was undertaken to provide additional evidence to a morphological trend which was identified in Section 3. This study was covered in Section 4.

The third phase of study consisted of using the results of the gouge morphology analysis to develop a 3D representative ice keel model and incorporate it into a physical scale model experiment. A simple prismatic wedge model keel was also developed and tested to compare to the representative 3D model. The results of the experimental program can be found in Section 5. The summary conclusions and recommendations of this thesis are included in Section 6.

2.0 FACTORS AFFECTING ICE GOUGE MORPHOLOGY

2.1 General

Before beginning a gouge morphology study, it is important to be familiar with environmental factors and processes involved in ice gouging. Identifying the factors, and understanding the processes aid in the development of a plan for how to conduct the bathymetric reconnaissance. The overall objective of this thesis is to develop a representative morphological shape for ice keel models, so the primary focus will be placed on identifying factors that can result in a morphological change along a gouge path. The secondary objective of this thesis is to advance the understanding of the gouge phenomenon by identifying the constraints, limitations, and general behaviour of pressure ridge ice gouging, and thus other factors not associated with keel morphology will also be considered.

The factors mentioned in this section are: ridge morphology, sediment strength and type, major wind events, and ice zonation. Ice strength is presumed to be a factor in gouging; however, it will not be covered in any comprehensive detail. Ice zonation is primarily qualitative and cannot be verified in a bathymetric study; however, it is covered in this section in order to place the gouge problem in context.

2.2 Gouge Factors

2.2.1 Ice Ridge Morphology

One of the main concerns with considering ridge morphology as a gouge factor is the inherent uncertainties in comparing a keel that has not been involved in the gouging process to one that has. This is primarily due to the notion that a keel may undergo a morphological change during the gouging process. One objective of the bathymetric study is to find evidence regarding change to keel morphology during the gouging process.

Morphological studies of ridges have been conducted for many years, due to the obstacle that ridges pose to marine traffic. In studies conducted by Timco and Burden (1997), an idealized model for first-year and multi-year ice ridges were proposed (see Figure 8 and Figure 9). These models were based on an analysis of 112 first-year ridges, and 64 multi-year ice ridges. Timco and Burden noticed common morphological trends and proposed ratios for physical parameters of the ridges, as seen in Figure 8, and Figure 9. Of particular interest is a proposed keel width (W_k) to keel height (H_k) ratio of 3.9, for first year ridges which could potentially be evaluated in a bathymetric study. A Scatter plot of the keel width (W_k) versus keel height (H_k), for first year ridges in the Beaufort Sea and temperate areas, can be seen in Figure 10. It can be noticed that the data shows a relatively linear trend.

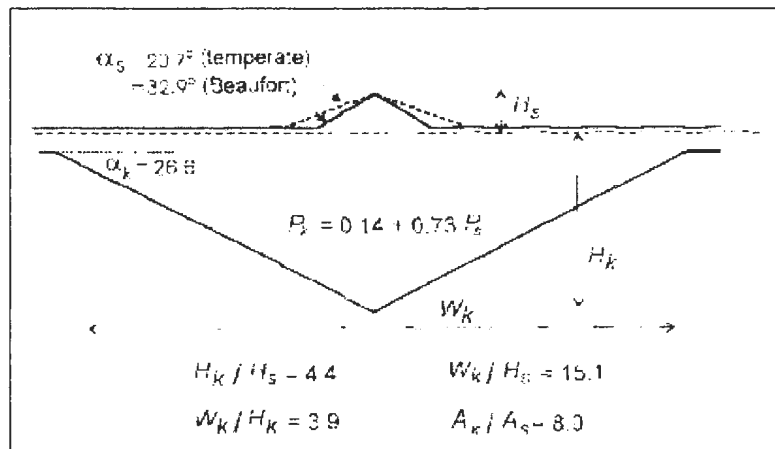


Figure 8: Idealized First-Year Ridge (Timco and Burden, 1997)

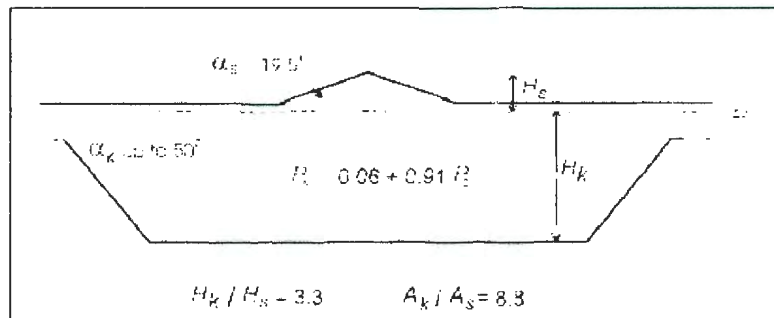


Figure 9: Idealized Multi-Year Ridge (Timco and Burden, 1997)

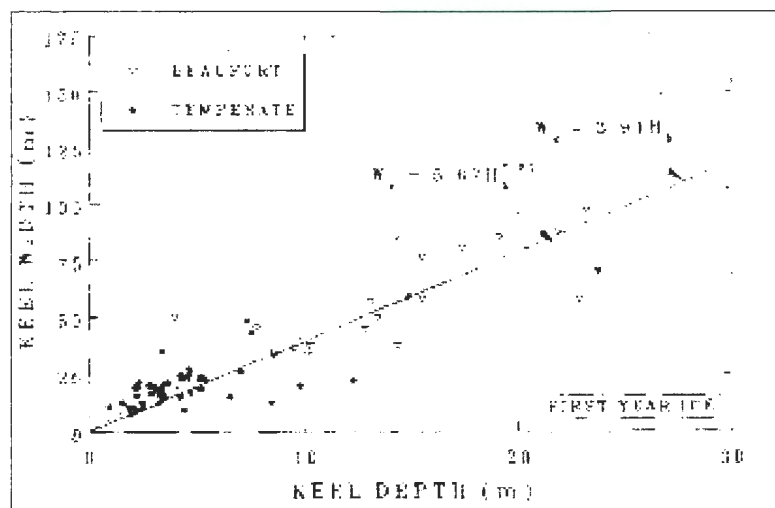


Figure 10: Keel Width Vs. Keel Depth for First Year Ridges (Timco and Burden, 1997)

Timco and Burden's finding of natural morphologic ratios in ridge structures is supportive of the theory of common keel morphology. However, the idealization has a number of limitations for use in a bathymetric study. Timco and Burden's idealization is fundamentally 2D, and does not mention any 3D relationships. Furthermore, the idealization is for the entire depth of a ridge, while for gouge studies we are mainly concerned with the bottom few meters that make contact with the seafloor. Timco and Burden's idealization of a ridge keel uses a single angle, much like the angle of attack methodology used for experimental keel models. However, based on observations made by Kovacs *et al.* (1973)(discussed in the following section), it is known that there is curvature around the base of the ridge.

Work published by Kovacs *et al.* (1973) illustrates an actual multi-year ridge, see Figure 11 below. Kovacs *et al.* (1973) comments that the shape of the keel can be described as roughly semi-circular to semi-elliptical. The curvature in the keel is believed to be caused by ablation due to relatively warmer water temperatures. Arguably, while there would be significantly less ablation, there should be some curvature around the bottom of the keel of a first year pressure ridge as well.

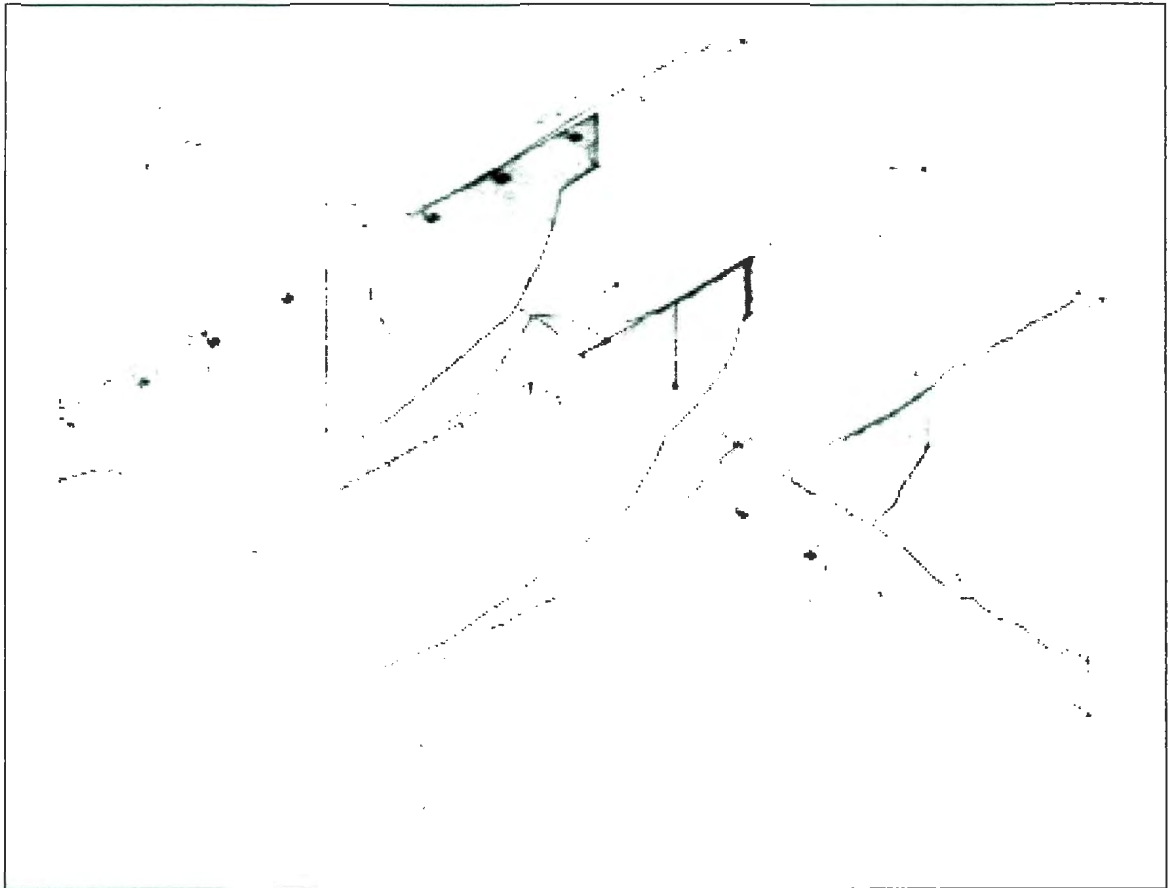


Figure 11: Structure of a Multi-Year Keel (Kovacs *et al.*, 1973)

Keel ablation is believed to cause an isostatic imbalance in multi-year keels which results in a downward deflection of the ice sheet near the ridge. This phenomenon also occurs with first-year ridges and is believed to be caused by an initial imbalance during the ridge forming process (Kovacs *et al.*, 1973).

The ice sheet of a ridge system is of interest, because of the added resistance that the sheet could provide to the upward vertical movement of the ridge during the gouging process. The ice sheet could possibly provide enough vertical resistance to gradually crush the keel between the ice sheet and the seabed. Conversely, the ice sheet could

potentially be a weak point in the ridge system. During the gouging process, one argument is that a ridge system is potentially analogous to a two way concrete slab-column system; gradually flexing until potentially experiencing a punching shear failure.

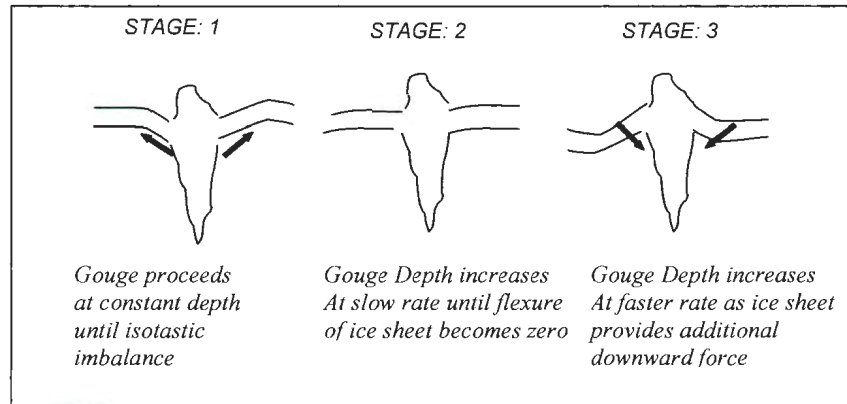


Figure 12: Proposed Three Stages of Gouge Based On Ice Sheet Flexure

If an ice ridge system does behave analogous to a concrete slab-column system then there may be indications in the type of vertical movement in a gouge path. There could be three distinct stages during a gouge event, as illustrated in Figure 12. In the first stage of gouging, the gouge may appear at a constant depth until the isostatic imbalance (noticed by Kovacs *et al.*, 1973) is overcome. Stage two to stage three of gouging would result in the gouge becoming gradually deeper as the additional vertical resistance of the ice sheet is mobilised. If the vertical resistance of the soil becomes greater than the downward force of the ice ridge system, then the keel may punch through the ice sheet, or alternatively, the keel may begin to crush.

Two distinct gouge paths may be observable from the possibility of punch through or crushing. In the case of crushing, a widening, or noticeable change in the overall keel morphology may be apparent. In the case of punch through, the gouge morphology may remain constant. A keel that has punched through would no longer have the vertical force of the ice sheet and the gouge path elevation could then appear to mirror the seabed elevation. Potentially, the free ice keel could be easily influenced by rotational forces, and appear to yaw frequently.

In a bathymetric review conducted by Blasco *et al.* (2007) it was noticed that during extreme gouge events, the vertical gouge profiles tended to follow a common theme, referred to as a three phase gouge, see Figure 13. In the proposed three phase gouge, phase one comprises gouging at a constant depth as the seabed slope increases, stage two consist of increasing gouge depth but with a gradual rise up in the vertical profile, and phase three is characterized by a constant vertical profile.

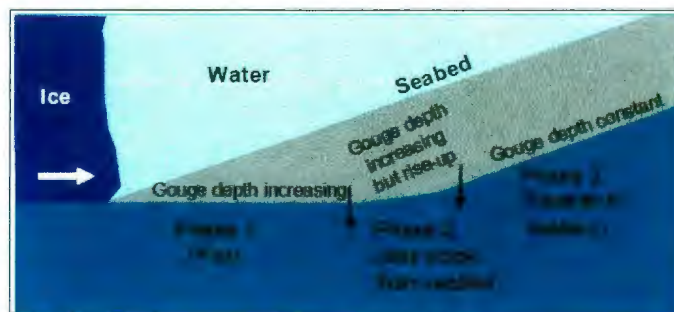


Figure 13: Three Phase Gouge (Blasco *et al.*, 2007)

It is possible that the vertical flexure of an ice sheet may explain the three phases of gouging as noticed by Blasco *et al.* (2007).

2.2.2 Soil Characteristics

The geotechnical properties vary significantly over the Beaufort Sea shelf. The sedimentation process along a coastal area usually results in coarse sediment (gravel and sand) deposited close to shore, and for finer materials (silt and clay) to be deposited further from shore. The sedimentation can occur in a gradual gradation as distance increases from shore. In the Beaufort Sea area there have been numerous sea level changes which can result in an uncharacteristic deposit of soil material. Figure 14 illustrates the varying surficial sediment over the Beaufort Sea shelf.

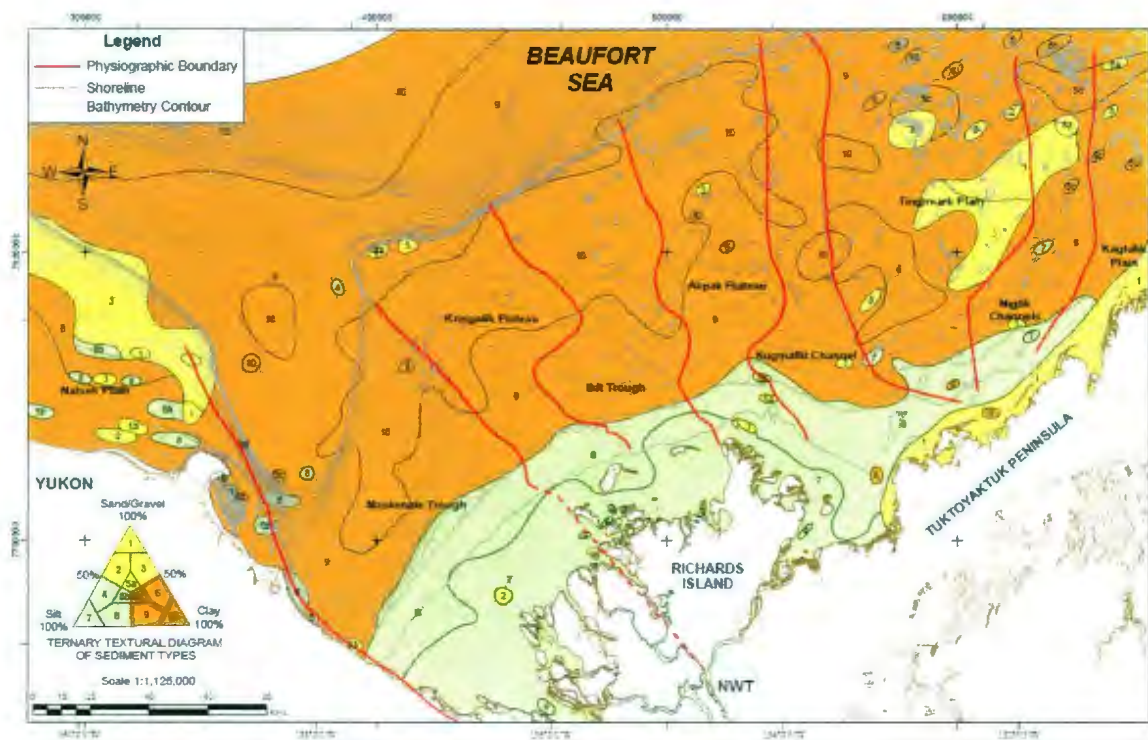


Figure 14: Beaufort Sea Surficial Sediment Map

The occurrence of glaciation from numerous ice ages has resulted in soil layers being scoured away (non-uniformly), as well as varying consolidation in clay. The active geologic setting results in a considerable challenge in geotechnical characterization of the Beaufort Sea shelf. Despite the convoluted geologic history, attempts have been made to develop a generic soil description for the Beaufort shelf, as can be seen in Table 1. The stratigraphic units in Table 1 have no associated thickness as they are highly variable, and in some cases not present.

Table 1: Geotechnical Description of Geologic Model (modified from O'Connor and Blasco, 1980)

Stratigraphic Unit	General Description
Unit A	<p>[Very] soft to firm (rarely stiff) clays or silty clays, usually containing traces of fine sand and organics, often in the form of fine laminations.</p> <p>The clays grade shoreward into grey, loose to very loose silts. Unit A may exhibit a complete range of plasticity, depending on the type and quantity of clay present.</p>
Unit B	<p>Is composed of a discontinuous and highly variable sequence of sands, silts and clays deposited in the transitional environment which accompanied the last sea level rise.</p>
Unit C	<p>In the near shore zones between Garry Island and Taker Point, Unit C consists predominantly of fine to medium grained, grey, brown or yellow sand. It normally contains a trace to some silt and only minor organics, but clay, silt and gravel layers have also been encountered in some areas. Consistency of this sand varied from loose to very dense.</p> <p>In some places Unit C may include an upper complex sequence of silty, fine sand interbedded with grey to black stony clay.</p>

Soil type is an important factor in ice gouge morphology for two reasons: first, the type of sediment dictates how well the gouge characteristics are preserved. Second, soil strength is believed to be a controlling factor in gouge depth.

Of particular importance for gouge bathymetry studies is the presence of clay. The type of clay referred to in unit A, is typically highly plastic. Plasticity refers to the clays ability to move and retain shape such that plastic clay can, in theory, retain the shape of an ice keel. In the occurrence of gouge turns and terminations in plastic clay it is theoretically possible to observe a cast of the keel face that created the gouge. In the case of multiple sharp direction changes it would be possible to develop a reasonable 3D profile of the gouging keel.

The presence of sand is particularly troublesome for gouge morphology studies. Due to a lack of cohesion, sand does not retain the shape of ice keels well. Sand also is susceptible to reworking by ocean currents. A bathymetric of an intensely gouged seabed in a clay environment is analogous to a downward glance at a plate of spaghetti, with literally hundreds of criss-crossing gouge paths, see Figure 15. A bathymetric image of a sand environment may show only a few shallow gouges due to reworking and removal of older features by bottom currents. This can lead to bias in the prediction of gouge events, and can also be misused in an argument supporting sediment strength in relation to gouge depth.

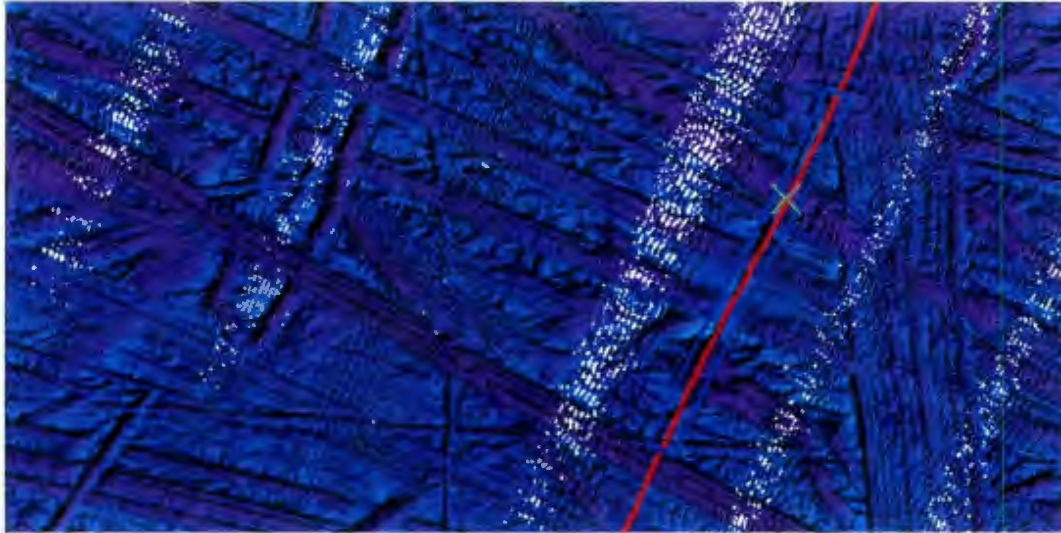


Figure 15: Multi-beam Image of Heavily Gouged Sea-bottom

The belief that ice gouge depth is controlled by sediment type and strength is a valid hypothesis. Observations of iceberg gouging, on the east coast of Canada, have shown that the sediment properties do limit gouge depth and influence the general gouge behaviour. However, pressure ridge ice is different from iceberg ice; the encompassing ice sheet can provide additional vertical and lateral force.

Of particular importance in regards to sediment strength is the potential for the pressure ridge ice keel to undergo physical change during the gouging process. The sediment strength may be such that the ice keel gets gradually, or abruptly, sheared away. There may also be potential for the keel to be crushed vertically. For this thesis, the preceding occurrences will be referred to as keel ablation.

In a geotechnical desk study conducted by EBA Engineering Consultants (1992) the attempt was made to correlate gouge depth with sediment type and strength. The study

focused on gouges that passed through the very soft to soft top layer of clay (Unit A) into much stronger clay (Unit B). One of the results from the study was:

“It is concluded that the strength of the seabed material does not appear to be the controlling parameter (at least in isolation) which will determine the ice penetration. It is believed that factors such as size of the iceberg, keel geometry, water plane area of the iceberg, inclination of the iceberg, and current and wind velocities may have stronger or equally controlling influence on the depth of ice scour penetration.” – EBA (1992).

C-CORE (2000), reanalyzed the data by EBA Engineering Consultants (1992), including observations of gouges in sand, and clay over sand. The C-CORE (2000) work did find a correlation between the soil type and the gouge depth, the results of the study can be seen in Figure 16. It is important to note, however gouges formed in sand are highly susceptible to ocean currents and in some cases can be filled in quite easily.

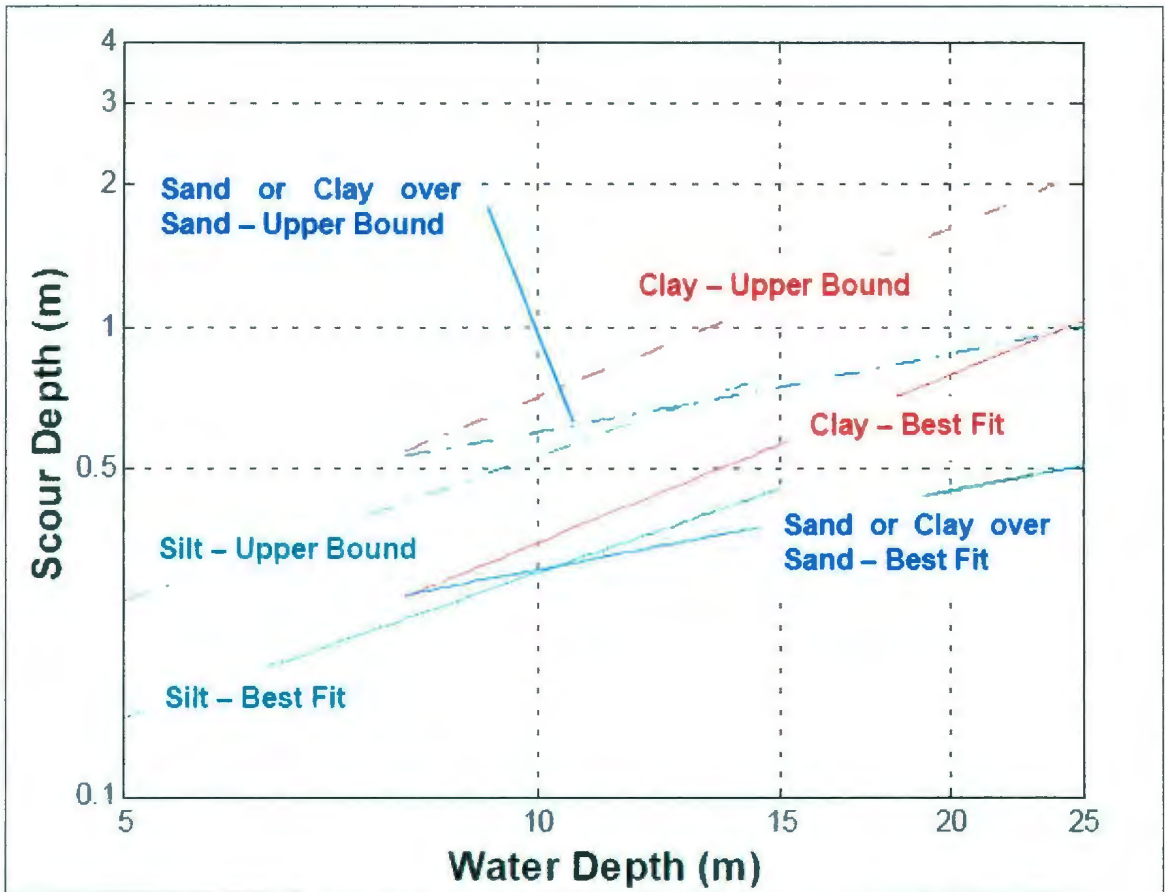


Figure 16: The effect of soil type on Gouge Depth (C-CORE, 2000)

In light of the previous studies, it seems that the bathymetric study conducted as part of this thesis is unlikely to prove, or disprove, that sediment strength limits the depth of gouging. There is, however, the possibility that gouge depth can be controlled through keel ablation, which can possibly be observed in a morphological study.

2.2.3 Extreme Wind Events

Wind is the primary driving force of Arctic ice (Thorndike and Colony, 1982). A potential hypothesis based on this fact is that extreme gouge events could be preceded, or occur in tandem, with an extreme wind event. A result of extreme wind events that is of particular importance to gouging is a temporary increase, or decrease, of sea level known as a storm surge.

The Beaufort Sea is considered to be micro-tidal. The tide on the Beaufort Sea shelf varies considerably and is often considerably less in deeper waters. Normal tides along the coast are typically around 0.25 m (Huggett et. al., 1975). Storm surges are associated with wind blowing from sea to shore. Strong winds blowing from shore to sea have caused temporary decreases in sea levels around Tuktoyaktuk Harbor (FOC, 1999); this type of sea level drop is known as a negative surge. In contrast, storm surges in the Beaufort Sea have been reported to increase the water level by as much as 3 m above normal sea level. In the Alaskan Beaufort there were reports of intensive ice gouging along the coast as a result of a 3 m storm surge that occurred in 1970 (Reimnitz and Maurer, 1979). Storm surges further out at sea do not normally cause the same level of tidal surge as close to shore in the summer months, but during the winter months the magnitudes of sea level change of offshore sites are close to that of nearshore sites (Henry, 1975).

Based on the description of the storm surge phenomenon, it may be possible that gouging may be preceded by a temporary increase, then decrease, in water level. Deep pressure ridges may be able to advance into locations normally too shallow to reach, and begin to gouge when the sea level begins to return to normal. There may be some indications in extreme gouge bathymetric profiles that this has occurred. As previously mentioned, wind events eventually subside, and thus, any temporary rise in sea level would rapidly fall to normal elevations. Post-surge sea level fall may be reflected in a gouge profile, in this type of situation, having the appearance of being vertically dropped. This type of movement is a consideration for future bathymetric study.

2.2.4 Ice Zonation

When first observing bathymetric images of the Beaufort Sea shelf, the impression that is given is that ice gouging is frequent, random, and occurs at any water depth. This is not the case. Through repetitive mapping it can be shown that the majority of gouging on the Beaufort Sea shelf occurs within a certain bathymetric interval, and is less frequent than would first appear. This may be due to the phenomenon known as ice zonation.

Ice zonation is best explained by evaluating the general ice formation process along the Beaufort Sea coast. During the fall of each year, ice first begins to form along the coastline, becoming attached to the coast. This is known as fast ice. As temperatures continue to drop, the ice can thicken and, close to shore, can attach to the sea floor, becoming what is known as bottom-fast ice. The ice also forms out from the coast extending seaward (FOC, 1999). As the fast ice extends seaward, ice is also being formed out at sea, which begins to drift towards shore. When the two ice masses meet the ice begins to crush and ice blocks are forced both under and over the adjacent ice sheets to create pressure ridges. During the ridging process in relatively shallow water, the ice rubble can reach the seafloor and spread laterally; Figure 17 illustrates this process.

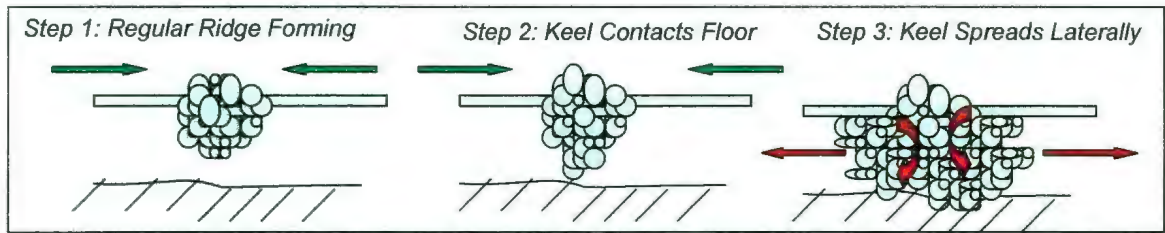


Figure 17: Stamukhi Process Illustration

The resulting ice formation no longer appears as the traditional idealization of an ice keel, but instead takes on the identity of a large grounded rubble field known as a stamukha (Figure 18).



Figure 18: Stamukhi in the Arctic

The geographical location of where the ice sheets meet is uncertain, however, there appears to be a break in slope at the 10 to 12 m isobaths that marks a boundary between a

zone of intense ice gouging seaward and a zone moderately affected by ice action, see Figure 19 (Hequette *et al.*, 1995). This is a likely candidate region for where the landfast and offshore ice sheets meet and thus where stamukhi would most likely begin to form.

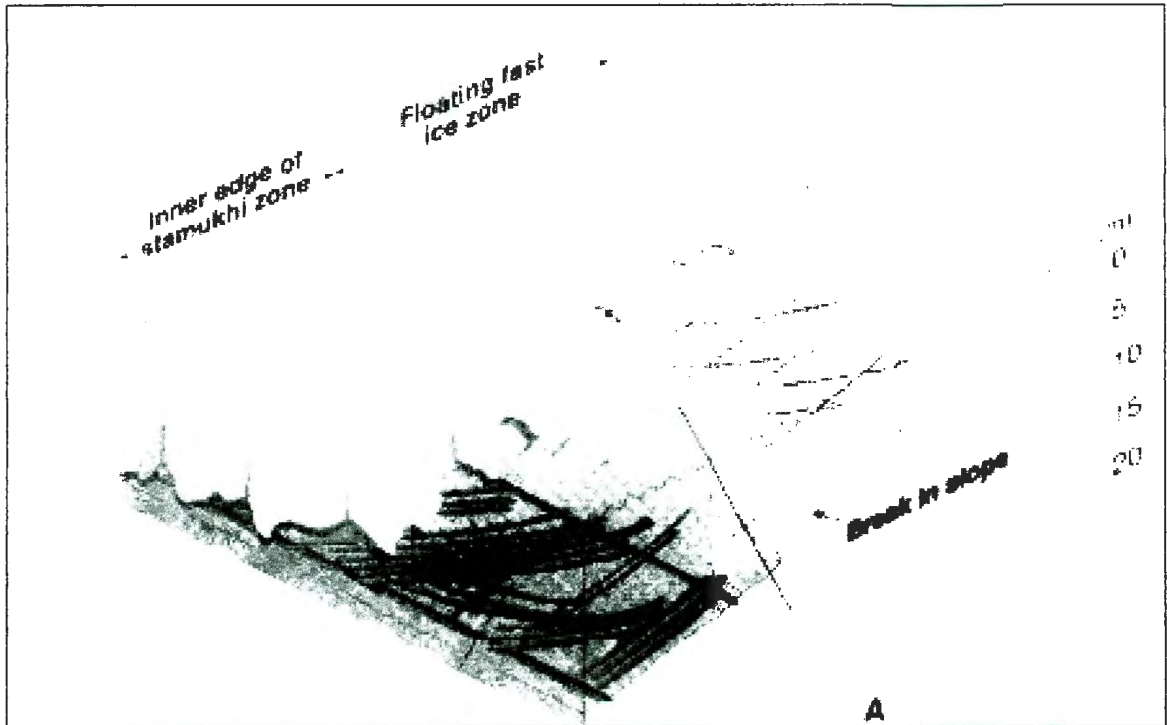


Figure 19: Shelf Break (Hequette *et al.*, 1995)

The reason for this break in slope, or why the ice appears to be hung up at this location, is not entirely clear. One hypothesis is that the break in slope is an artifact of a history of ice grounding at the same location. Another theory is that the break in slope marks a former shoreline when the sea level was much lower (Hequette *et al.*, 1995).

The stamukhi become well-grounded onto the seafloor and act as a barrier to further ice incursion; this becomes known as the stamukhi zone. The stamukhi zone becomes an

integral part of the extending fast ice zone. Eventually the ice sheet continues to form seaward from the stamukhi. As the landfast ice sheet continues to advance, more offshore sea ice is encountered. What follows appears to be a repetitive sequence of ridging and fast ice extension. As the water depth increases, the ridges can fully form and ground into the seabed. These ridges can be described as a grounded ridge zone. Eventually the water depth becomes such that the ridges no longer gouge, known as a floating ridge zone.

The edge of the fast ice varies in location from year to year. The water depth at the edge of the fast ice is approximately 20 m, but can also be deeper based on the annual ice extent. Seaward of the land fast ice is the active shear zone. The active shear zone can be described as highly dynamic with movement taking place throughout the winter. This zone can contain first year ice, or multiyear ice from polar pack ice incursions. Deep keel ridges from first year-ice have been known to form in the active shear zone. Multi-year ice ridges can also be present (Timco and Frederking, 2009).

It is unclear by how much ice zonation is influenced by: sediment type, bathymetry, or seasonal variation. Descriptions of ice zonation can vary from author-to-author, for example, contrast can be seen in the proposed ice zonation by Hequette *et al.* (1995), and by Reimnitz *et al.* (1978), in Figure 20 and Figure 21. Work by Hequette was conducted in the Canadian sector of the Beaufort Sea, while Reimnitz work was based on the Alaskan Shelf. In Figure 21, Reimnitz includes nomenclature used by other authors; as

previously mentioned, it is unclear if the difference in zone representation is due to regional variability, seasonal variability, or possibly due to attention to detail in graphic illustration.

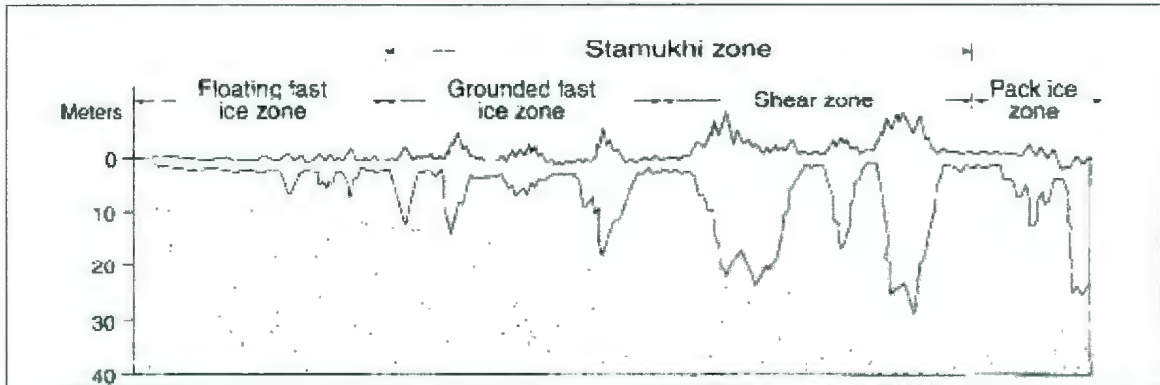


Figure 20: Ice Zonation (Hequette *et al.*, 1995)

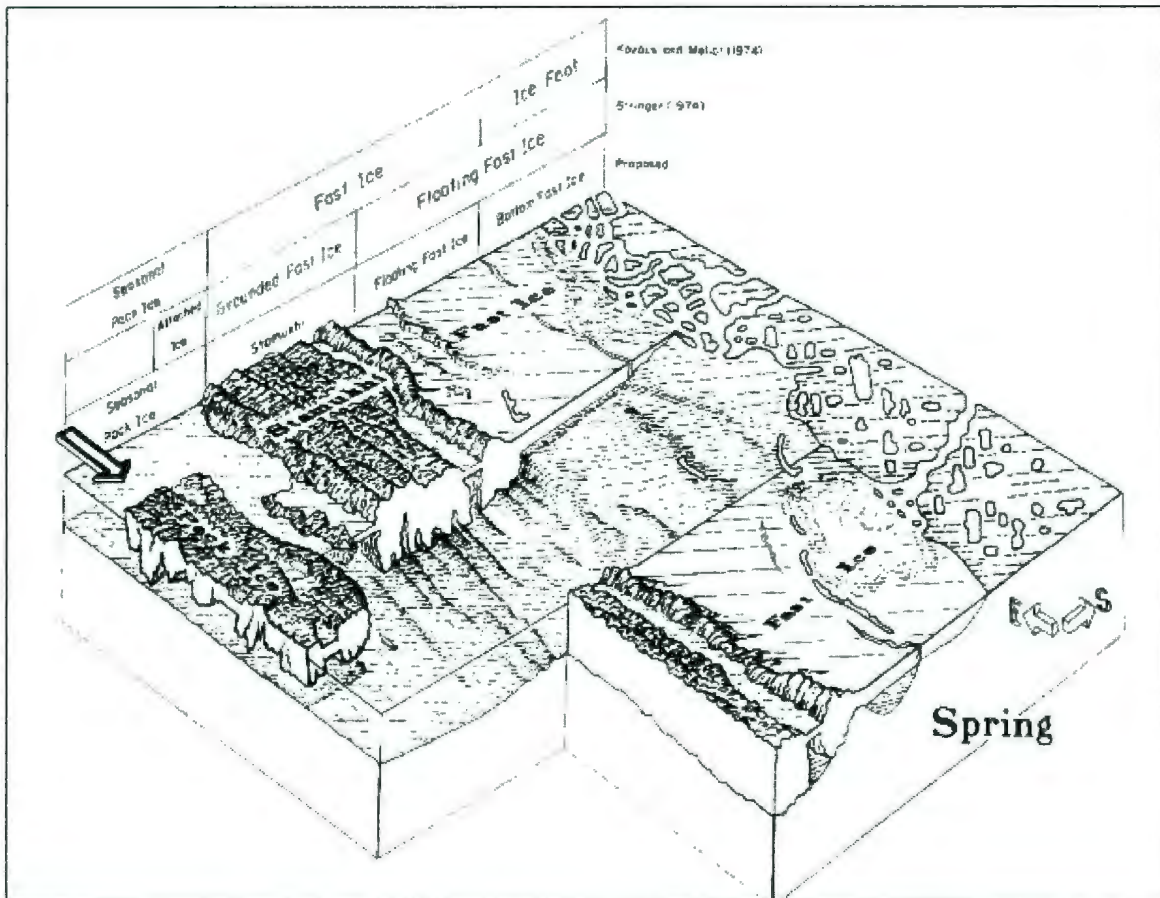


Figure 21: Ice Zonation Variations (Reimnitz *et al.*, 1979)

There are a number of trends and theories that can be drawn from the observation of ice zonation. As is observable in Figure 20 and Figure 21, the general trend is for ice keel structures to become progressively deeper, the further from shore. The barrier system created by such ice zonation implies that gouge depth is largely a factor of water depth. The fast ice barrier extends out to approximately the 20 m isobath, which implies that a gouge occurring in water depth greater than 20 m is possibly due to the incursion of a pressure ridge created in the active shear zone.

When considering the type of gouges that would be encountered past the ice fast edge it is largely speculative. However, work conducted by Obert and Brown (2011) on ice ridges in the Northumberland Strait, showed that, of the types of ridge shapes that were possible, triangular keels appeared to be deeper than other keel shapes. Whether this type of morphological trend would hold true for the Beaufort Sea is speculative. From the Northumberland Strait data, the general theme of ridge morphology appears to be multi-keels or multi-finger keels, and is also observable in the Beaufort Sea Bathymetric data.

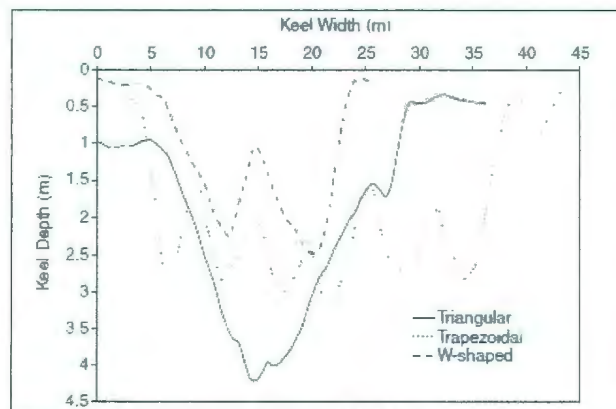


Figure 22: Pressure Ridge Keel Morphology in the Northumberland Strait (Obert and Brown, 2011)

In terms of the gouge morphology study, not a great deal of the ice zonation factor is relevant. Of some importance is the observation of deep keels tending to be triangular in shape, however it is unclear if this observation is true for the Beaufort Sea.

The significance of the ice zonation phenomenon is the implication that the types and drafts of ice keel features may be predictable, and thus reflected in the gouge record on the seafloor. There are indications of two possible gouge systems: one being the ice zonation system from the winter freeze-up and the other system due to active shear zone ice advancing after the breakup of the ice zone barrier. Two separate systems would mean that predictions from traditional methods of statistical processing may have to be re-evaluated.

2.3 Discussion

Understanding the factors and the associated theories in the ice gouge phenomenon serves as a starting point for a bathymetric study. The factors discussed that are of particular interest for a bathymetric study are: vertical flexure of ice sheets, ice keel ablation during gouging, and sediment strength affects. These factors are potentially quantifiable since they could result in the measurable change of vertical and horizontal profiles of ice gouge paths.

In the following bathymetric study, although primary focus will be on obtaining morphological characteristics of ice keels, attention will also be placed on the movement characteristics that may support or argue against the factors mentioned above.

3.0 EXTREME GOUGE MORPHOLOGY STUDY

3.1 Introduction

Real time observation and keel morphology measurements of an extreme gouging keel is, arguably, not practical. The uncertainty of when and where an extreme gouge occurs, and the physical scale of the ice structures involved, would require an immense amount of resources to undertake such a study. The only practical method of studying extreme keel morphology is to study the morphology of their gouges. While there are limitations to a gouge morphology study (which will be discussed) currently there are no other options available.

For this thesis five bathymetric data sets containing extreme gouges, on the Canadian Beaufort Shelf, were obtained from the Geological Survey of Canada. The gouges are herein referred to as “Gouge 1” to “Gouge 5”. The approximate locations of these gouges can be seen in Figure 23. After communication with personnel from the Geologic Survey of Canada, it was revealed that the gouges were formed in a plastic clay sediment. and the most important detail of these gouges is that they experience sharp directional changes. The combination of these conditions creates prominent end-berms, which allows for the three-dimensional analysis of ice keel morphology. In addition to the study of morphology, general behavior of the ice ridge was interpreted based on observable changes in gouge path elevation and change in orientation.

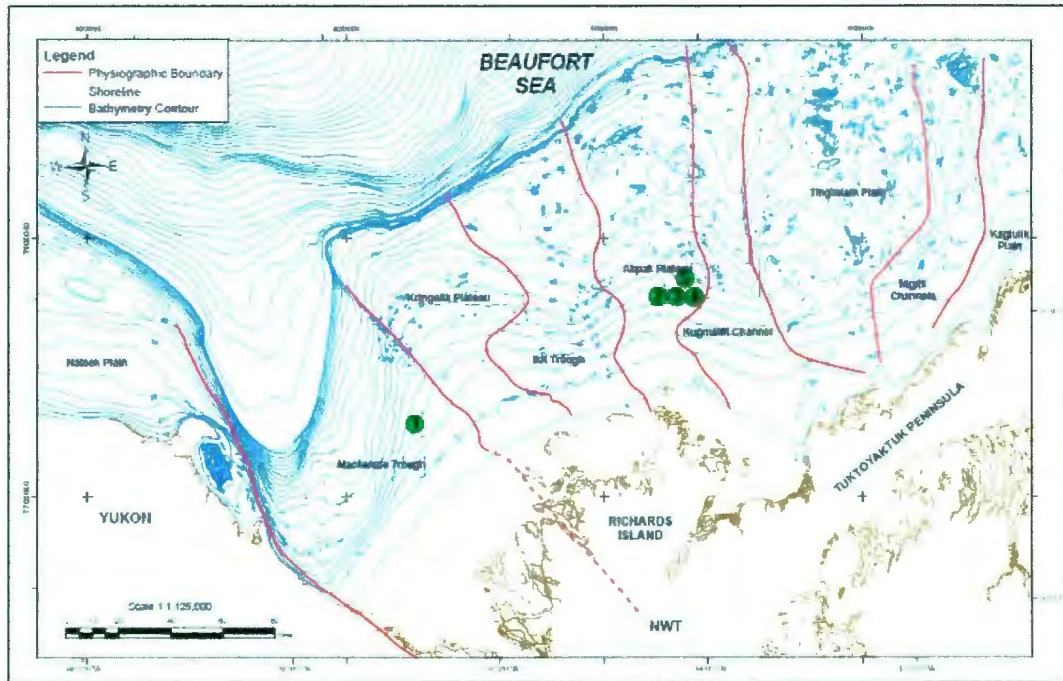


Figure 23: Extreme Gouge Locations

The overall goal of this study is to compare a 3D representative keel to that of the commonly accepted prismatic wedge model. To do this, two models need to be created from the following study. A classical wedge shape model can be designed based on a representative angle of attack of the end-berms in the gouges. A representative 3D model will be more complex; as multi-planar curvature will have to be evaluated.

The attack angle of each gouging ice keel will be obtained by evaluating the average slope of the end berms, using ArcGIS software (discussed later in this section). The average attack angle, which will be used to develop the prismatic model, will be based on the average of the attack angles of each keel from Gouge 1 to Gouge 5.

For the development of a 3D representative keel model, profile lines taken through end berms in the gouge direction changes will be used to obtain general curvature and shape in the vertical direction. Curvature in the horizontal direction is believed to be semi-elliptical to parabolic, based on observations by Kovacs *et al.* (1973); however, this will be confirmed by evaluating the general gouge morphology of keel impressions in end-berms. The proportions of: width (the longer side), thickness (the shorter side) and depth (gouge depth from relative seabed) are evaluated in each gouge set to obtain a dimensionless ratio which can be used to evaluate if a common proportion exist among ice keels. In order to test the common proportion theory, the overall gouge and prominent individual keels (or keel fingers) will be studied.

In a bathymetric study, it is recognized that there may be a general uncertainty over the ability of soil to retain the shape of the indenting keel. This is certainly the case for non-cohesive sediment (sand) but, cohesive sediment (clay) is believed to be able to retain the general shape of an ice keel much more effectively.

The PRISE Physical scale model test conducted by C-CORE in a medium strength silt-clay test bed showed that the side wall slope angles were approximately 45 degrees, even though the model keel had 90 degree sides. For this reason, the gouge morphology study undertaken in this thesis will not consider side wall slopes as accurately representing the true morphology of the ice keel, however there is still a valid reason to study the side wall slopes of gouges.

When a clay sediment is very soft it may not have enough shear strength to retain a physically imposed shape. With very high water content, which is associated with very soft clay, the soil may deform plastically. After an initial disturbance, over a period of time, very soft clay can plastically “slump” into a shape that may be supported by what strength the soil does have. During the gouging process the sediment strength can be reduced by disturbance during the gouging process. Also, the removal of overburden material can result in a lowering of the shear strength due to reduction of overburden stress.

The side berms of a gouge are presumed to be formed relatively rapid during the gouge process. It is likely that if clay sediment were to slump or plastically form into some natural shape it would occur in the side slopes. End berms are believed to be under ice load for a significant period of time, and may have consolidated to form a shape that is more representative of the actual ice keel shape. The main argument formed by these observations is that: if the side slope angles are significantly different than the end berm angles then we can be more confident that the gouge morphology is not due to a natural slumping of material.

3.2 Methodology

3.2.1 Overview

The computer program ArcGIS 10, by ESRI, was used to process multi-beam ASCII raster data into 2D and 3D visual terrain models. There are two components of ArcGIS 10 that were used in the processing of bathymetric data: ArcMap and ArcScene. ArcMap is the program that was used to conduct the quantitative analysis of the data. The tools within ArcMap that were primarily used include the “Interpolate Line” function (with “Create Profile Graph” function), and the slope raster overlay (used in conjunction with “Surface-Contour”). Arc Scene was used to create 3D rendered terrain imagery and was particularly useful for visualizing the terrain morphology.

3.2.3 ArcMap

In ArcMap, the raster data appears visually as a top down map with a color gradient used to depict the relative elevation. By this it means that each bathymetric interval is color coded. Due to the relative contrast in elevation, more than one color scheme was used in order to better visualize gouge morphology features, see Figure 25a.

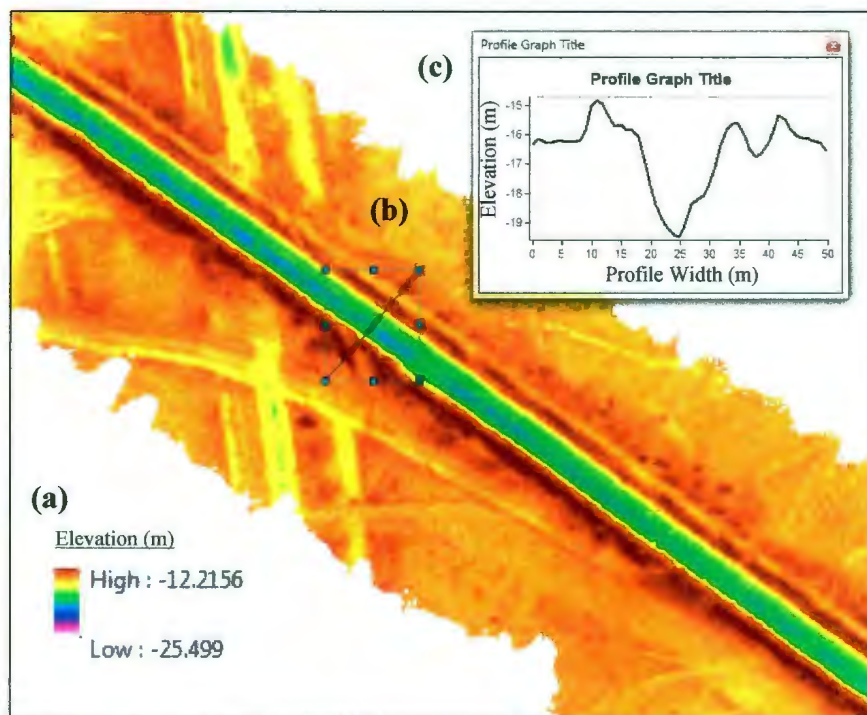


Figure 25: Screenshot from ArcMap (a) Color elevation legend (b) Interpolate Line (c) Profile Graph

A number of tools were used to analyze the bathymetric data. One of the most common was the “Interpolate Line” function (used with “Create Profile Graph”). This allowed for a line to be drawn that would return a 2D elevation profile of the data, see Figure 25b and Figure 25c, respectively. This function was instrumental in rapidly observing profiles. Due to scaling issues, a vertical exaggeration is automatically applied to profile plots by

the ArcGIS software. Vertical exaggeration helps visualize the vertical component of the gouge, but can give the wrong impression of the true morphology of the gouge. An example of how this can be misleading can be seen in Figure 26. In this figure the two images are of the same profile. The profile on the left (Figure 26a) has a vertical scale exaggeration of 12:1, whereas the profile on the right (Figure 26b) has a 1:1 exaggeration and is how the gouge would appear in nature. The use of vertical exaggeration does allow for the identification of features that would be indiscernible when viewed in a 1:1 scale, which is why profiles illustrated in this thesis can have variable degrees of exaggeration.

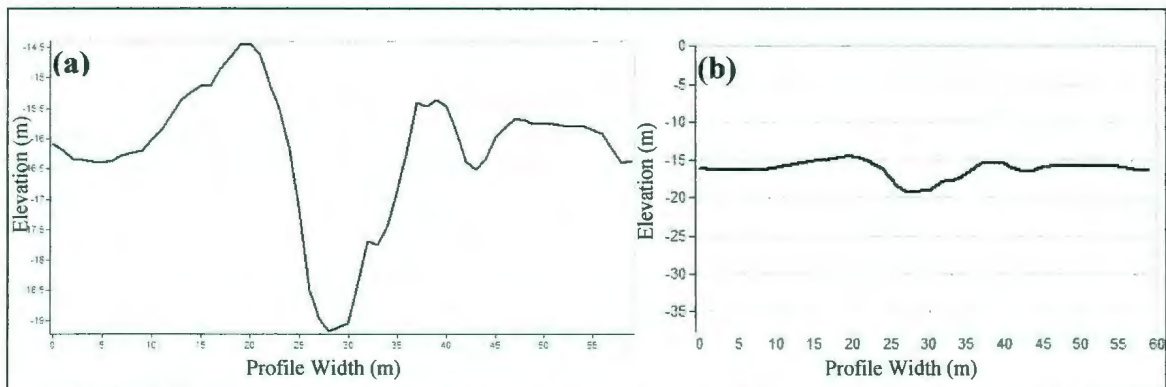


Figure 26: Profile Vertical to Horizontal Scale difference (a) 1:12 (b) 1:1

When using the interpolate line function, care must be taken. The direction in which the line is drawn matters to the orientation of the profile displayed. Another issue related to the interpolate line function arises when attempting to find the 2D profile of a gouge. If the interpolate line is not perpendicular to the gouge path, then the resulting profile plot gives the impression that the gouge is wider than it actually is.

One tool that is used extensively in the processing of the following bathymetric data is the slope raster overlay. For the slope overlay, an algorithm in ArcMap calculates the slope gradient for each cell, based on the elevations of the surrounding cells. It does this by calculating the elevation gradient in the respective x and y planes and using the square root of the sum of squares. The method in which this is done is outlined in the Figure 27, below.

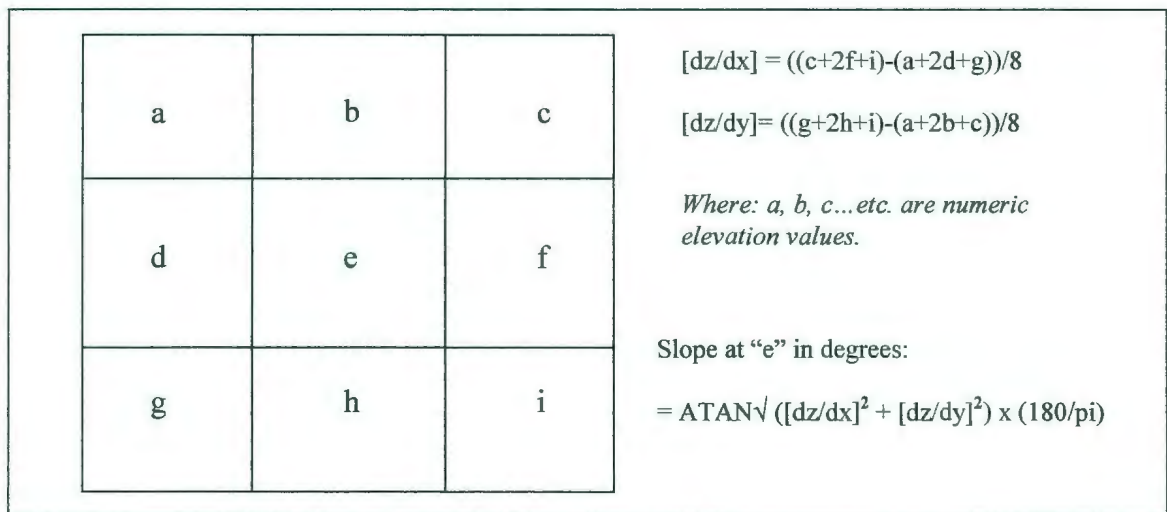


Figure 27: Raster Slope Algorithm (Modified from ArcGIS 10 help page)

The slope values for each cell can be overlaid on the 2D map, and has the visual appearance of a raster image superimposed on the ArcMap scene, an example of this can be seen in Figure 28. When used in conjunction with contour lines, the value and direction of the slope gradient can be ascertained. This is based on the premise that the steepest path on a slope is perpendicular to contour lines. As can be seen in Figure 28, the approximate direction and slope angle of a cell are indicated, the arrows have been added to illustrate the approximate direction of cell slope.

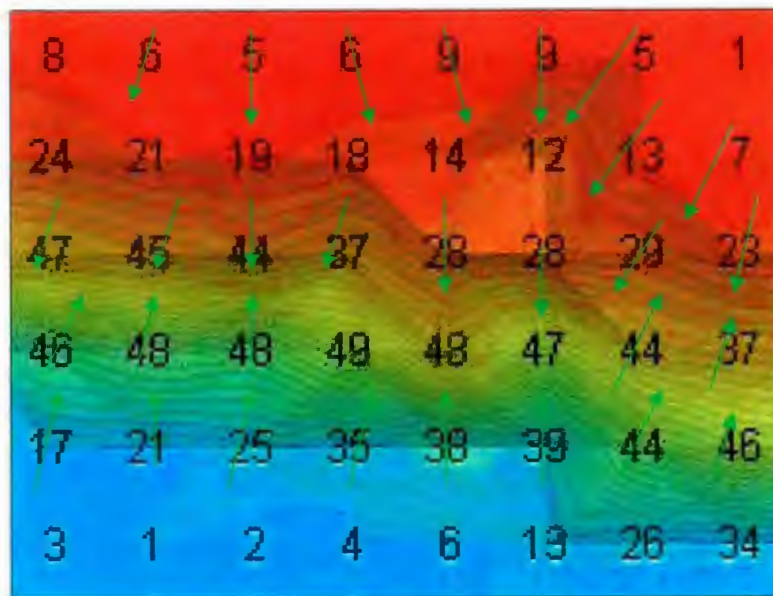


Figure 28: Example of Slope Raster Overlay

The use of the slope raster overlay, and contour lines, allow for fast and easy quantitative analysis; but in order to better assess the overall morphology, the use of rendered 3D imagery is also used in this thesis.

3.2.4 ArcScene

ArcScene can produce rendered 3D imagery of geographical data, which can be navigated and viewed from many different viewpoints. The use of 3D rendering is a powerful tool, and adds an entirely different level of observation to the study of gouge morphology. Though the dynamic use of rendered imagery was instrumental in the gouge bathymetry study, throughout the following section, only a few rendered images are included to better illustrate the gouge morphology.

3.3 Gouge 1 Study

3.3.1 Overview

Gouge 1 was created by a multi-fingered ice keel. An overview of the gouge study area can be seen in Figure 29. Based on the direction change, it can be discerned that the gouging begins on a southwest to northeast trajectory (Leg A). After approximately 3.8 km of gouging the gouge comes to a stop (Direction Change 1). The gouge then changes directions and begins moving on a west-northwest to east-southeast trajectory (Leg B). At approximately 7.3 km into the gouge, the gouge begins to make a gradual direction change to a northwest to southeast trajectory (Leg C) until it finally comes to an abrupt stop after approximately 10.3 km of observed gouging (Termination Point).

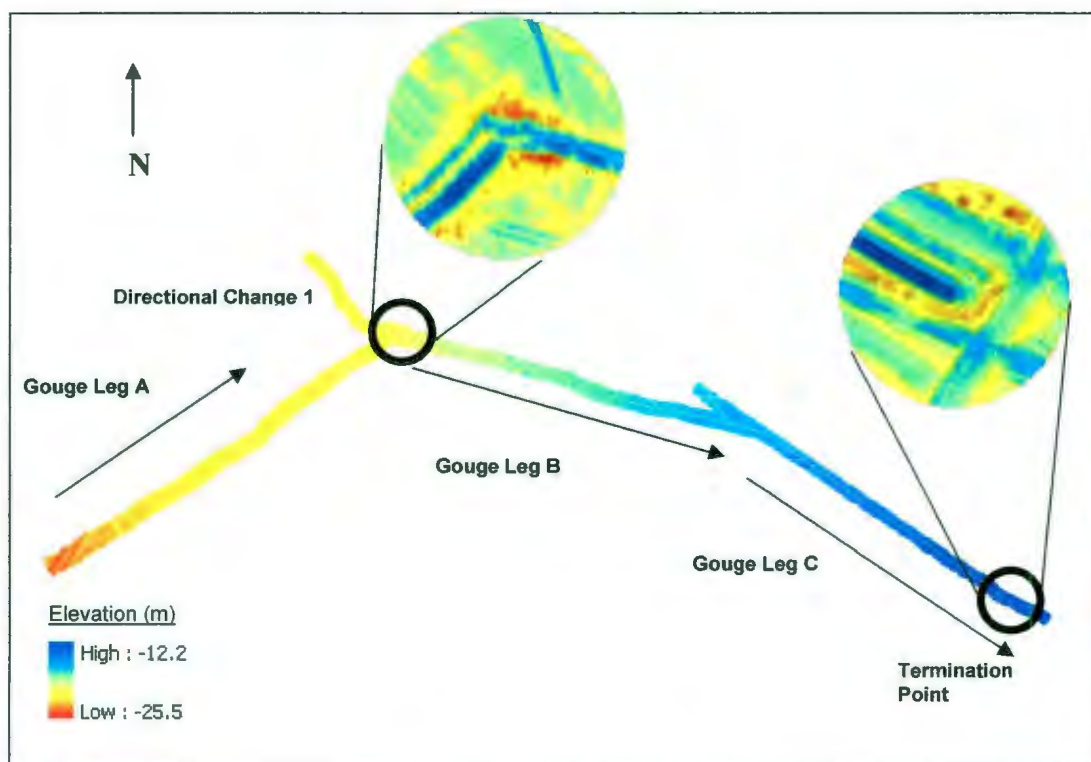


Figure 29: Gouge 1 Study Area

At its deepest point the gouge was measured to be 4.1 m deep with a width of approximately 12 m. The gouge begins in approximately 22 m water depth and begins to gouge progressively deeper as the seabed elevation begins to rise. An overview of the gouge and relative seabed elevation can be seen in Figure 30. The gouge elevation remains relatively constant up until the first direction change. After the first direction change, the gouge depth increases, however, not as fast as the seabed elevation is rising. There are three additional gouge depth increase changes: one at approximately 5.6 km, when the gouge path trajectory alters, becoming more south east; the second depth increase change occurs at the commencement of the second direction change, and the third appears to be a sharp rise in elevation approximately 100 m prior to the termination.

For purposes of analysis the gouge has been divided into three “legs” and two inflection/termination points; these are shown in Figure 29. The two main points of interest, for morphology, are the location of the first direction change and the termination point. The second direction change occurs gradually and is used to delineate Leg B and Leg C. The gouge path legs are studied for signs of morphological changes that can be equated with changes in keel shape and for evidence that may explain rise-up of the gouge path elevation. The side wall slopes in the gouge path legs are presumed to be unrepresentative of the true keel morphology; this assumption is based on the PRISE centrifuge model tests which showed that the vertical side wall keel models resulted in side wall angles of 45 degrees due to slumping, C-CORE (1996) and Woodworth-Lynas *et al.* (1995).

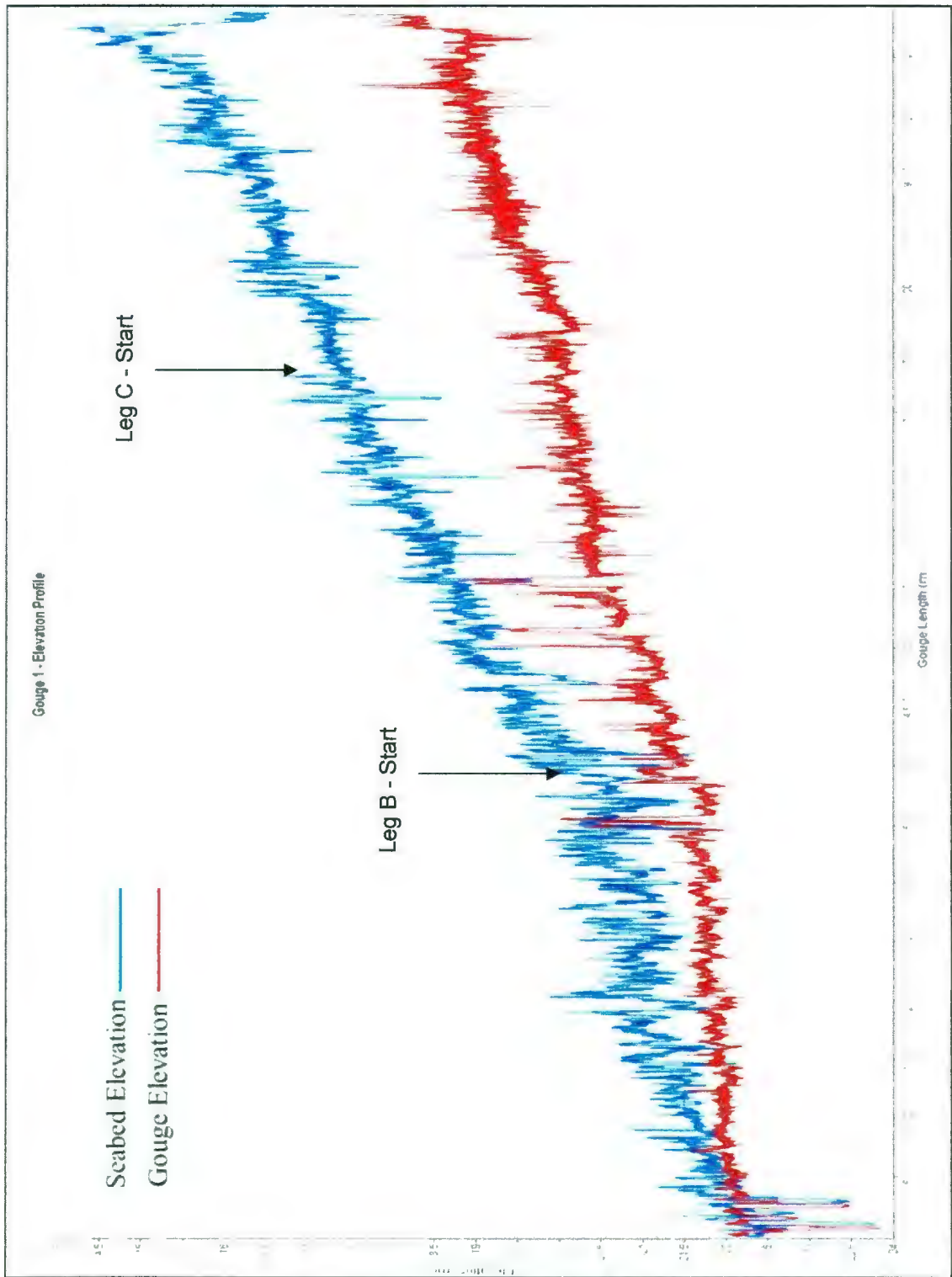


Figure 30: Gouge 1 – Elevation Profile

3.3.2 Gouge 1 - Leg A

Leg A is approximately 3.8 km in length and leads up to the first direction change. The gouge elevation during this phase remains relatively constant, as the seabed slopes at approximately 0.05 %. Leg A provides an opportunity to determine if the ice keel undergoes any drastic morphological change. When “leg A” is first observed, only one keel finger set is gouging, however, at the 1.1 km post a separate keel finger touches down. Figure 31, provides an overview of “leg A”, and the touchdown of the additional keel.

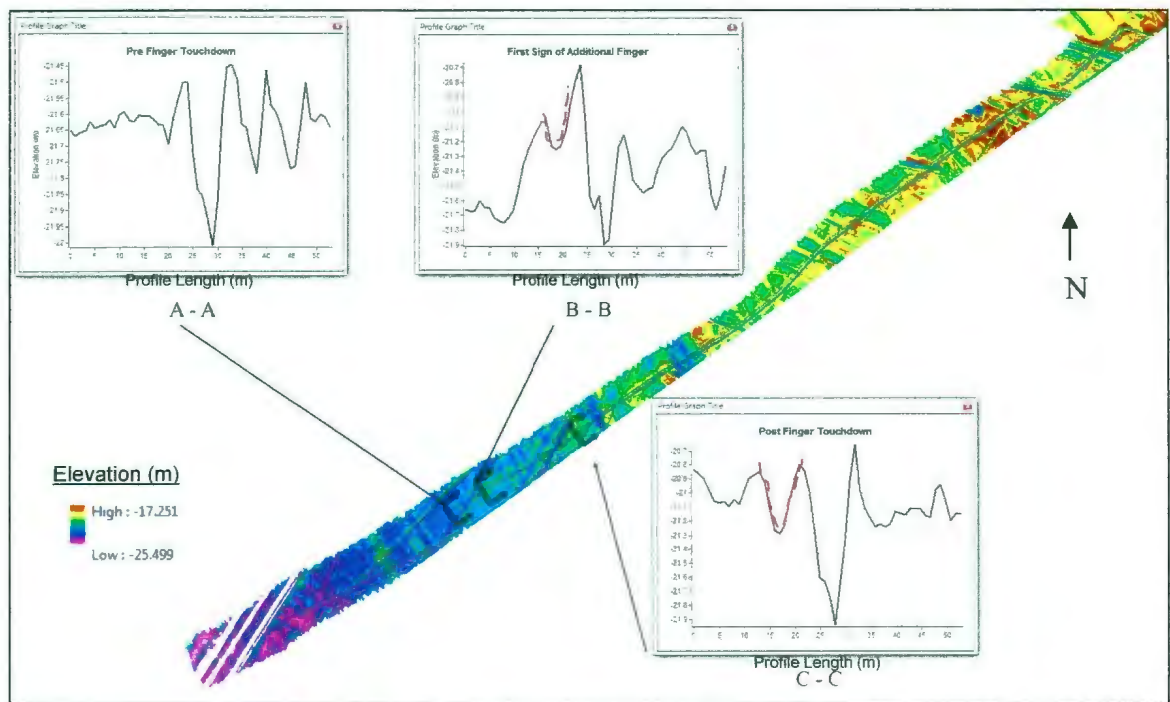


Figure 31: Gouge 1 - Leg A - Overview

The additional keel finger appears to be much smaller than the main keel finger. If keel ablation, or keel restructuring, occurs during gouging then it could possibly be observed in two structures of unequal size and properties. Figure 32, shows that the elevation of

the two keels, while there is considerable variation, change at the same rate over a distance of 2.7 km. If keel restructuring does occur, then it would be expected to be seen during the beginning of a new gouge path. Alternatively, restructuring may be on such a small scale that it is not obvious in gouge 2D profiles

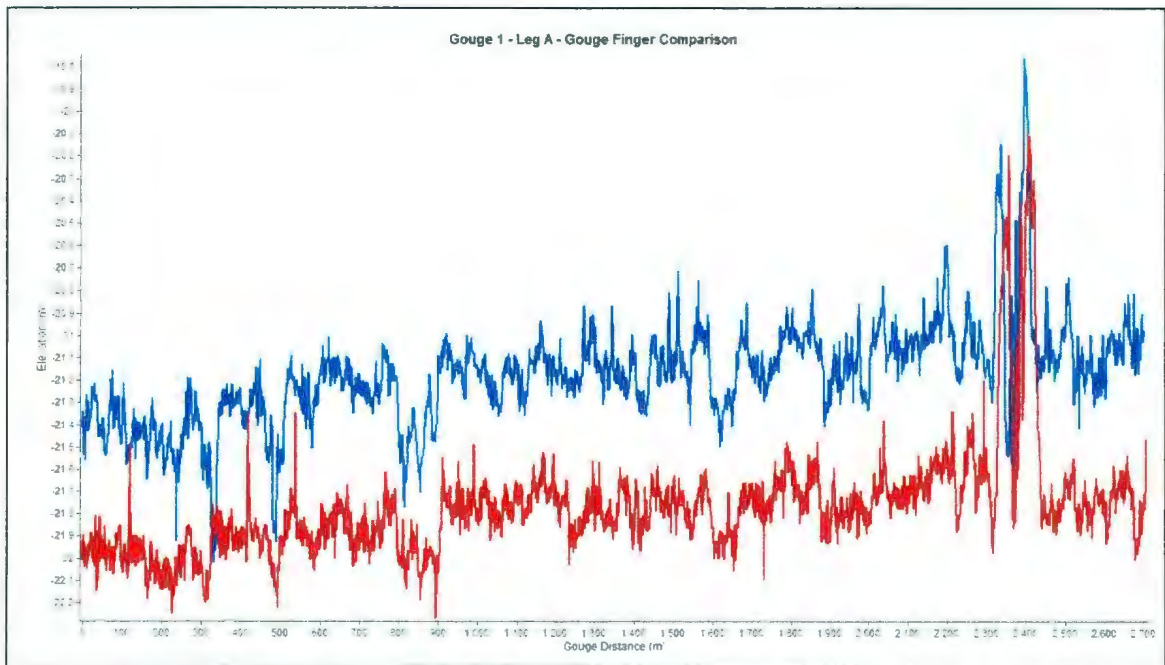


Figure 32: Gouge 1 - Leg A - Relative Finger Elevation

When viewing 2D profiles of the gouge, there is uncertainty of the true morphology of the ice keel. The relative positions of the keels' fingers are not always obvious. In a multi-finger gouge, it may be possible that a gouge path from a lead finger may be totally obliterated from a lagging keel finger. In the case where there is little lateral staggering, it may be possible that the lagging keel finger partially infill's a leading keel finger.

3.3.3 Gouge 1 - Direction Change 1

The end berm resulting from the direction change provides evidence of the slope angles of the ice keel, and the indentations in the berm provide clues to the horizontal shape of the ice keel. An overview of the direction change area can be seen in Figure 33. The width of the gouge before the direction change is approximately 20 m with a depth of 1.5 m, giving a width-to-depth ratio of 13:1. After the direction change the width is approximately 10 m with a depth of 1.2 m; giving a width-to-depth ratio of approximately 8:1. It is suspected that the true gouge depth after the direction change was still 1.5 m, but was obscured due to infill from the lagging keel; this would put the ratio at approximately 6.5:1 after the direction change.

Cross section profiles taken before and after the direction change shows that the keel fingers (Figure 33) appear to be slightly overlapping. From the shape of the gouge it is presumed that the smaller keel finger was leading the larger keel finger; this is seen when comparing the relative position of the keel finger indentations in the end berm. The cross section profile, after the direction change, also seems to indicate that the smaller keel was leading.

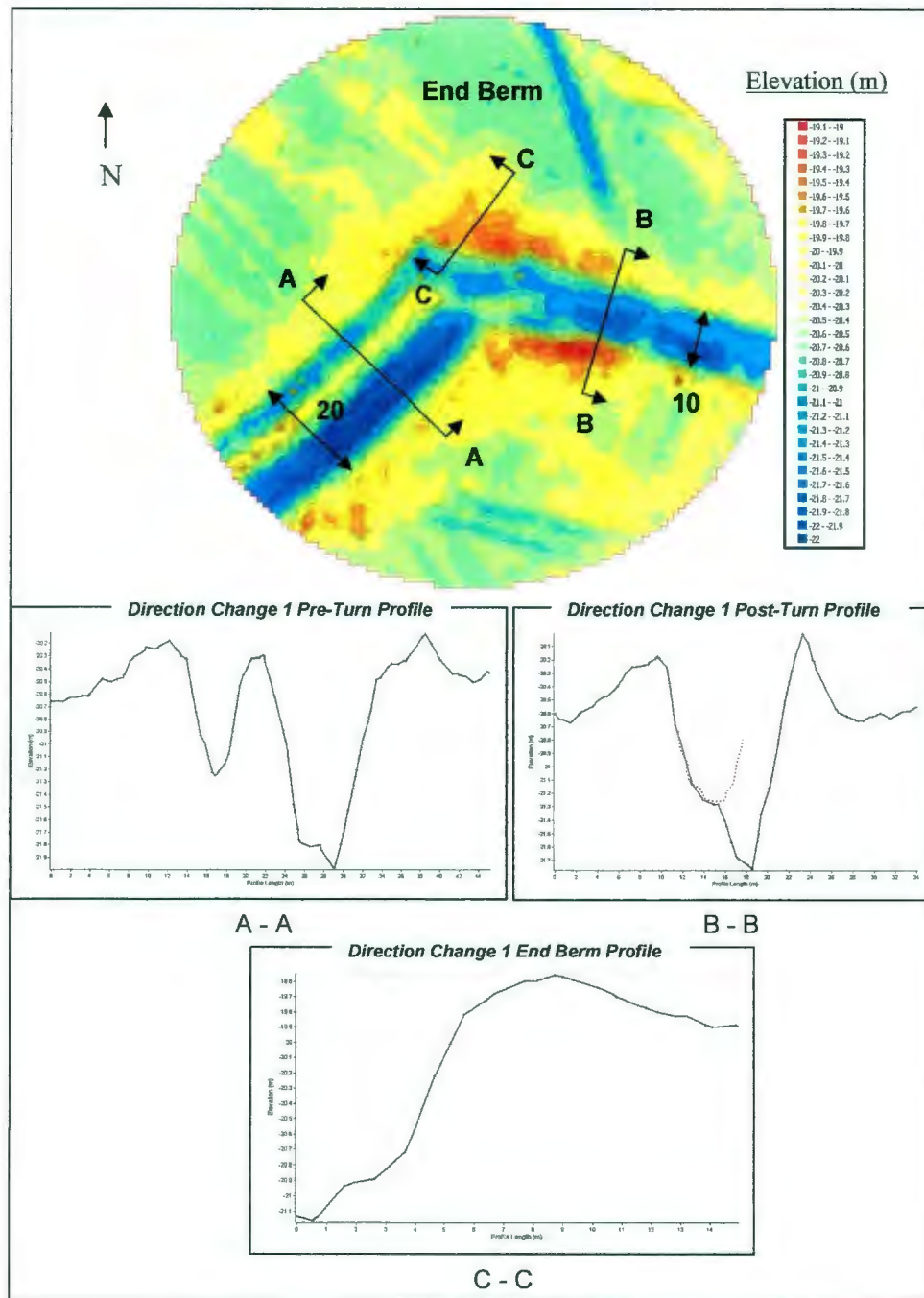


Figure 33: Gouge 1 - Direction Change 1 Overview

In theory, the lagging keel finger gouge would be less likely to be influenced by the leading keel finger gouge. If focus is placed just on the large keel, which was lagging,

we find that the width-to-depth ratio for the individual keel is approximately 8:1 before the gouge. After the direction change we see that there are indications in profile “B-B” (Figure 33) that the smaller keel is now lagging, the morphology is noticeably different, and the elevation is now 10 cm deeper than before the direction change. It appears as if this lagging keel is depositing material in the now leading gouge finger’s path. If we presume that the leading gouge path is at the same elevation that it was prior to the direction change, taking into account a reduction in width, it would mean that the width-to-depth ratio for the formerly lagging keel would be less than 6.7:1. If symmetry is assumed, a width for the keel of approximately 8m can be assumed, this would mean that the large keel would have a width-to-depth ratio of approximately 5.3:1 after the direction change.

Slope angles for the end berm are in the range of 26 to 33 degrees, with an average slope angle of approximately 30 degrees; this can be seen in Figure 34. Based on the increasing angles in the end berm it is determined that the gouging portion of the ice keel had a curved shape changing from convex near the base of the keel, to straight in the main gouging portion, to slightly convex at the seafloor. Indentations in the berm also indicate that the horizontal shape of the keel is circular. Side berm angles prior to the direction change were in the range of 19 to 24 degrees; this is much lower than the 45 degrees that was observed in the PRISE experiments.

There is some uncertainty over the applicability of studying the end berm to deduce the shape of the leading edge of the keel; it is possible that the smaller keel may have re-shaped the end berm profile as the keel changed direction. It is, however, considered still usable for the purposes of this thesis.

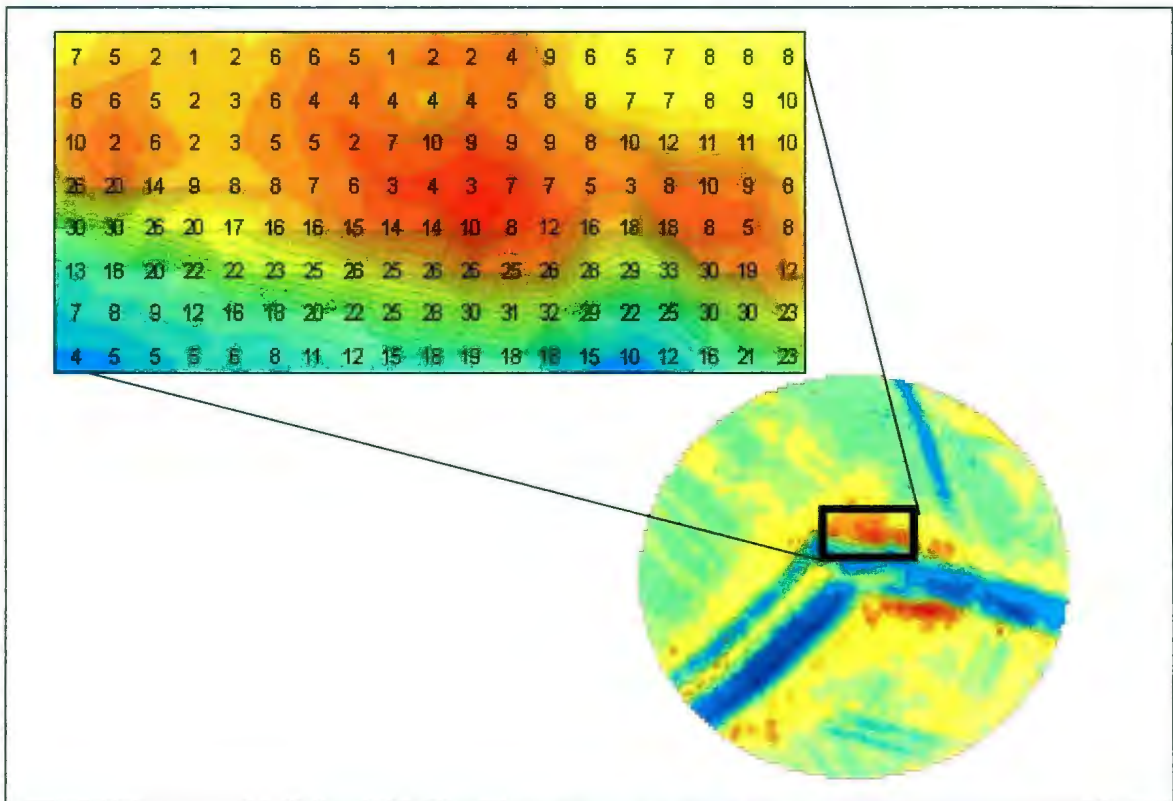


Figure 34: Direction Change 1 Slope Overlay

3.3.4 Gouge 1 - Leg B

During Leg B the ice keel is at its smallest observed width-to-depth ratio. The gouge, during Leg B, also experiences the development of an additional keel finger. The elevation change during Leg B was approximately 0.06 % during the initial portion. After approximately 2 km into leg B the gouge elevation rate changed to 0.03 %. The seabed slope remains relatively constant at 0.09%.

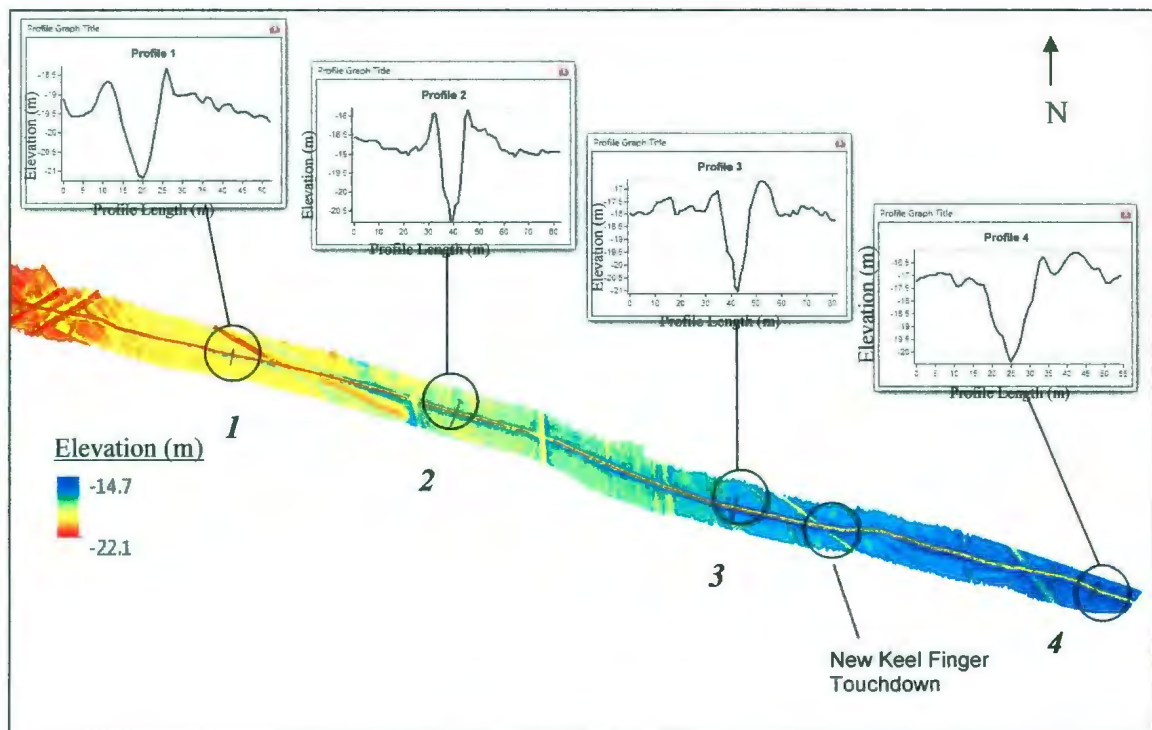


Figure 35: Leg B – Overview

From cross-profiles along Leg B, the smallest observed width-to-depth ratio was 3.5:1. Figure 35 shows an overview of Leg B, profile parameters from the figure are displayed in Table 2. The keel reached its deepest penetration depth along Leg B at the location of Profile 3; this is thought to be due to the presence of high berms from previous gouging

in the region. A trend that is noticeable in Table 2 is the decrease in width-to-depth ratio as the gouge depth increases. This trend can imply that the keel sides are becoming steeper with increased depth; a possible characteristic of curvature. This also may be due to artifacts in the data; more observations are required in order to verify if this trend is applicable to other gouges.

Table 2: Gouge 1 - Leg B- Profile Parameters

Profile	Width (m)	Depth (m)	W: D Ratio
1	9	1.7	5.3:1
2	9	1.8	5:1
3	11	3.1	3.5:1
4	11.5	2.8	4.1

The touchdown of an additional keel finger occurs at approximately 6.4 km, which can be seen more closely in Figure 36. Profiles taken before, and after, the touchdown of the additional keel are morphologically very similar, and have the exact same width-to-depth ratio of 5:1, at a gouge depth of 2.4 m; this indicates that the keel finger did not appear as a result of morphological change. The touchdown of the keel finger occurs at the crossing of a previous gouge with Gouge 1. The side berms from the previous gouge appear to have been high enough to make contact with the keel finger. Slope data shown in Figure 37, show side berms have maximum angles ranging from 44 to 49 degrees; this is in agreement with the PRISE results, which observed a 45 degree angle slope.

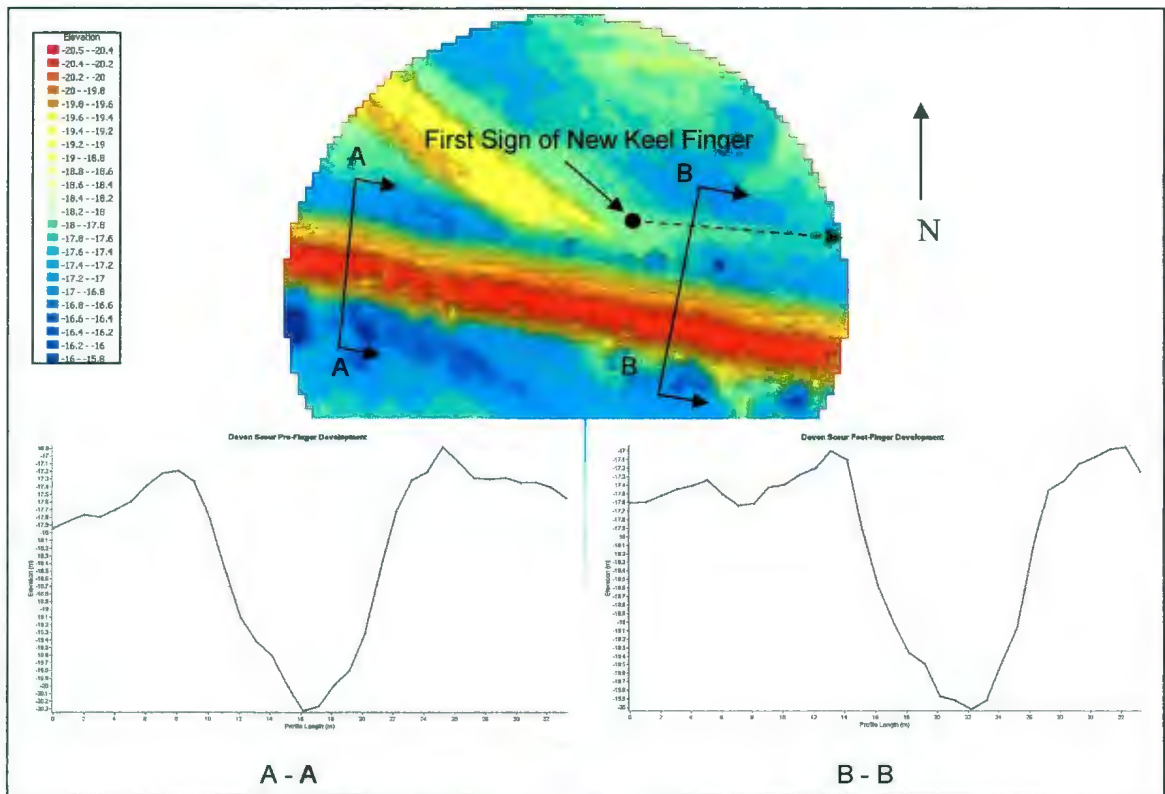


Figure 36: Gouge 1 – Leg B – Additional Keel Finger

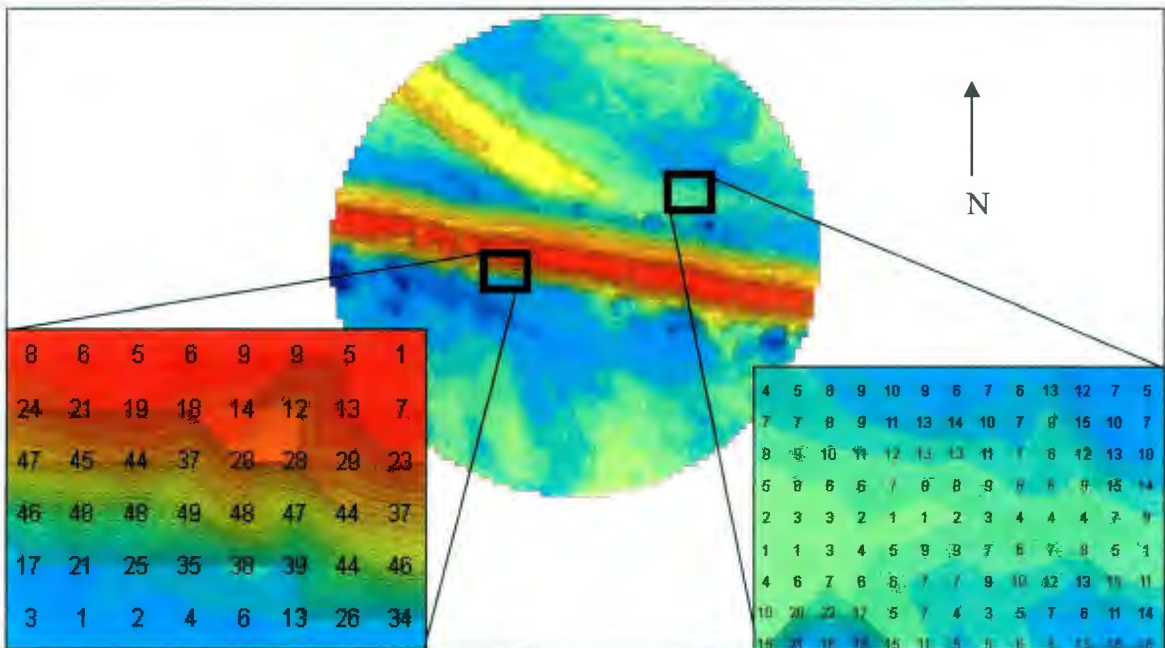


Figure 37: Gouge 1 – Leg B – Direction Change Slope Raster Overlay

3.3.5 Gouge 1 - Leg C

During Leg C, the gouge slope was relatively constant at 0.05 %; the seabed slope was also relatively constant at 0.07 %. Leg C is of particular interest for two reasons: first, the deepest gouge depth in Leg C also happens to be the deepest gouge point of Gouge 1; second, as observed in Figure 30, there was an abrupt change in elevation near the end of the gouge.

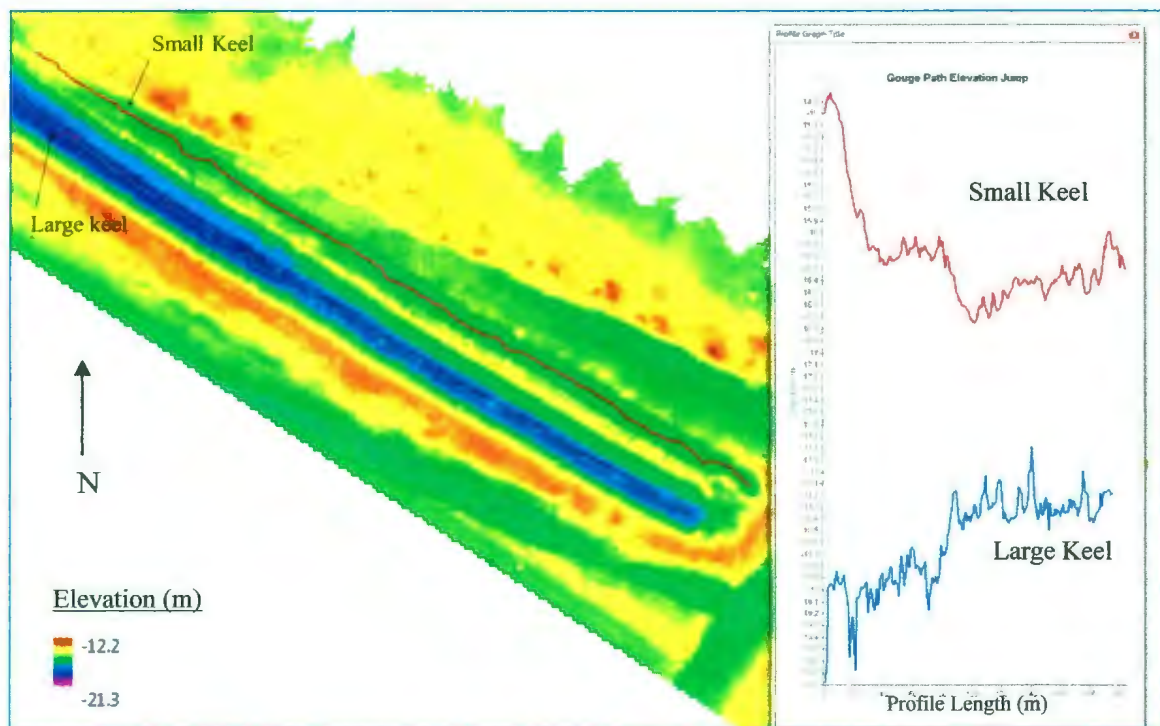


Figure 38: Gouge 1 - Leg C - Sudden Elevation Change

It was found that when the main gouge path suddenly became shallower by 0.5m, the additional keel, from Leg B, became deeper by nearly the exact same amount; this can be seen in Figure 38. Profiles taken before and after the drastic change in elevation do not show any signs of catastrophic keel morphology changes, see Figure 39. There appears

to be no other logical explanation but a sudden vertical failure in the larger ice keel finger accompanied by a vertical drop of the remaining ice. In Figure 39a, the profile just before the elevation jump happens to be the deepest observed point in the entire gouge. The actual depth is speculative, because Gouge 1 appears to have entered a previous Gouge path, and thus the relative seabed elevation is much higher than normal. However, the approximate depth to undisturbed seabed is estimated to be 4.1 m. The width-to-depth ratio at this point is approximately 2.9:1. Curiously, there is significant elevation variation in the gouge path, it is unclear if isolated point of significant gouge variation is due to erroneous data, or if the variation is due to inconsistent soil infilling.

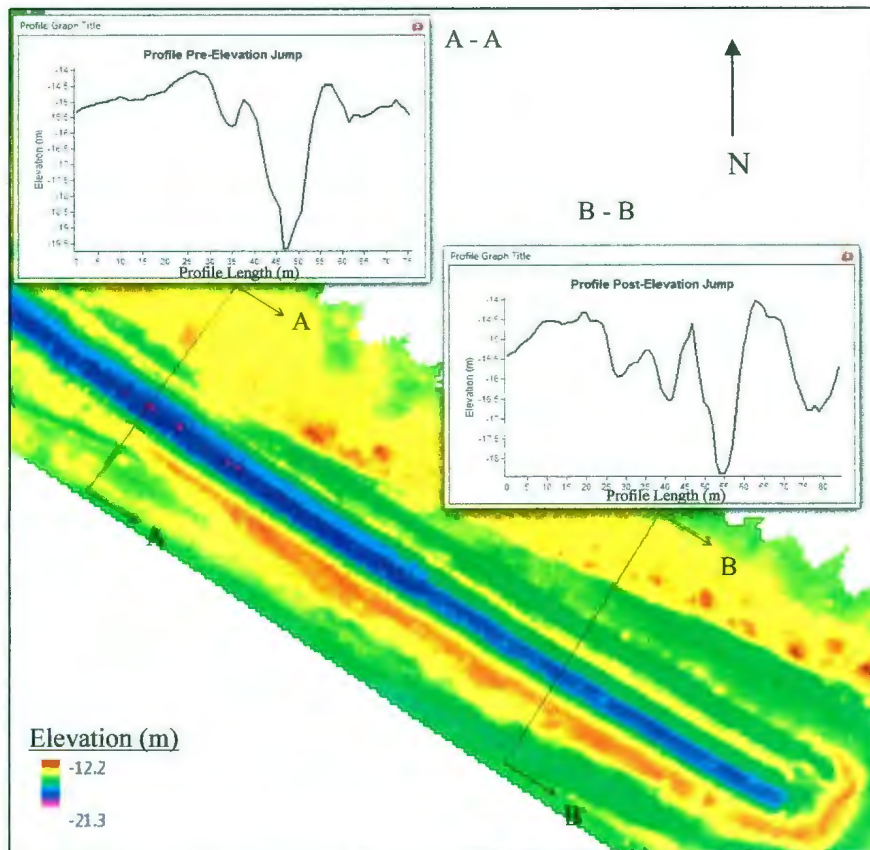


Figure 39: Gouge 1 - Leg C - Before and After Elevation Change Profile

3.3.6 Gouge 1 - Termination Mound

Given the abrupt end to the gouge, it was expected that the ice keel would have left an impression on the end berm. However, based on the failure of the larger keel finger, it is unlikely that the impression would be representative of the morphology that had created the previous 10 km of gouging.

Figure 40 shows an overview of the termination point area. Just before the termination point the gouge is approximately 24 m wide, with a depth of 2.5 m; this gives a width-to-depth ratio of 9.6:1.

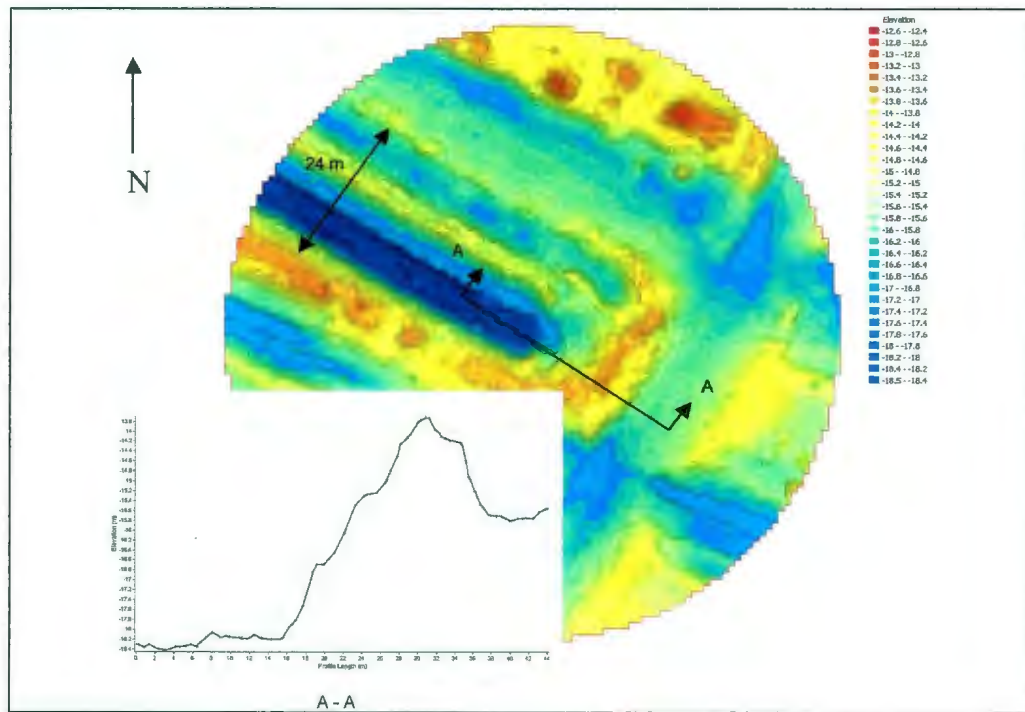


Figure 40: Gouge 1 - Termination Mound Overview

The terminal berm of Gouge 1 has been disturbed by a more recent gouge event that passed through the end berm at approximately 90° to the orientation of Gouge 1 (Figure 42). It is unclear if the gouge crossing has influenced the slope angles on the termination berm.

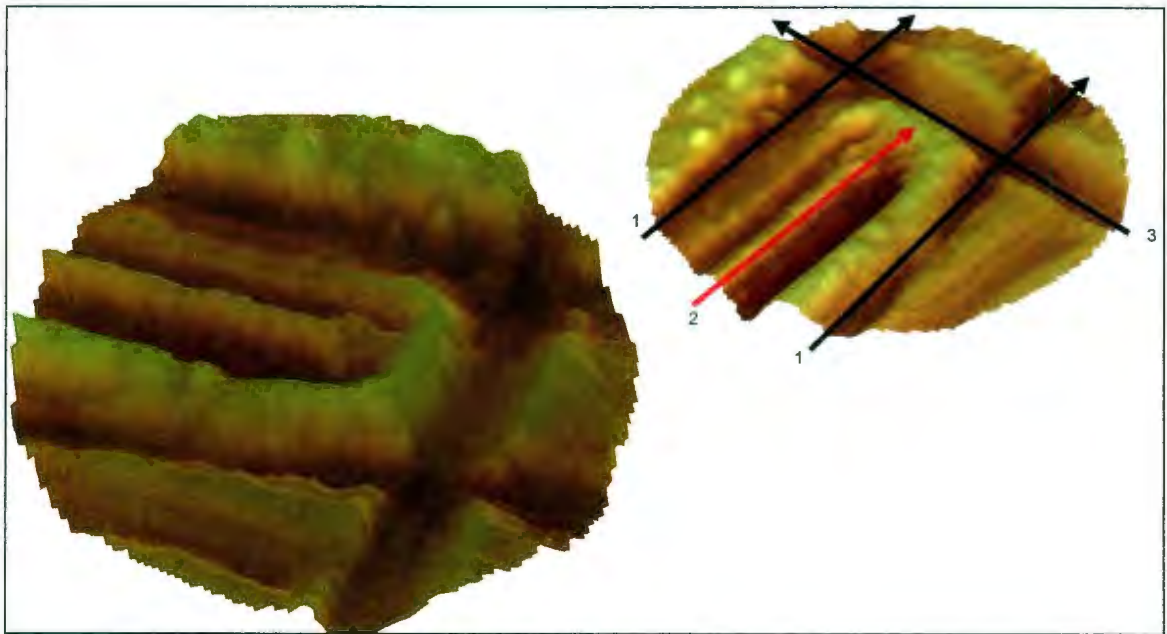


Figure 42: Gouge 1 - Rendered Image- Termination Mound Gouge Interference

3.4 Gouge 2 Study

3.4.1 Overview

Gouge 2 was created from a multi-finger keel and was recorded for approximately 15.3 km. The gouge path is first surveyed moving from the northwest to southeast, in a water depth of approximately 33 m. The keel changes direction and moves to the southwest. The gouge morphology changes considerably. The occurrence of a sharp jump in seafloor elevation also occurs, at approximately the 5.5 km, due to the vertical destruction of a keel finger. At approximately 10 km, the gouge reaches a water depth of approximately 27 m, and changes direction to the North West, back into deeper water. The maximum gouge depth seen in this gouge was approximately 4 m; the maximum width was approximately 66 m. The width-to-depth ratio for the overall gouge varies from approximately 20:1 to 10:1. An overview of the gouge area can be seen in Figure 43.

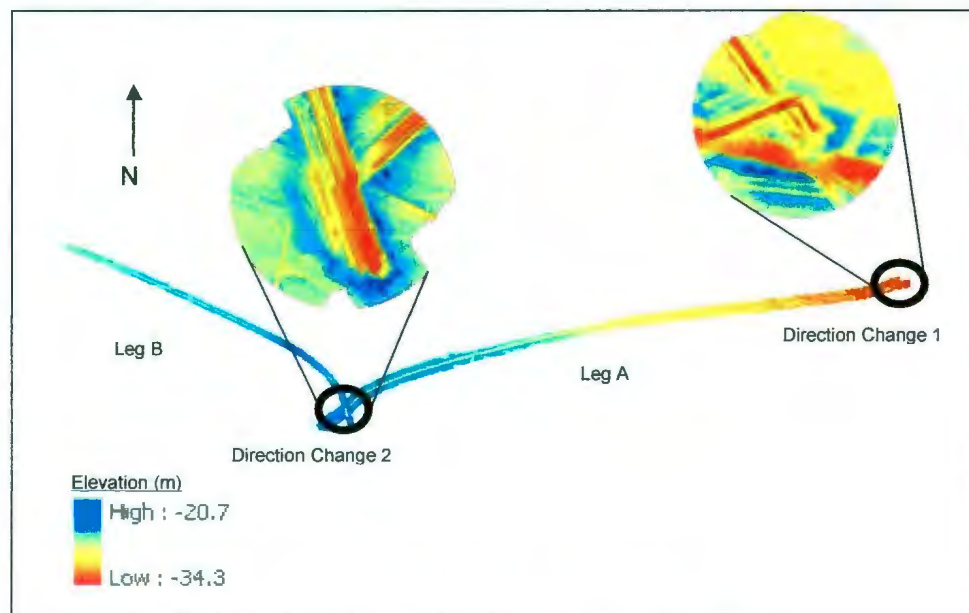


Figure 43: Gouge 2 - Study Area Overview

The elevation profile of Gouge 2 can be seen in Figure 44. Initially the seabed slope is approximately 0.05 %. The gouge is relatively linear, increasing at a rate of 0.015 %. At approximately 5.5 km there is a sharp decrease in the gouge elevation followed by a decrease in gouge elevation of approximately 0.03 %; the seabed rate of change still remains at 0.05 %. The elevation profile shows that between approximately 10 km and 11 km the seabed rises to its shallowest elevation. It is unclear if this is actually the case, or if active gouging in this section artificially gives the impression that the seabed has risen.

For ease of study Gouge 2 is divided into three sections. Direction Change 1, Leg A, and Direction Change 2 (Figure 43). Leg B, was found not to contain any events of significance, or interest, and was excluded from the study.

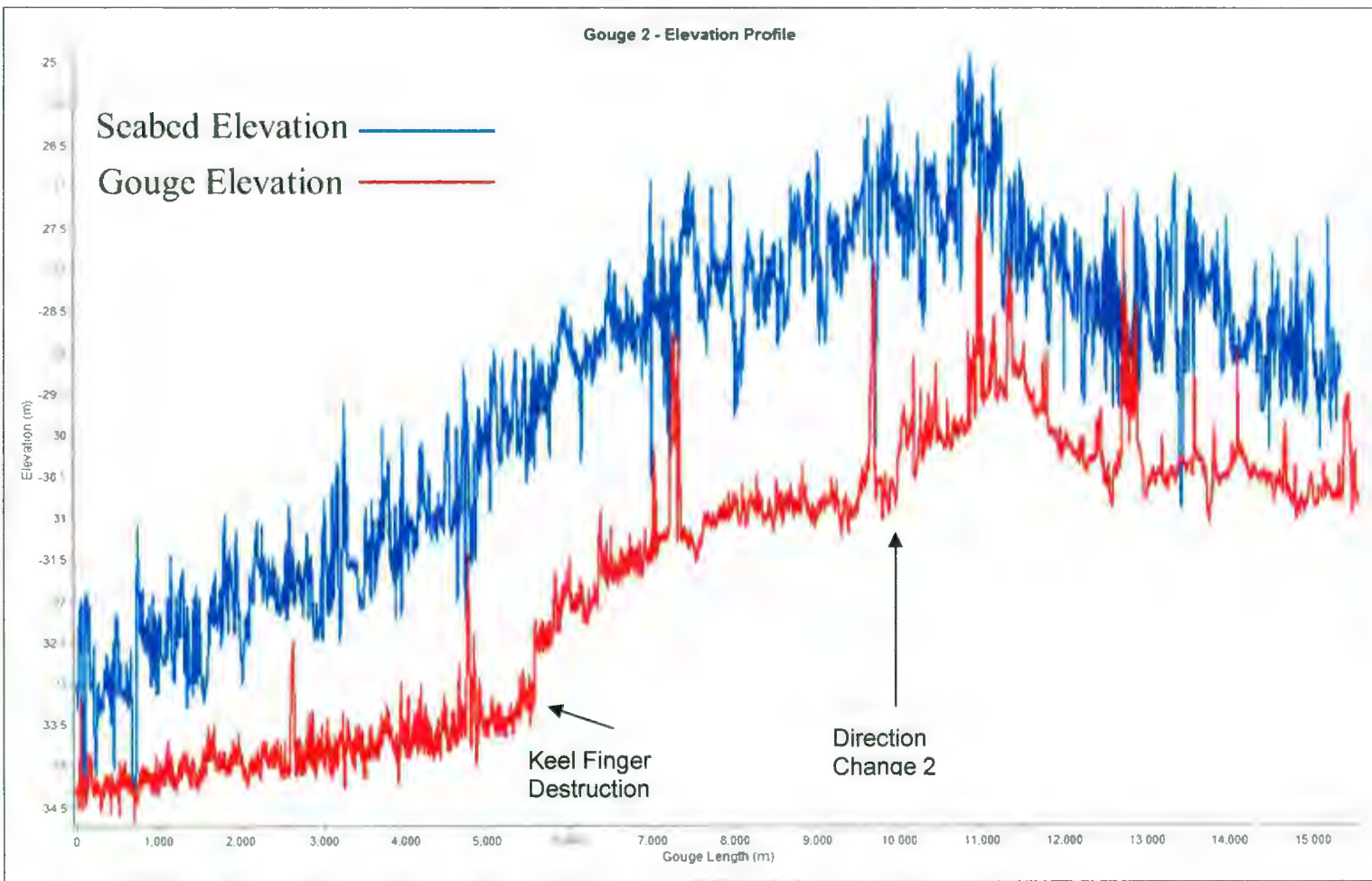


Figure 44: Gouge 2 - Elevation Profile

3.4.2 Gouge 2 - Direction Change 1

Direction Change 1 is gradual and little can be obtained from the section in terms of morphology. An overview of Direction Change 1 can be seen in figure Figure 45. The ice keel that created Gouge 2 comprises three keel "fingers", based on gouge morphology. The keel moved into the change of direction region from the northwest before stopping. It then moved approximately 10m to the East, and stopped. It moved 25 m northwest, where the keel appears to have rotated approximately 90 degrees and then proceeded on a west-southwest trajectory. The relative trajectories of the individual keel fingers are labeled 1 to 3 in Figure 45.

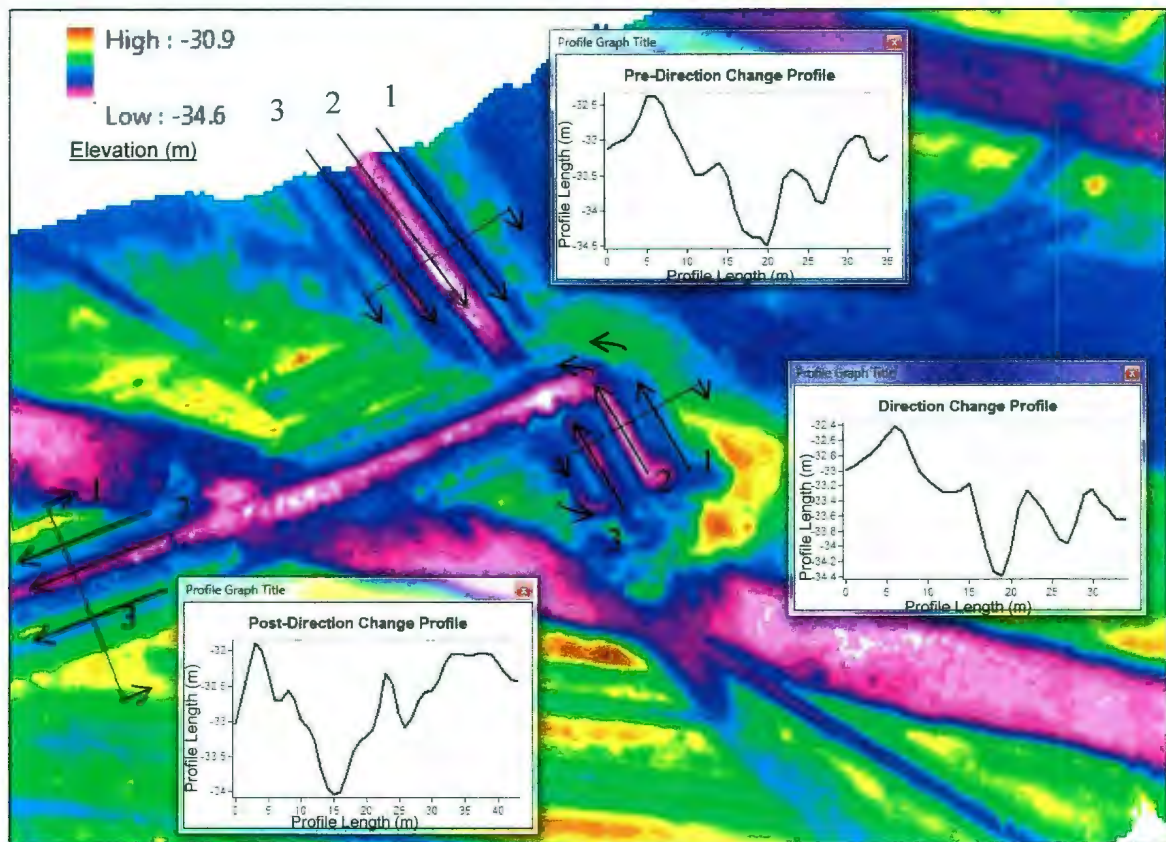


Figure 45: Gouge 2 - Direction Change 1 Overview

Profiles taken at different points of the direction change (insets in Figure 45) show that lateral separation of the keel fingers are approximately the same; the overall width-to-depth ratio before and after the direction change are also the same value of 15:1. This supports the interpretation that the ice keel had rotated. This would also explain how the larger keel finger could appear to have been lagging before, and after, the direction change.

Since the larger keel finger (“2” in Figure 45) appears to have been lagging before and after the direction change, it is less likely to have been influenced by infill from the other keel fingers. The width-to-depth ratio for keel finger “2” is approximately 8:1.

Direction Change 1 is a good example of how complex keel movement can partially erase the gouge path and make the interpretation of rotational movement much harder.

3.4.3 Gouge 2 - Leg A

During Leg A, the gouge profile undergoes considerable changes from the end of Direction Change 1 to the beginning of Direction Change 2. Profiles taken at several locations across the gouge clearly illustrate changing morphology along the gouge route. The gouge appears to be created by a single multi-finger keel up to the 5 km location, when the touchdown of an additional keel finger is first discernible. By 9.3 km (Figure 46) an additional multi-finger keel is visible. Parametric data of the profiles contained in Figure 46 can be found in Table 3. Maximum side wall slopes in the gouge during Leg A ranged from 29 to 43 degrees.

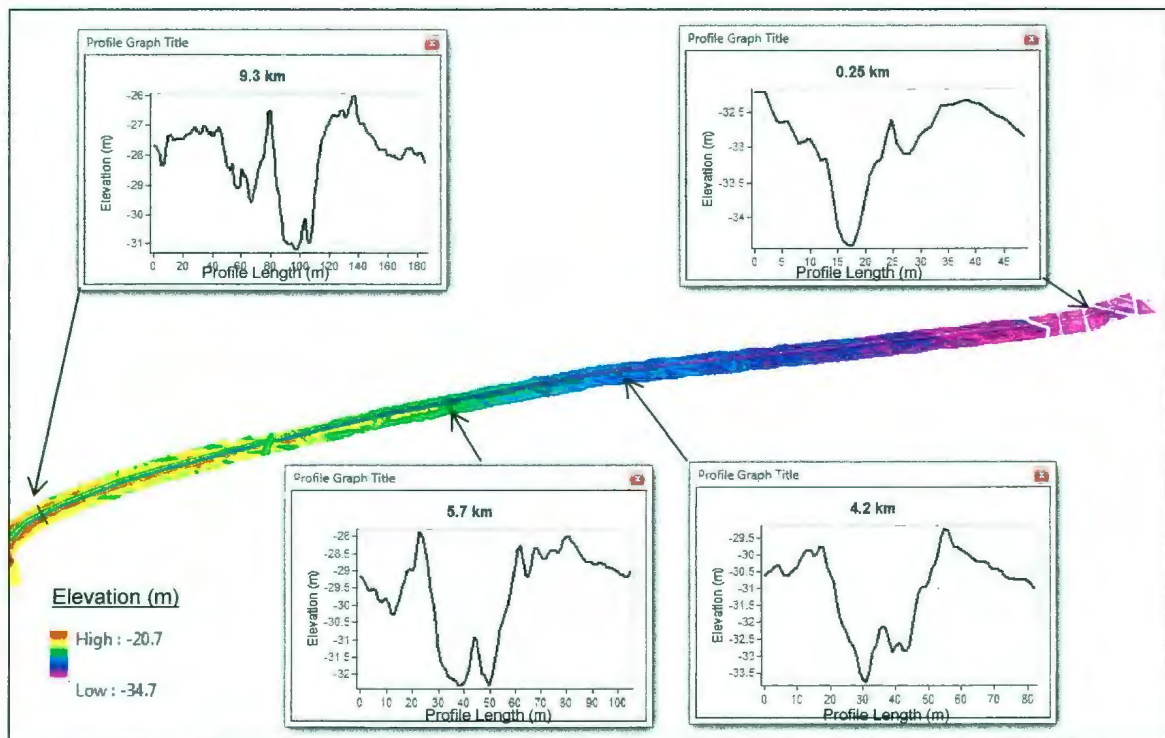


Figure 46: Gouge 2 - Leg A – Profile Comparison

Table 3: Gouge 2 – Leg A – Profile Parameters

Profile	Width (m)	Depth (m)	W: D Ratio
0.25 km	8	1.1	7.7:1
4.20 km	27	2.8	9.6:1
5.70 km	34	3.3	10.3:1
9.30 km	66	3.6	18:1

The disappearance of an individual groove indicates that the keel finger which created the groove was sheared off (Figure 47 denoted in red). The relative constant elevation of the smaller keel finger indicates that a sudden change in overall keel elevation did not occur.

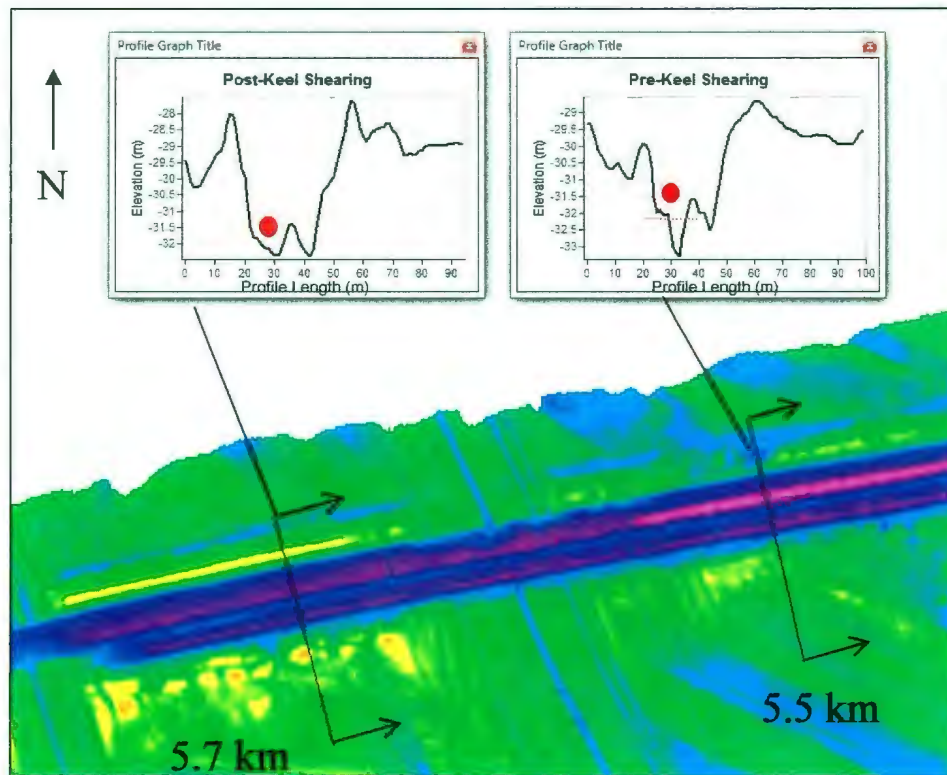


Figure 47: Gouge 2 - Keel Being Sheared

3.4.4 Gouge 2 - Direction Change 2

It is presumed that the presence of two prominent berms would give an ideal opportunity to study keel morphology, however, this is not the case. Direction Change 2 was a complex event, with signs of keel finger shearing and possible rotation. An overview of Direction Change 2 can be seen in Figure 48.

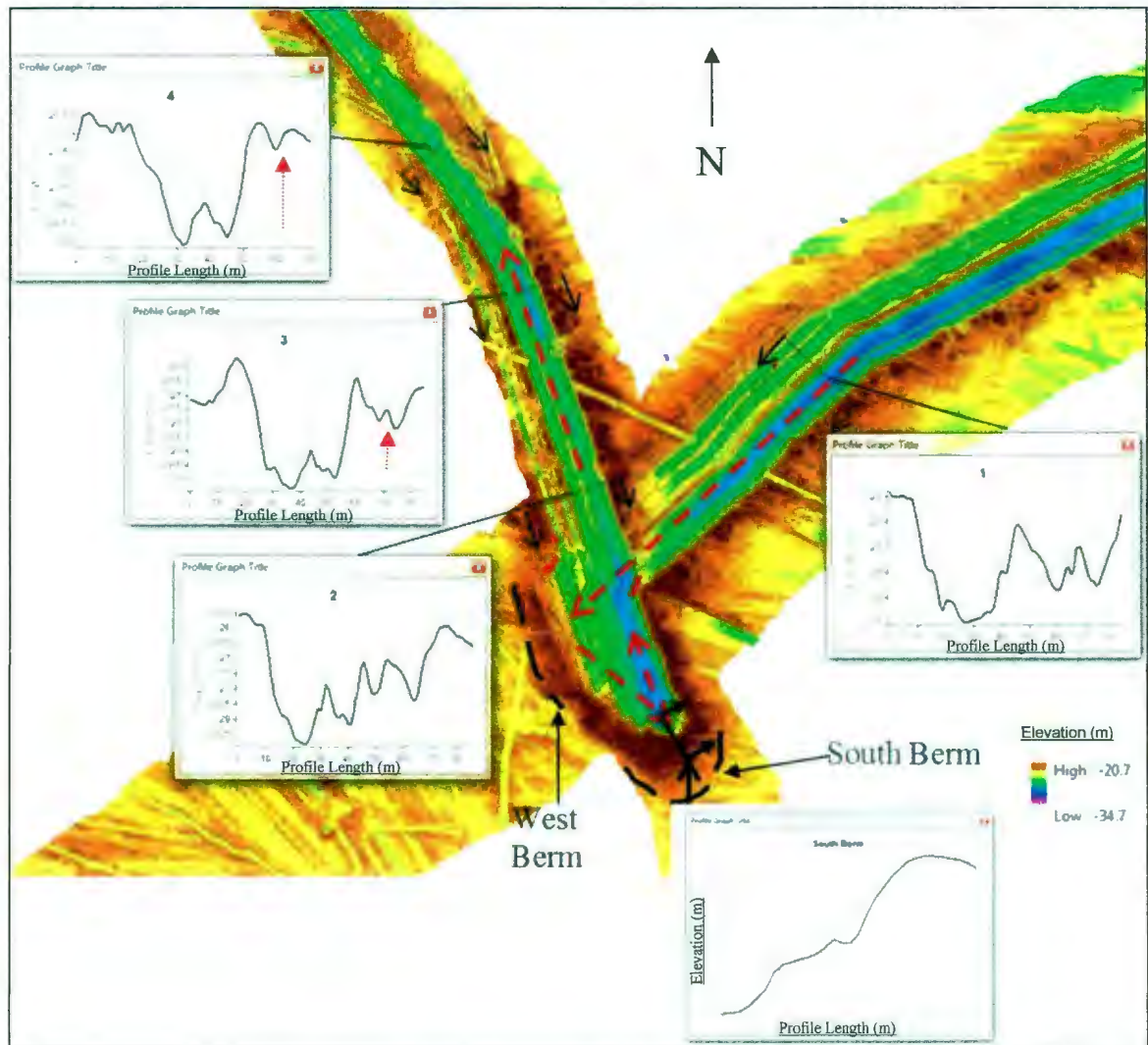


Figure 48: Gouge 2 - Direction Change 2

The keel can be seen moving from the East. It is believed that the keel came to an abrupt stop and began to move southeast for approximately 100 m. The keel then began to move to the Northwest. Rounded features on the side walls, and non-uniform infill of the gouge path, prior to the direction change, could indicate that there was a significant amount of vertical rotation (yaw). The similarity in profiles (1 to 4) also appears to support that the keel possibly made a near 90 degree rotation.

It can be observed that the elevation of the smaller keel set is drastically changing during and after the direction change. Profiles 2 to 4, show that the elevation difference between the smaller keel set and the larger keel set is increasing until eventually the smaller keel finger set is no longer discernible. This is believed to be due to a gradual shearing away of the smaller keel (ablation). From the profiles, it does not appear that the larger keel set is experiencing any significant ablation.

The West berm appears to have been strongly influenced from the South, and North, movement of the keel, and is thus not considered to be representative. The South berm is considered more representative of general morphological characteristics of the scouring face of the Gouge 2 keel. A stepped like appearance in the south berm profile, in Figure 48, is most likely a result of keel fingers leading a deeper keel. The keel fingers in the berm profile seem to indicate a slightly rounded toe at the base, but becoming relatively

linear. Each individual keel in the South berm shows a convex circular appearance in the horizontal direction.

A slope raster overlay of the South berm can be seen in Figure 49. The maximum slope angles range from 25 to 41, with an average of approximately 33 degrees.

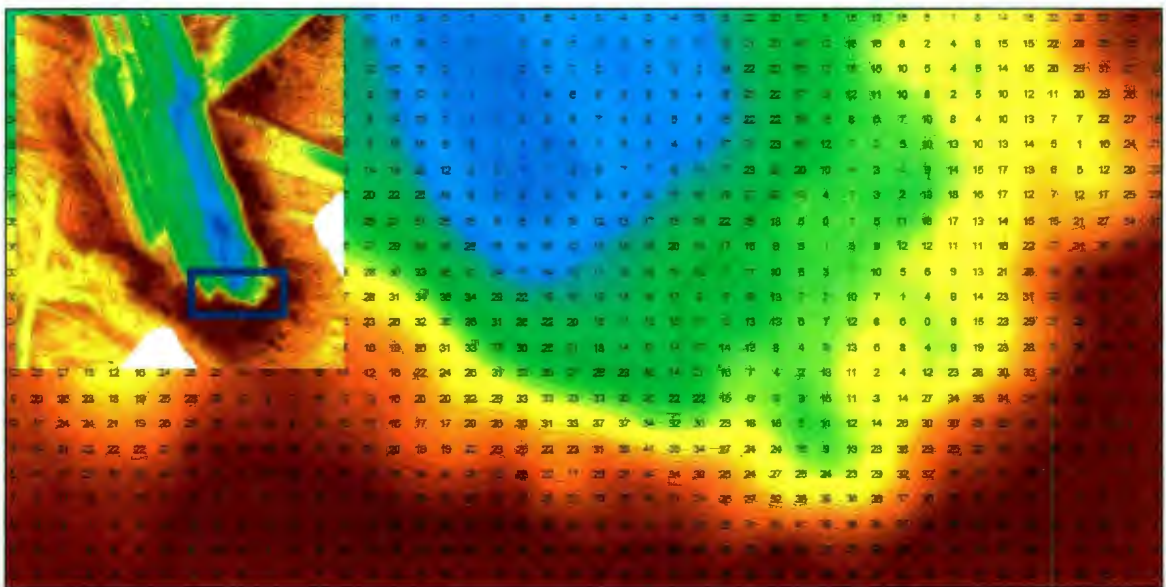


Figure 49: Gouge 2 - Direction Change 2 - Slope Overlay

3.5 Gouge 3 Study

3.5.1 Overview

There are four events observed in Gouge 3 that provide insight into the behaviour and shape of the ice keel. The first event is a transition zone, which occurs at 1.6 km into the scour; the second is a transition zone, which occurs at 2.3 km into the scour; the third event is also a transition zone, which occurs at 2.8 km into the scour path. The final event is the termination of the gouge. An overview of the scour area can be seen in Figure 50.

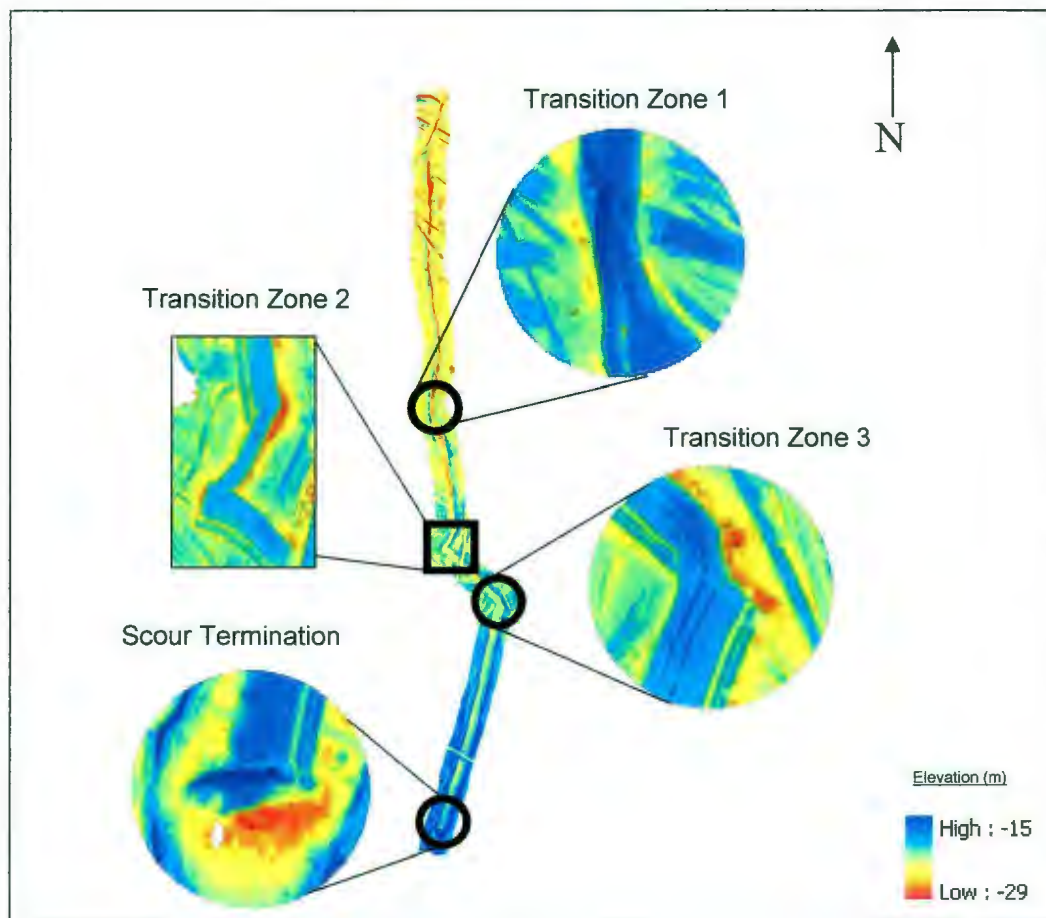


Figure 50: Gouge 3 - Overview

Gouge 3 is observed for approximately 4.1 km. Unlike Gouge 1, Gouge 3 depth appears to be relatively constant, thus it is likely that the keel was gouging for a significant period of time before being first observed in this data set. The gouge begins in the North in water depth of approximately 22 m and proceeds to the south into shallow water where it terminates in water depth of approximately 19 m. The maximum width of this scour was observed to be 40 m. The maximum gouge depth observed in this gouge was approximately 2m. The width-to-depth ratio of this gouge varies from approximately 22:1 to 10:1, depending on orientation. Gouge 3 is a multi-finger ice keel, at some points several keel fingers can be observed. There are two prominent finger sets observable in this gouge.

Elevation profile data for Gouge 3 shows a steady reduction in the elevation of the gouge over the length of the gouge, see Figure 51. The rate of elevation decrease of the gouge is approximately 0.07%. The seabed slope is also noticed to be approximately the same value. This indicates that the gouge depth stays relatively constant over the gouge path.

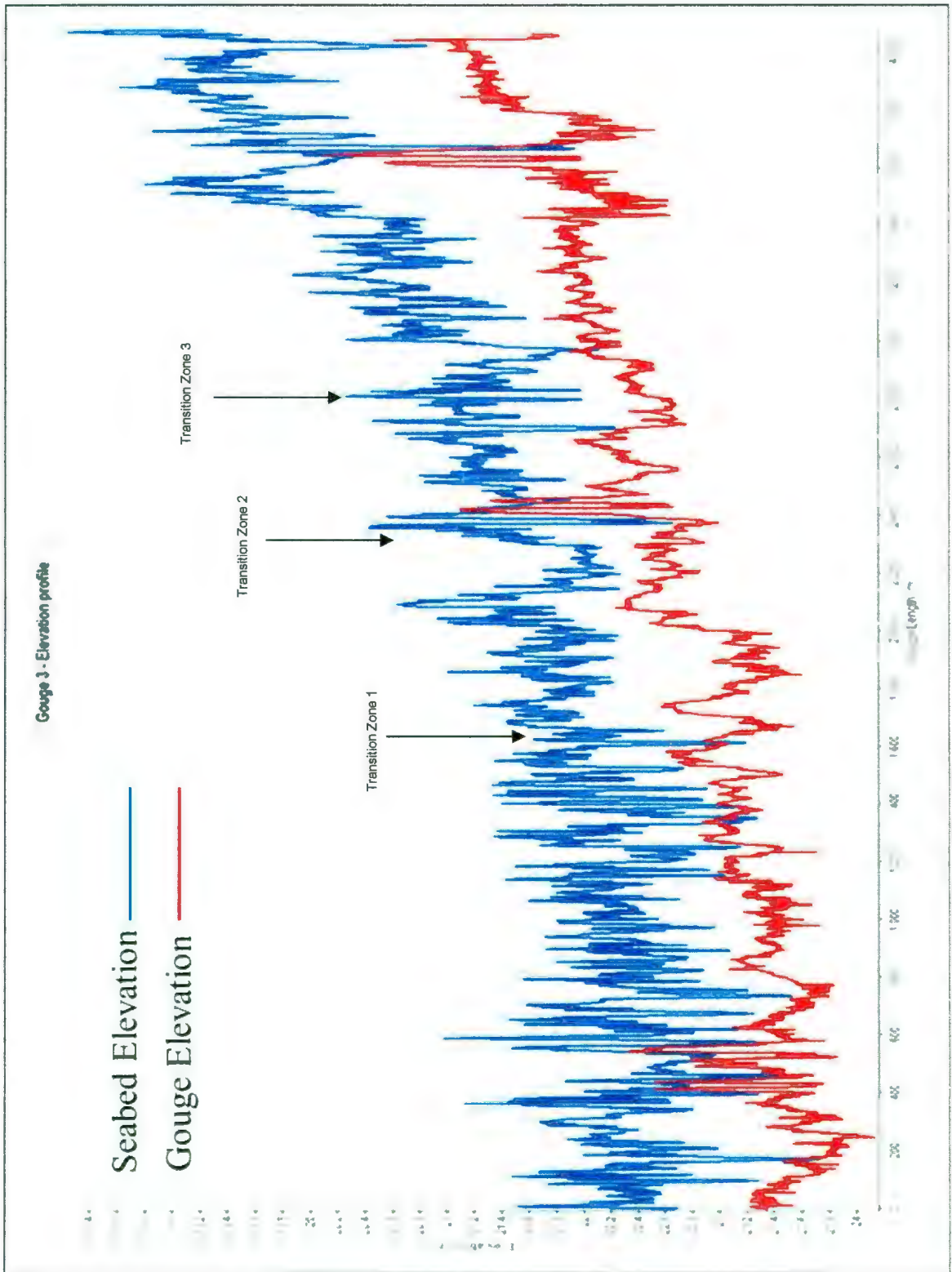


Figure 51: Gouge 3 - Elevation Profile

3.5.2 Gouge 3 - Transition Zone 1

Transition Zone 1 was the first occurrence in the gouge path of a unique event. Based on the pattern of gouging as seen in Figure 52, the ice keel appears to be in the process of yawing. Profiles 1 to 3, taken through the transition, show similar keel finger elevations, but with a change of keel lateral staggering. The keel widths from profiles 1 to 3 are 30 m, 22 m, and 45 m, respectively. The gouge depth remains constant at approximately 2 m, despite the significant change in width. The rotation was completed in less than 100 m of gouge travel, and the transition process is observable. It is presumed that such movement may be due to interaction with other surficial ice structures.

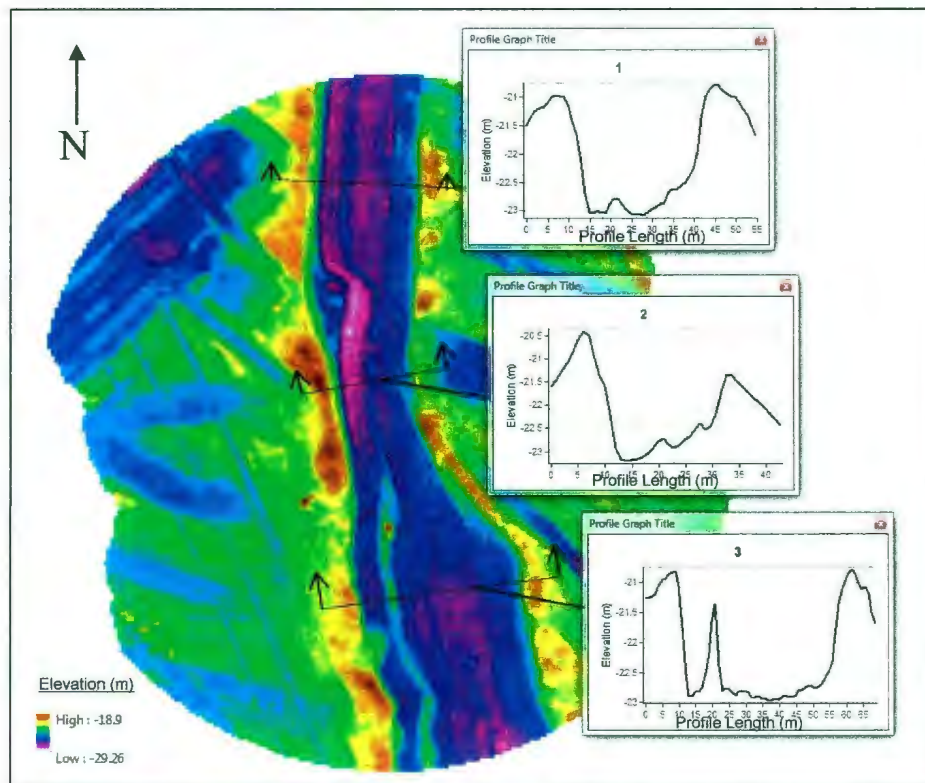


Figure 52: Gouge 3 - Transition Zone 1

3.5.3 Gouge 3 - Transition Zone 2

An overview of Transition Zone 2 can be seen in Figure 53. Transition Zone 2 has two distinct direction changes which can provide insight into the keel morphology. The first direction change contains a vertical rotation; the second is a near 90 degree direction change in which the keel doubles back on itself, resulting in a well-developed berm with presumably a relatively undisturbed impression.

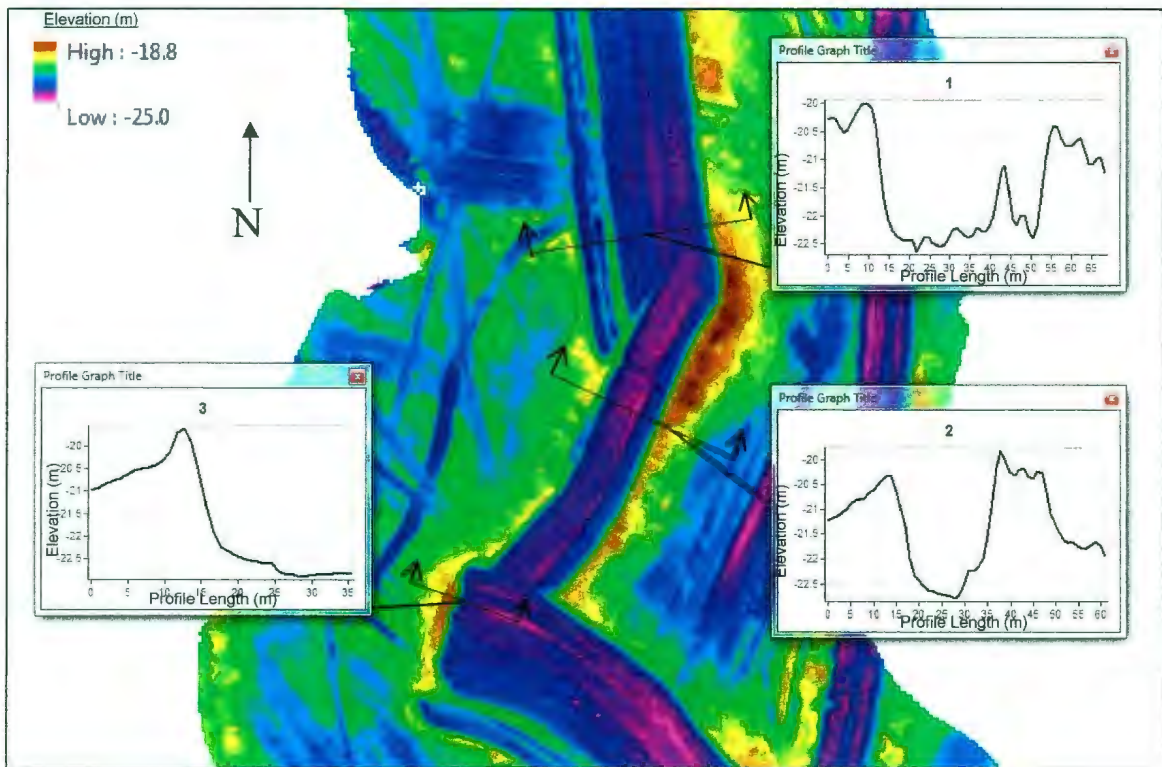


Figure 53: Gouge 3 - Transition Zone 2

Profiles 1, and 2, show that the width of the keel is 40 m before the direction change and 20 m immediately after. This implies that the keel has an approximate 2:1 ratio of width-to-thickness. Considering only the large keel, the width-to-depth ratio before the

direction change is approximately 15:1, but indistinguishable after. The West berm, from the second direction change, shows that the keel was rounded at the base, but had a relatively linear face; this can be seen in Profile 3, of Figure 53. A slope raster overlay of the west berm can be seen in Figure 54. The maximum slope angles range from 30 to 42 degrees, with an average of 36 degrees.

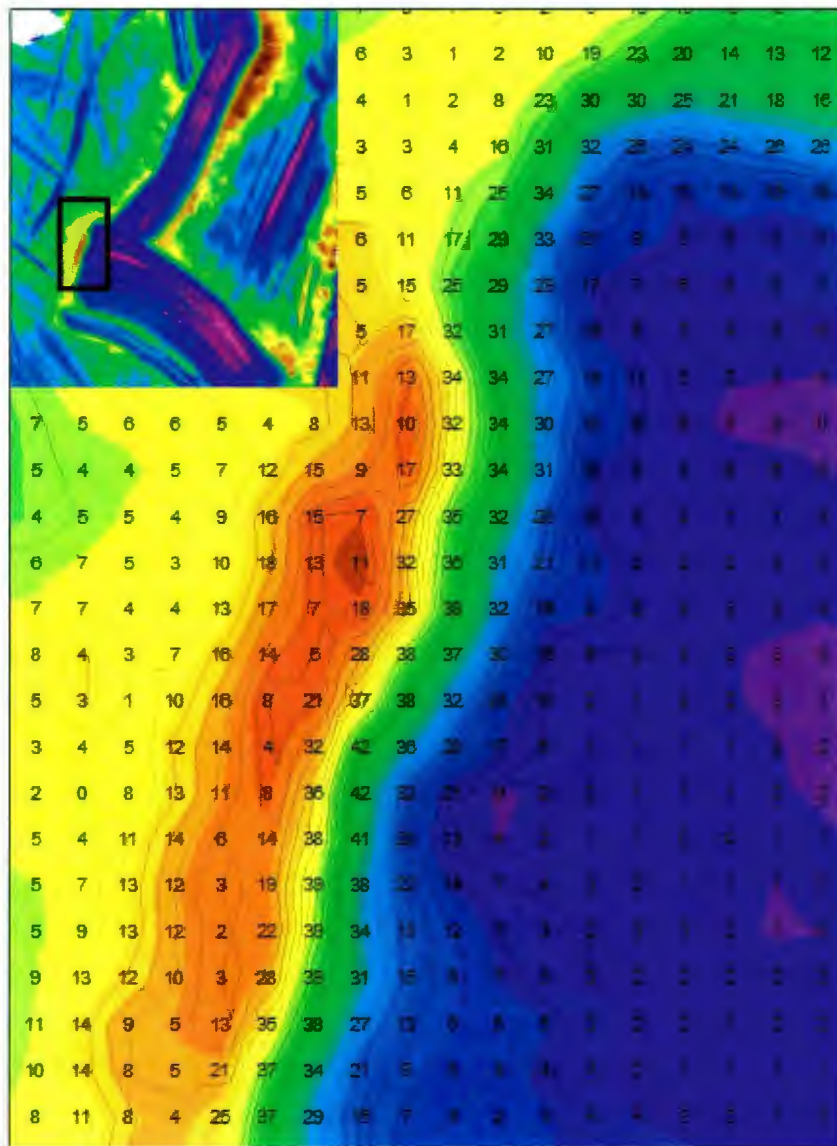


Figure 54: Gouge 3 - Transition Zone 2 - West Berm Slope Raster Overlay

3.5.4 Gouge 3 - Transition Zone 3

Transition Zone 3 occurs at approximately 2.8 km into the gouge path. An overview of the gouge area can be seen in Figure 56. The morphology of the gouge indicates that the keel performed a 90 degree rotation. This can be observed by the bottlenecks during the direction change, and by mirror opposite profiles taken before and after the direction change (Profiles “A-A” and “B-B”). After the direction change, there is evidence that the ice keel backtracked to the North before resuming gouging to the south; this movement results in a partial berm being created. The general morphology of the prow of the keel indicates that the keel has an elliptical type shape.

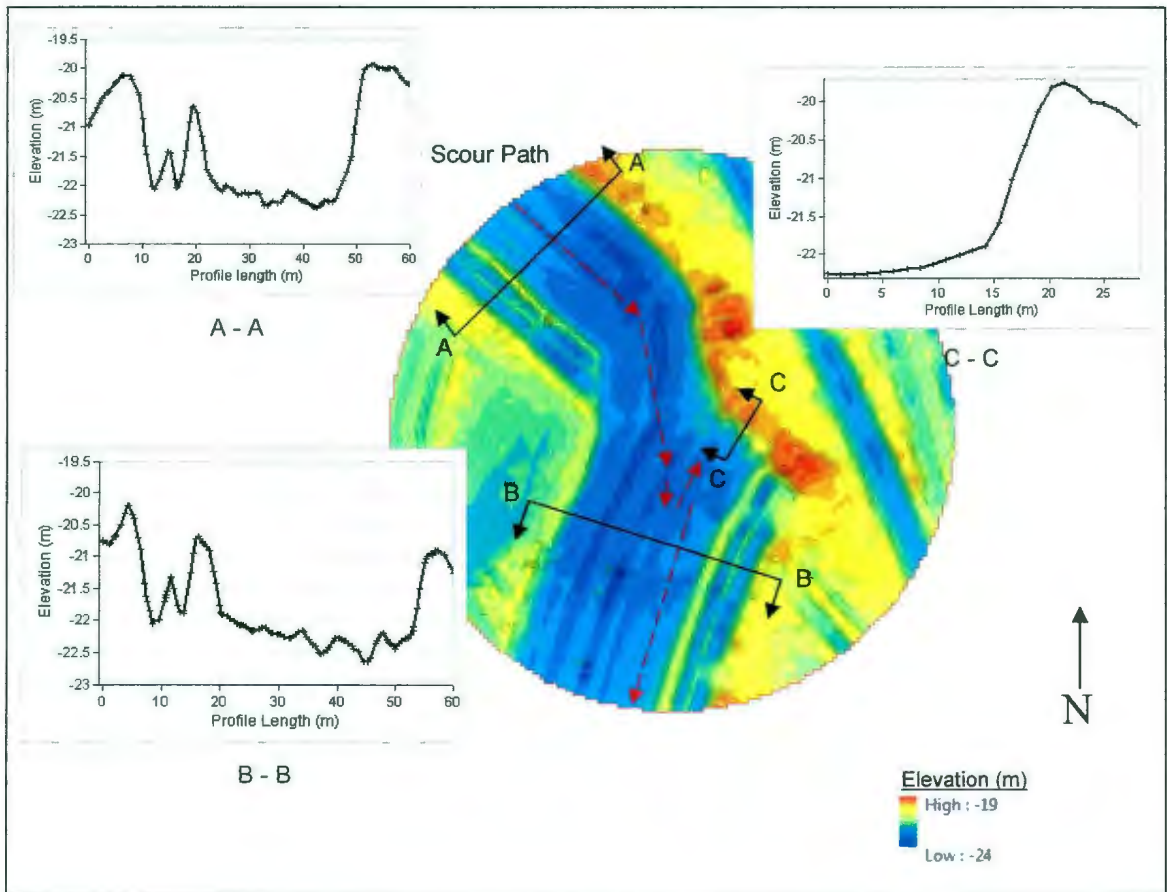


Figure 56: Gouge 3 - Transition Zone 3

Slope data for the partial berm can be seen in Figure 57. The maximum slope angle for the berm was 36 degrees. The average slope angle for the berm was approximately 30 degrees; this was very similar to the end berm in Figure 54, which had an average of 31 degrees.

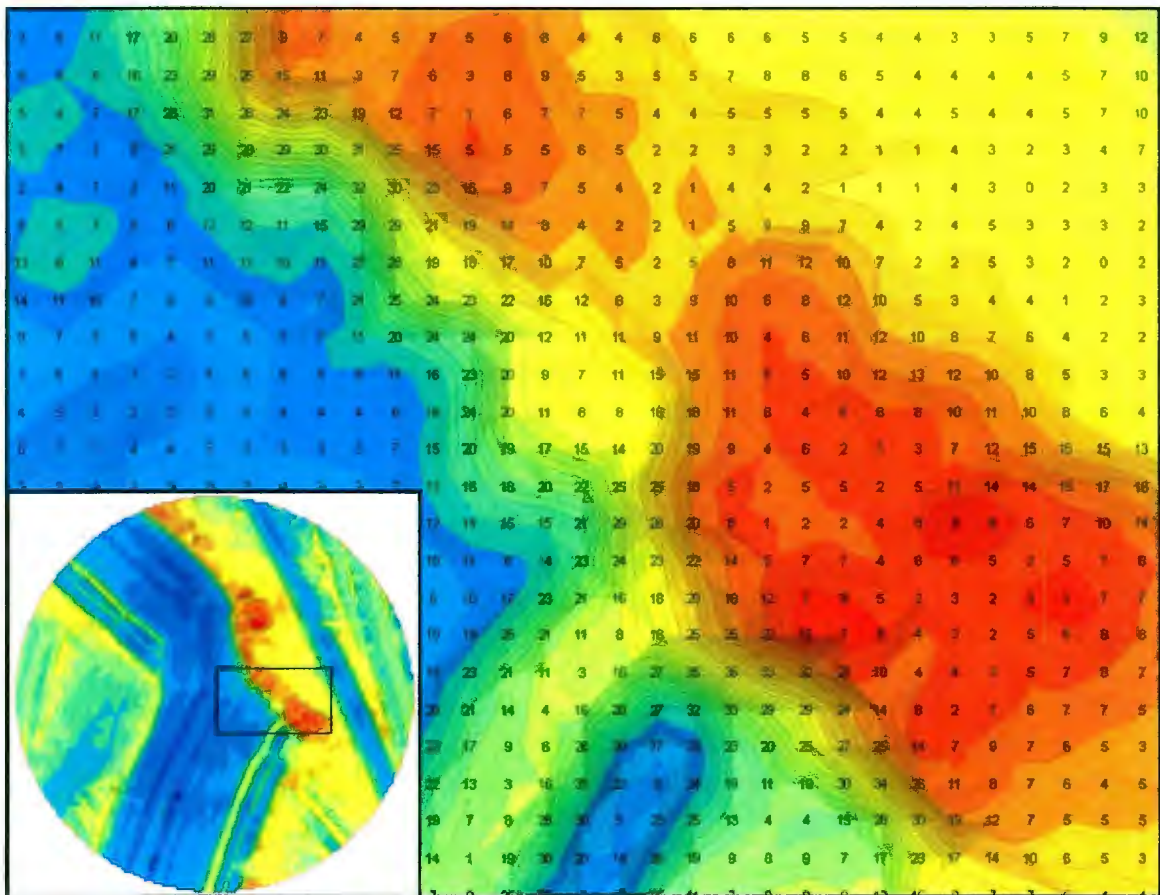


Figure 57: Gouge 3 – Transition Zone 3 – Slope Raster Overlay

3.5.5 Gouge 3 – Termination Point

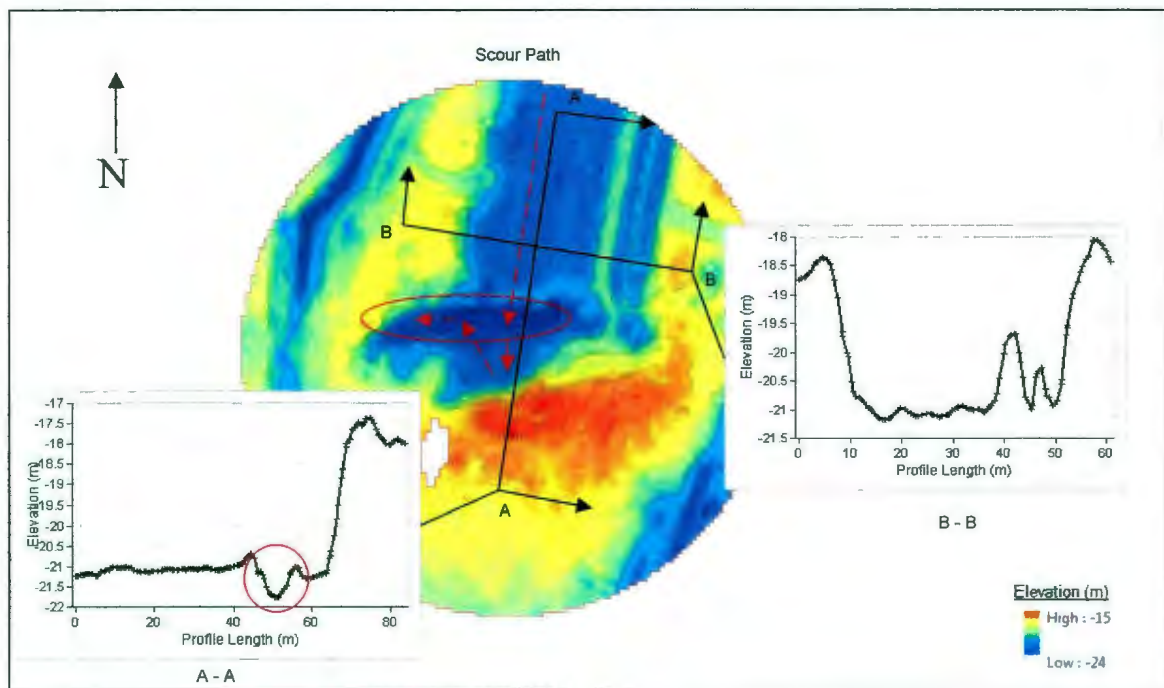


Figure 58: Gouge 3 - Termination

An overview of the gouge termination area can be seen in Figure 58 . The keel is known to have traveled in from the North. It is then presumed to have stopped, back tracked, and moved laterally approximately 10 m to the West, until it finally came to rest. Profile “B-B” taken before the gouge termination shows that no obvious morphological changes occurred to the keel since Transition Zone 3. There are two points of interest in the termination area. The first is a prominent South Berm, and the second is a relatively unique trough-like feature.

The South berm in the termination area is partially disturbed from an apparent Westerly drift; however, a section in the middle of the berm appears to be relatively unscathed and

3.6 Gouge 4 Study

3.6.1 Overview

The Gouge 4 study area can be seen in Figure 60, below. Gouge 4 occurred in the immediate vicinity of Gouge 3, and crosses the Gouge 3 path in two different locations (highlighted in red in). Much like Gouge 3, Gouge 4 shows very erratic movement, and as can be seen in Figure 61, maintains a constant gouge depth.

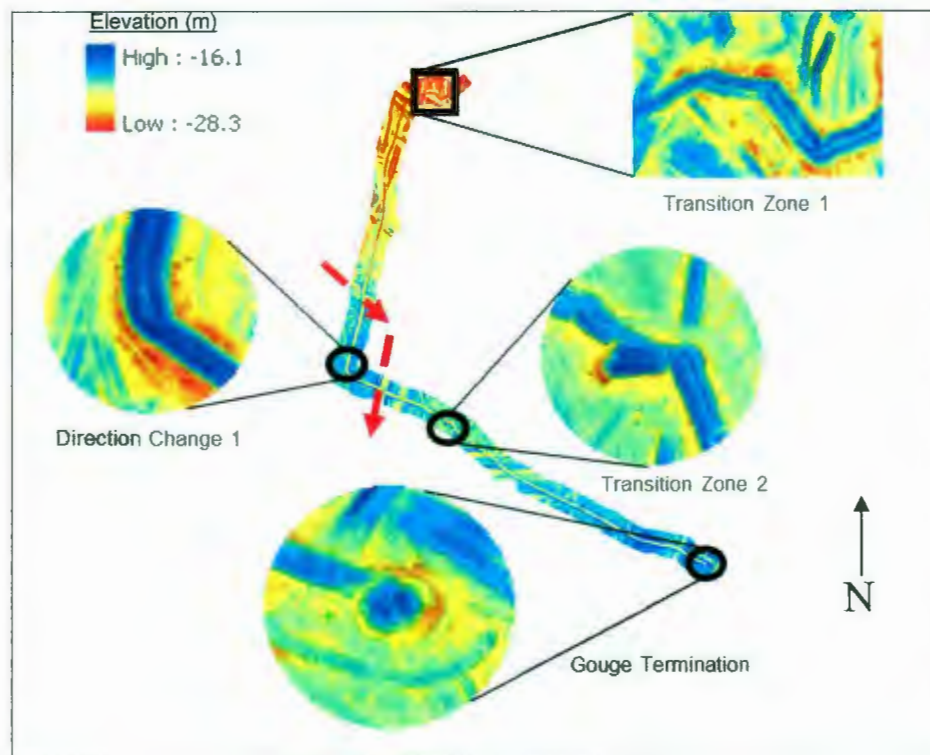


Figure 60: Gouge 4 - Study Area

Gouge 4 was created from a multi-finger ice keel. The observed length of the gouge is approximately 5 km. The maximum width of Gouge 4 is approximately 20 m. The maximum depth of this scour is approximately 2 m. The width-to-depth ratio for this scour varies from 7:1 to 15:1.

The elevation profile for Gouge 4, in Figure 61, shows that the gouge elevation rate occurs at approximately the same as the seabed slope; this indicates that the depth of gouge is relatively constant throughout the gouging process. Initially the rate change is approximately 7 % in elevation decrease. At the 2.2 km point there is a change in direction in which the keel begins to move into deeper water, but then gradually begins to move back into shallow water where the elevation is decreasing at a rate of approximately 3 %.

Gouge 4 contains four areas of interest: the first is a transition zone which occurs at approximately 200 m into the scour; the second is a direction change which occurs at approximately 2.2 km into the scour; the third is a transition zone which occurs at approximately 3 km into the scour, and the fourth event is the termination of the scour

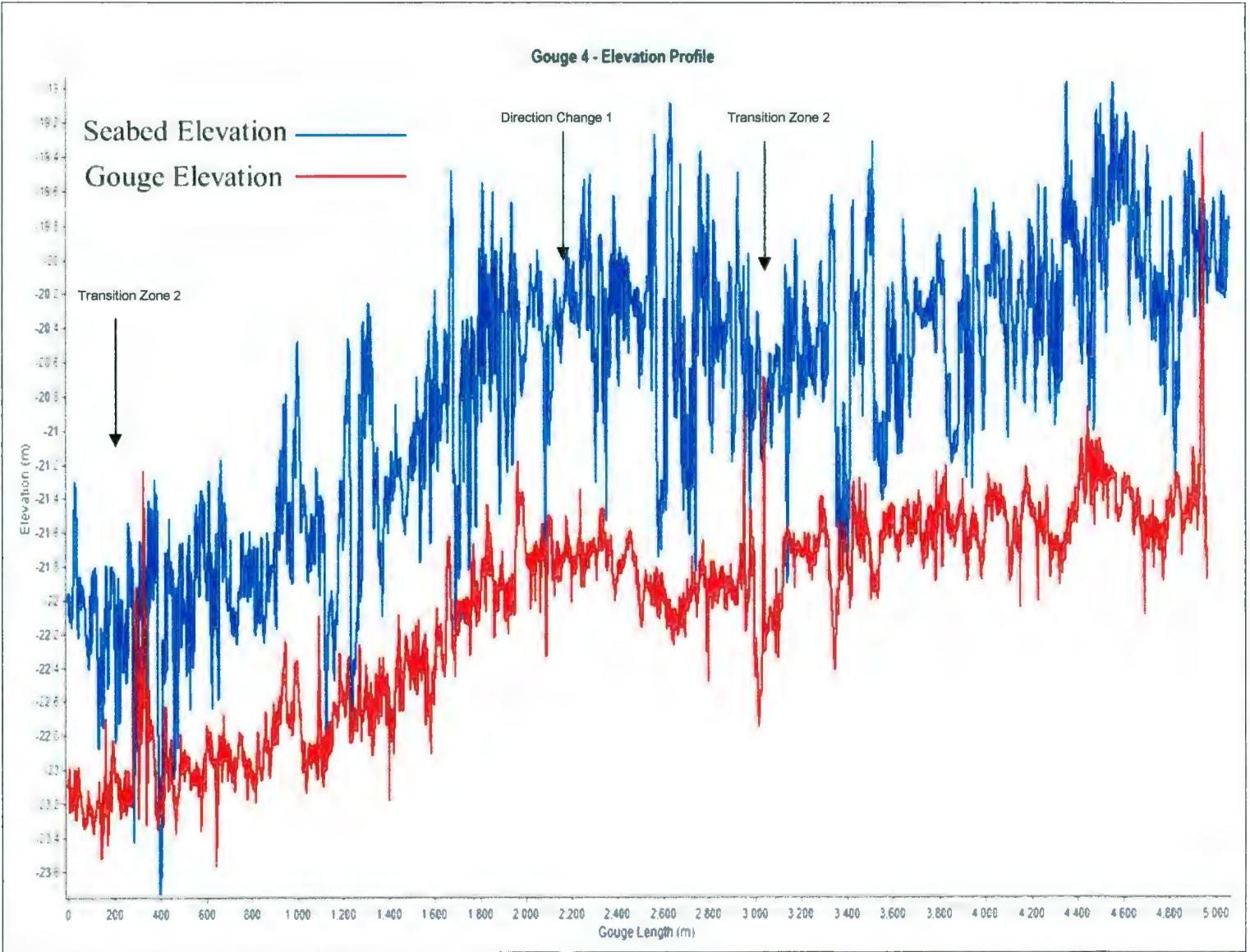


Figure 61: Gouge 4 - Elevation Profile

3.6.2 Gouge 4 - Transition Zone 1

Transition zone 1 occurs, at approximately 200 m; this area shows signs that the ice keel underwent numerous direction shifts, as well, there are indications that the ice keel underwent yawing. Figure 62 shows cross sectional data from the area. Based on these profiles it can be determined that the ice keel does not change its morphology. Variations in the keel dimensions indicate a slightly different orientation, which is characteristic of vertical rotation. The width of the gouge prior to entering the zone area is approximately 18 m. Upon leaving the area, the width is approximately 12 m. Based on the orientation of the keel it is presumed that the width-to-thickness of the ice keel is approximately 1.5:1.

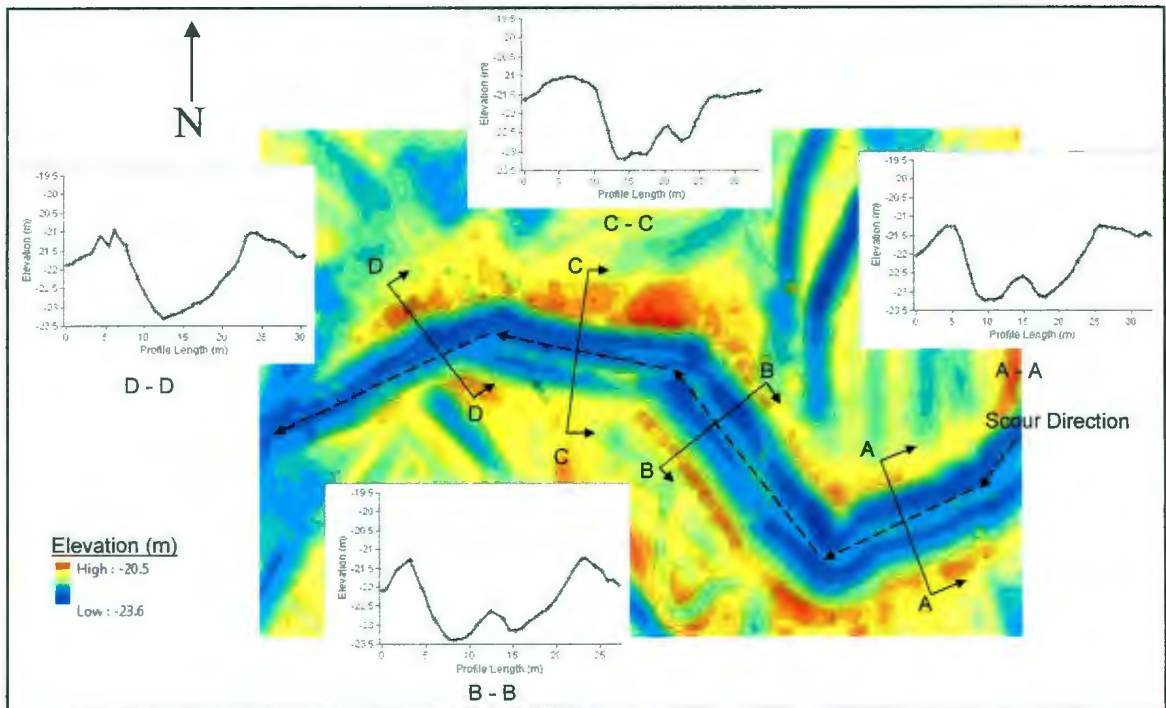


Figure 62: Gouge 4 - Transition Zone 1

3.6.3 Gouge 4 - Direction Change 1

Direction Change 1 occurs at approximately 2.2 km into the gouge path. The gouge is observed to have been travelling in from the North and then changing direction by approximately 45 degrees. The direction change was not sharp or abrupt, and thus a prominent berm was not created. An overview of the gouge area can be seen in Figure 63. Base on the morphology in the gouge path, it is presumed that the keel rotated vertically clockwise during the direction change. The width of the gouge prior to the direction change is approximately 20 m and approximately 12 m after the direction change. This indicates that the width-to-thickness of the ice keel is approximately 2:1. Cross section profiles taken before and after the direction change clearly shows the two keel fingers.

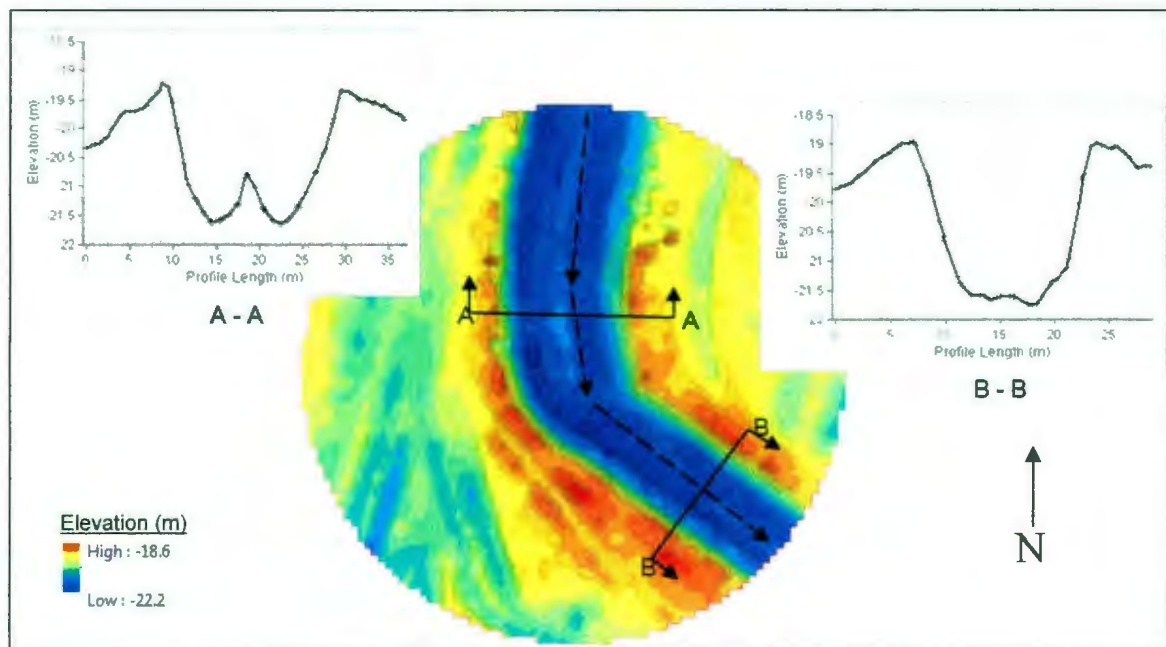


Figure 63: Gouge 4 - Direction Change 1

Width-to-depth ratios for the individual keels are relatively uncertain. Prior to the direction change it is estimated that the individual keels may be 10 m wide. After the direction change it is unclear, assuming total overlap a keel finger could be 15 m wide. This would give individual keel ratios of 5:1 before the direction change and 8:1 after.

Slope data for Direction Change 1 can be seen in Figure 64. The maximum side slope values on the West berm range from 30 to 42 degrees, while the East berm side slope ranges from 27 to 34 degrees. What is interesting to note is that the slope angles on the west and east berms are not equal to each other, and can vary up to 10 degrees. This is significant, because the two ice keel fingers are approximately the same size. A measurable difference in the side slope morphology of two approximately equal keels indicates that the side slope angles may be related to the morphology of the ice.

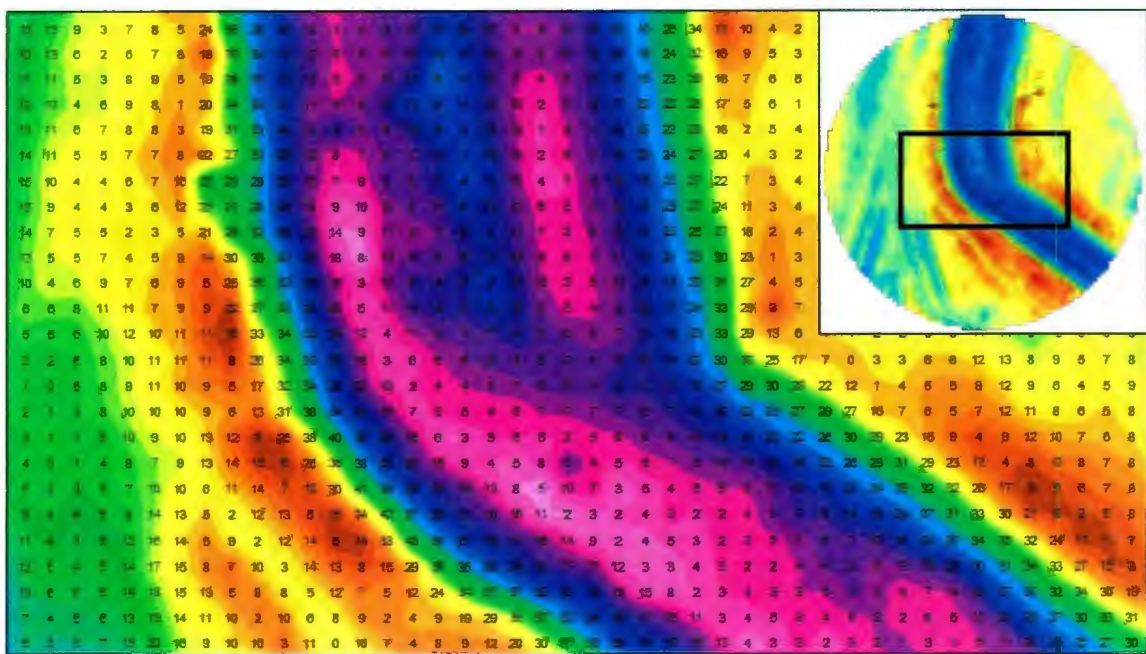


Figure 64: Gouge 4 - Direction Change 1 - Slope Raster Overlay

3.6.4 Gouge 4 - Transition Zone 2

An overview of Transition Zone 2 can be seen in Figure 65. This event occurs at approximately 3 km into the scour, and can be characterized as oscillatory. The shape of the scour prior to entering the area, and after, is nearly identical; this can be seen in cross section profiles “A-A” and “B-B”. This indicates that no significant morphological change occurred during the movement in the transition zone. The type of movement in this zone creates numerous berms. However, upon inspection the west berm (indicated by profile line “C-C”) appears to be free from rotation movement, and is likely to be the most representative.

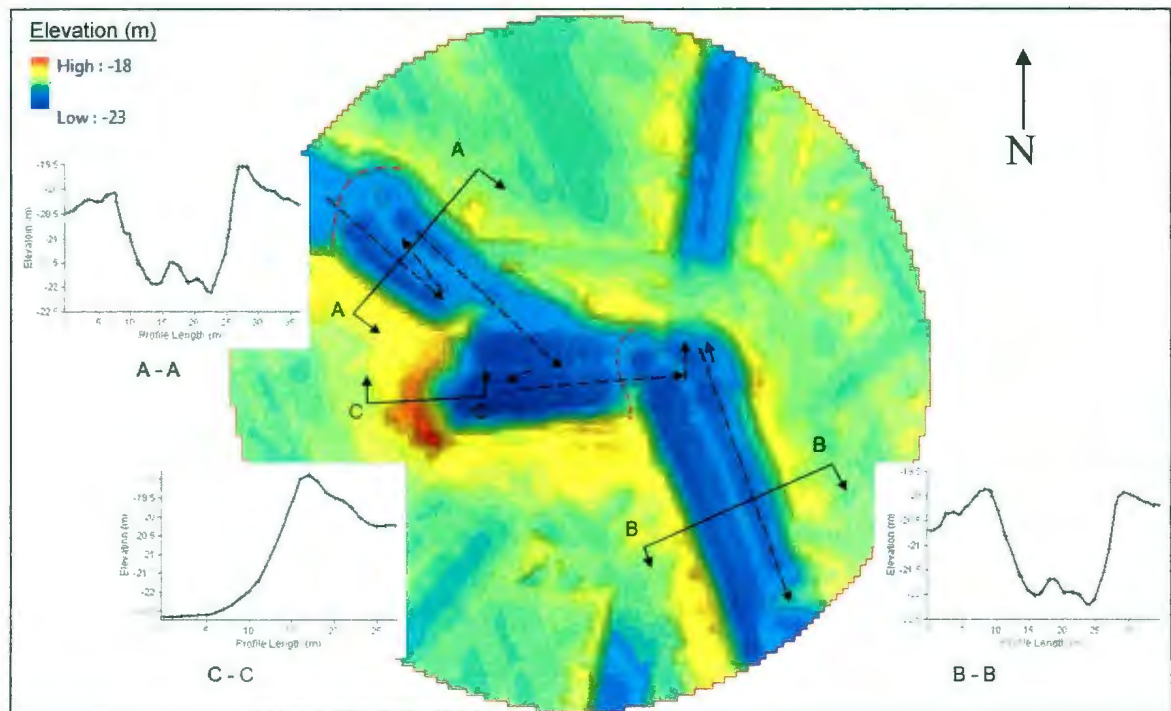


Figure 65: Gouge 4 - Transition Zone 2

From profile “C-C”, in Figure 65, it is observable that there is significant curvature along the bottom toe of the keel but, becomes relatively linear. The plan view in Figure 65 shows that there is significant convex curvature in the horizontal direction.

Slope data for Transition Zone 2 can be seen in Figure 66. The maximum slope angle observed in the west berm was 39 degrees, with an average of approximately 37 degrees. The rate of curvature of the keel prow changes from one to eight degrees per meter.

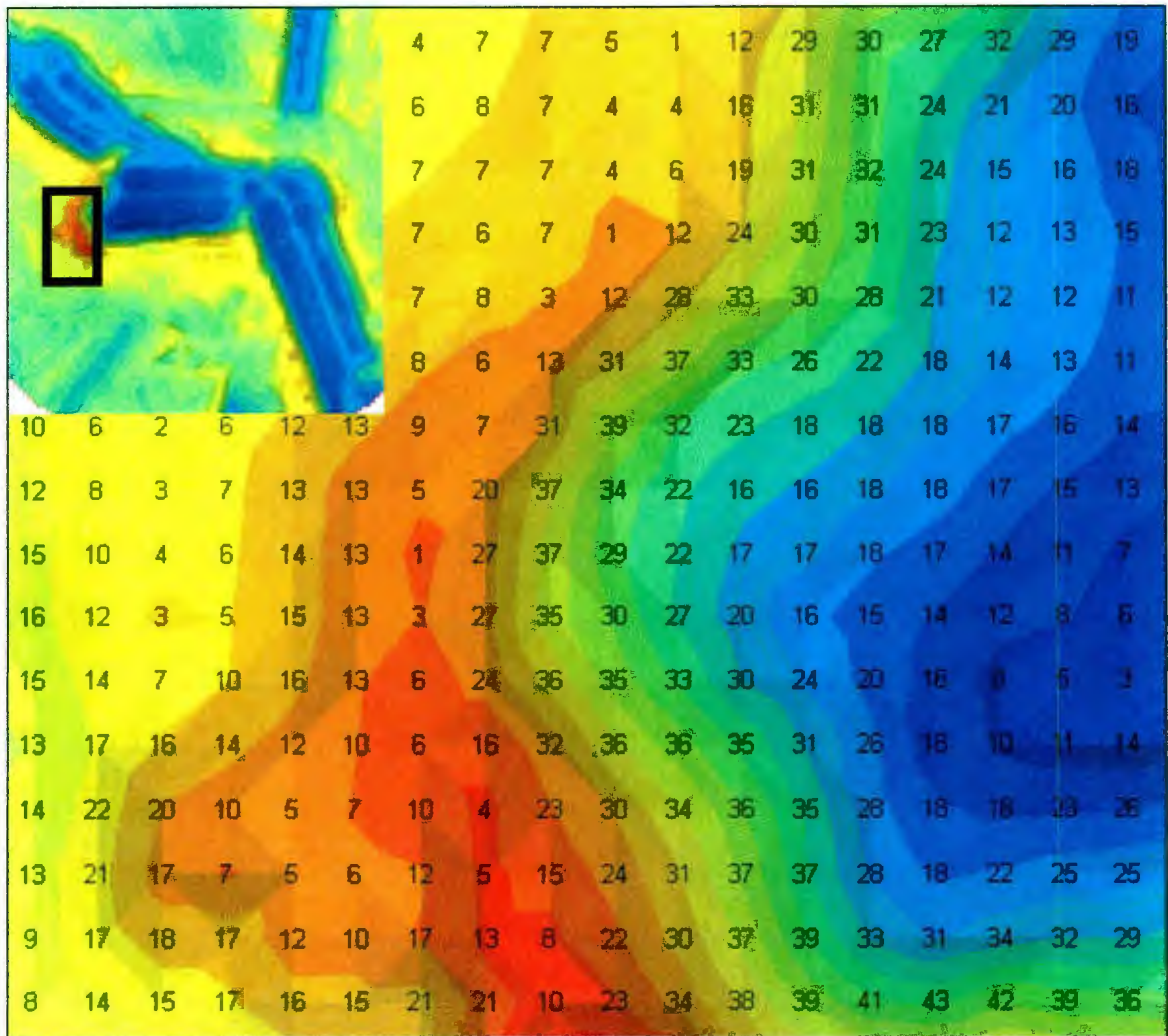


Figure 66: Gouge 4 - Transition Zone 2 - Slope Raster Overlay

3.6.5 Gouge 4 - Rotation Point

The termination of the gouge produces a very unique shape; this can be seen in Figure 67. Initially, the gouge appears to have come to an abrupt stop and descended vertically. Upon further inspection it was noticed that the dimensions appeared to be 1:1 width-to-thickness (20 m width), which is contradictive of previous observations in the gouge path. An adjacent gouge to the south was observed that appeared to mirror Gouge 4 (highlighted in red). It is believed that this keel may have been part of the same pressure ridge, however, is separated from the Gouge 4 keel by 32 m.

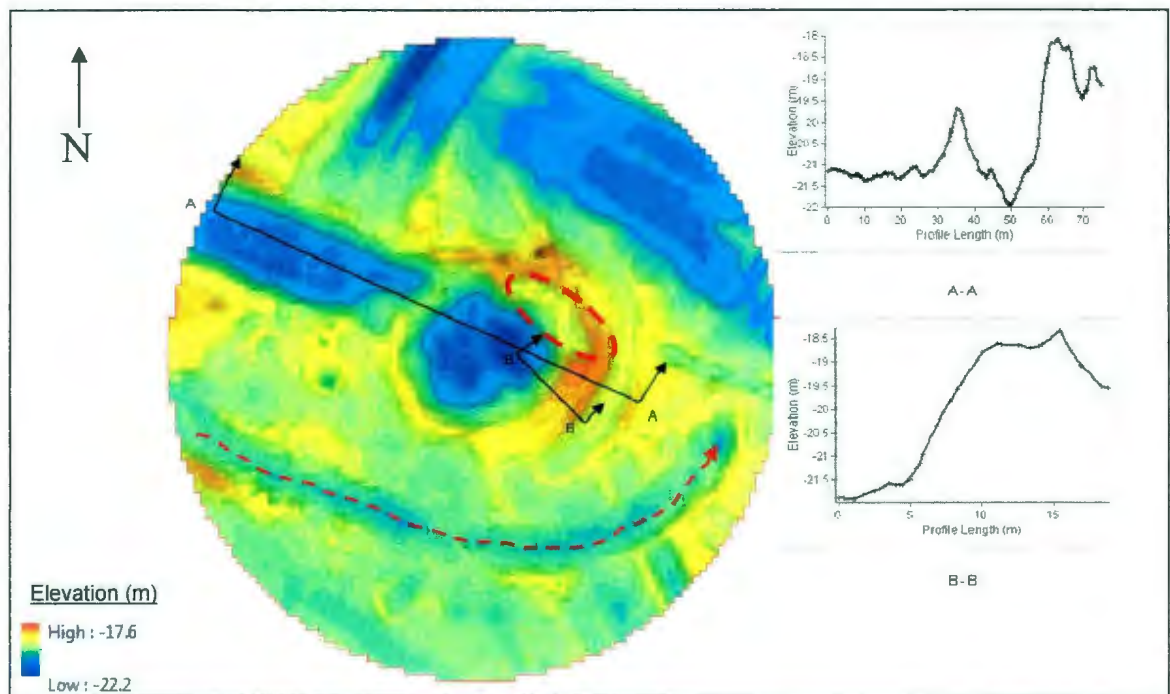


Figure 67: Gouge 4 - Termination

The movement of the South keel shows a counter clockwise rotation about Gouge 4, while the Gouge 4 keel remains in place; this would explain the approximate 1:1 ratio.

From profile “A-A” in Figure 67, it can be observed that the keel descends by approximately 0.6 m from the preceding gouge elevation; this was also the observation for Gouge 3. Initially it was unclear if the vertical drop was due to a decrease in water level, or from the vertical rotation. An unusual impression (denoted by a red circle) does not appear to be created from a circular rotation, but from a vertical descent. This indicates that the unusual impression was created after the rotation, and is likely due to a drop in elevation, possibly due to a significant tidal drop in the sea level.

3.7 Gouge 5 Study

3.7.1 Overview

An overview of the Gouge 5 dataset can be seen in Figure 68, below. There are two points of interest in the gouge dataset; the first is the inception of the gouge; the second is a direction change (at 2.5 km into the gouge), in which the keel back tracks.

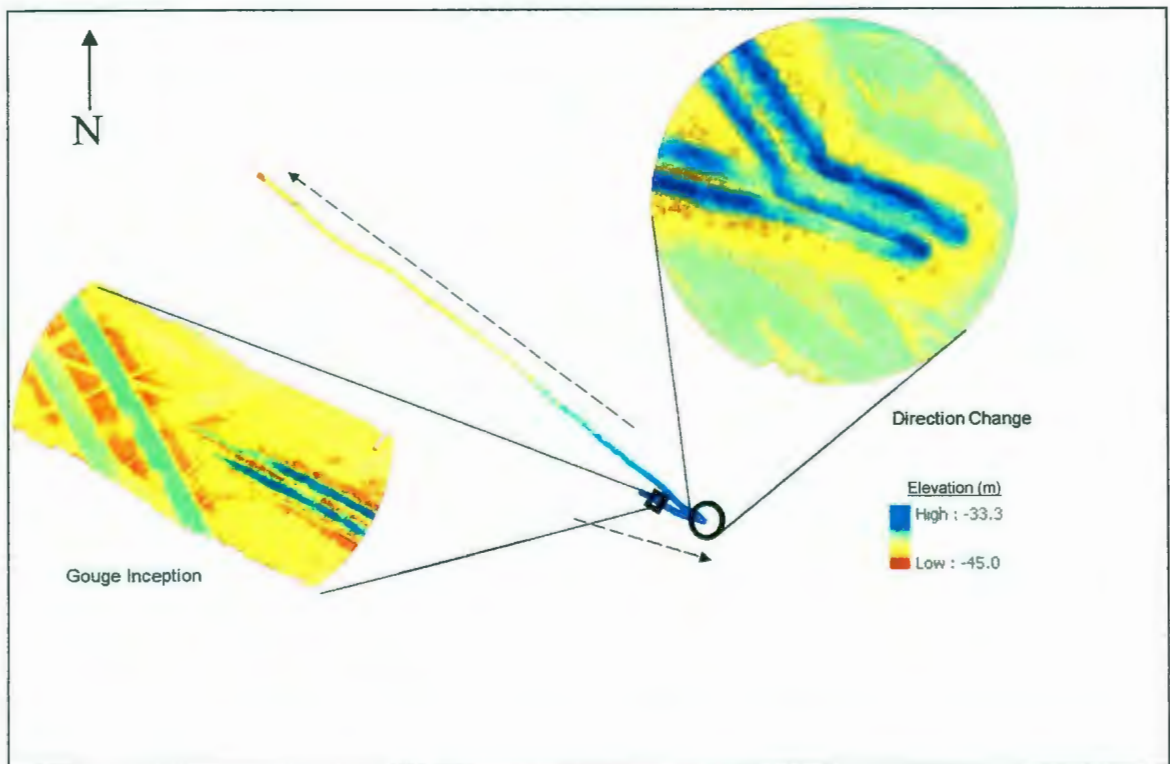


Figure 68: Gouge 5 - Overview

Gouge 5 begins gouging on a Northwest to Southeast trajectory; it then comes to an abrupt stop and begins to backtrack at nearly the opposite trajectory. The elevation profile of Gouge 5 is very unique; this gouge descends vertically up to 4 m in a travel distance of only a few hundred meters. Once it achieves maximum depth, the gouge

profile remains constant; the gouge path appears to develop contradictive to expectations. The Gouge elevation profile for Gouge 5 can be seen in Figure 69. The total length of the gouge was in excess of 23 km; the profile in Figure 69 was stopped at approximately 18.5 km due to the disappearance of keel 2, and the relative indiscernibility of the gouge elevation from the relative seabed elevation.

The maximum width of Gouge 5 is approximately 55 m, however, the depth is more difficult to ascertain. The maximum depth appears to be approximately 4 m to 4.5 m but, due to the staggering of the keels, it is estimated that the deepest point may be 5.5 m to 6 m. This would make Gouge 5, one of the deepest gouges observed in the Beaufort Sea.

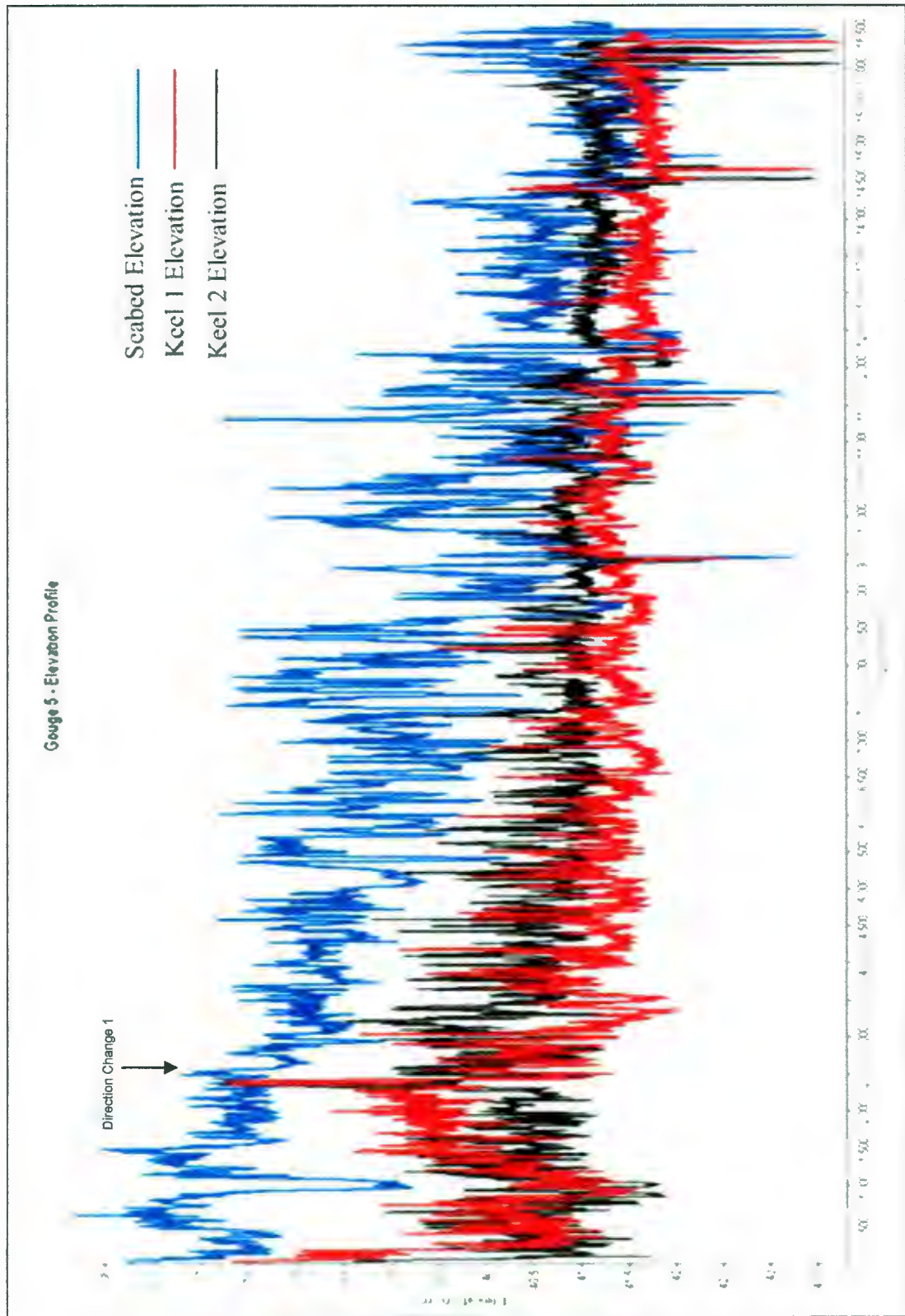


Figure 69: Gouge 5 - Elevation Profile

3.7.2 Gouge 5 - Inception

Gouge 5 is a gouge which contradicts the expected behavior of the gouge process. From the moment it first touches down on the seabed it travels approximately 200 hundred meters before obtaining an observable gouge depth of approximately 4 m. The actual gouge depth is believed to be greater than 4m. The true gouge depth appears to be hidden by the order of gouging. An overview of the gouge inception area can be found in Figure 70.

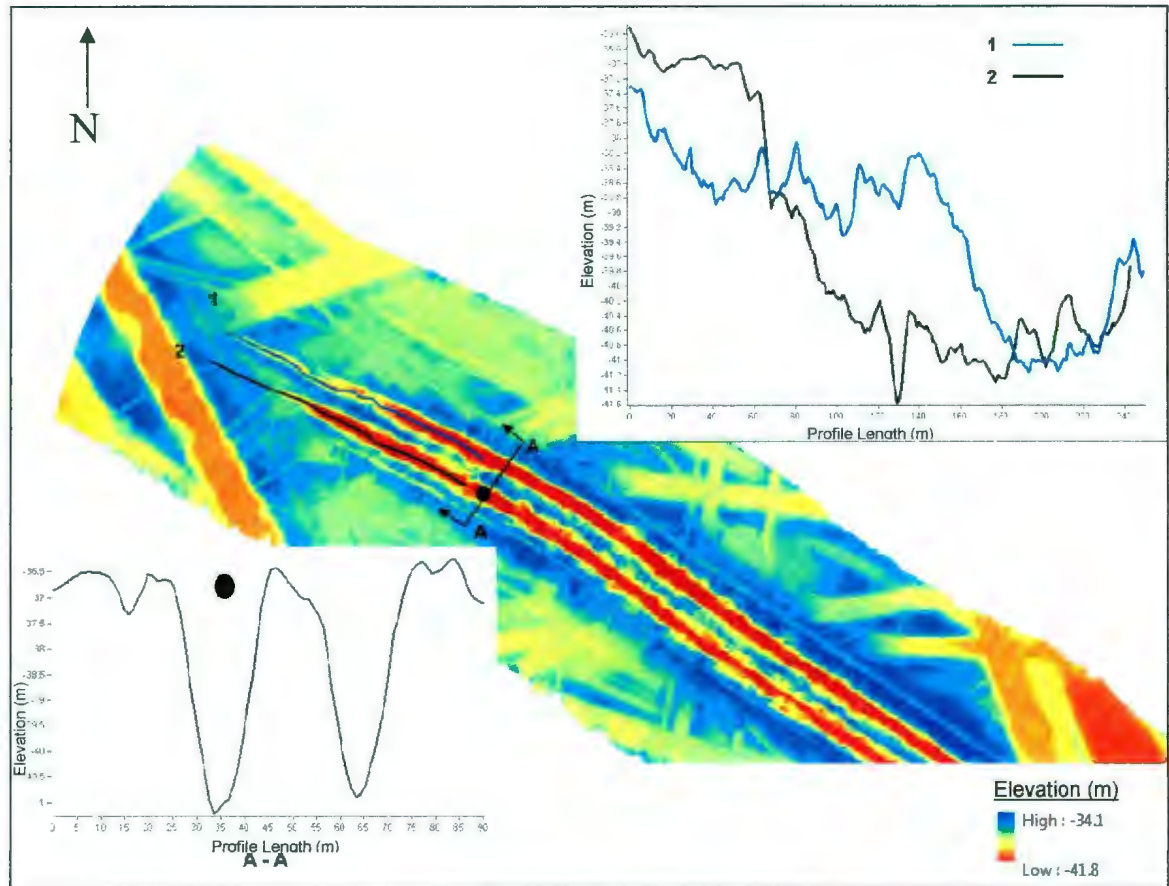


Figure 70: Gouge 5 - Inception Area

Two profile lines line (“1” and “2” in Figure 70) show the elevation of each of the keels of Gouge 5. Keel 1 can be seen to start gouging first, the relative elevation difference between keel 1 and keel 2 is approximately 1 m to 1.8 m before keel 2 begins to actually gouge. As keel 2 begins to gouge it can be noticed that keel 2 overtakes keel 1 as the deepest point in the gouge, despite keel 1 initially being deeper than keel 2. Profile “A-A” also illustrates how keel 2, appears to be deeper and wider than keel 1.

The width-to-depth ratio of the gouge in the early stages is approximately 12:1; if it is considered that the true depth of the gouge is actually closer to 5.8 m, then the ratio becomes approximately 10:1. If only keel 2 is considered (as keel 1 may have been influenced by keel 2), then the individual keel width-to-depth ratio is approximately 5:1.

3.7.3 Gouge 5 - Direction Change

An overview of the direction change area can be seen in Figure 71. Based on morphological evidence in the direction change it is known that keel 1 is actually leading in the order of gouge. It is likely that the profile for keel 1 is being strongly influenced by the follow on action of keel 2. Initially, it was presumed that keel 1 may have been altered during the gouging process, yet, the elevation profile in Figure 69, shows that after the direction change (at approximately 2.5 km) the elevation profile shows a switch, during which keel 1 becomes the deeper point by approximately 0.5 m to 0.8 m. Profiles taken before and after the direction change (“A-A” and “D-D”) clearly shows that the once deeper profile becomes the shallower profile (black dot used to identify keel).

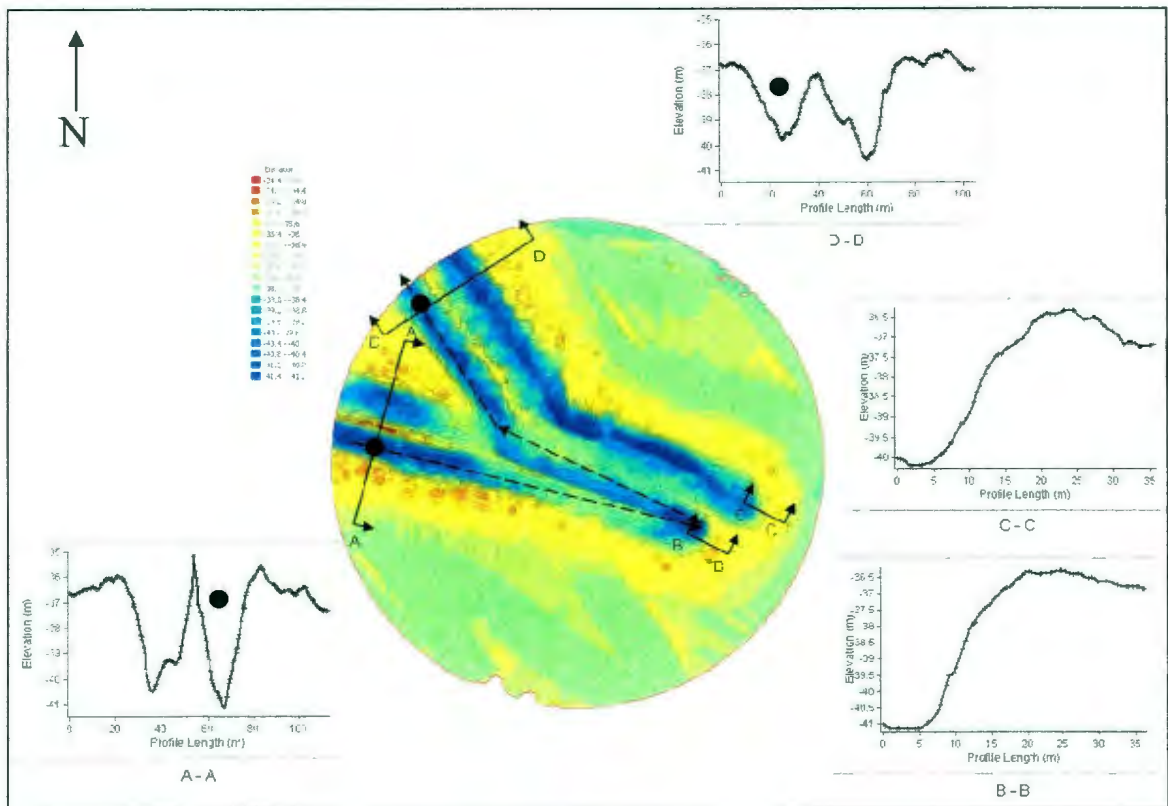


Figure 71: Gouge 5 - Direction Change

Profiles “B-B” and “C-C”, in Figure 71, show that the keels have a curved toe but, after the initial curvature, has a relatively linear slope. There does appear to be a slight step like appearance, which may be a result of the individual ice blocks of the keel.

It can be noticed that, despite being ahead by approximately 25 m, and eventually becoming the lagging keel, the gouge profile of keel 1 (“C-C”) is not deeper than the profile for keel 2 (“B-B”). It is unclear why the gouge profile does not indicate at the end berm that the keel 1 gouge profile is deeper than the keel 2 profile. It may be possible that the gouge was in-filled due to slope failure along the middle berm.

The trajectory after the direction change was at an approximately 45 degree angle to the initial direction, however, the keel appears to have the same gouge signature similar to that observed before the direction change. The width-to-depth ratio immediately after the direction change, for the overall structure, is approximately 12:1. For the deeper individual keel (keel 1), the width-to-depth ratio is approximately 8:1. Shortly after, the direction gradually changes back to the same trajectory as before the direction change. The overall width-to-depth ratio changes back to approximately 10:1 for the entire gouge, and 5:1 for the individual gouge. This would indicate that keel 1 has approximately the same width-to-depth ratio as keel 2, even though they have different depths. Based on the gouge being relatively new, this is either an indication of a common morphology of ice structures, or possibly related to soil characteristics.

Slope data for the direction change can be seen in Figure 72. The average slope angle for the keel 2 was approximately 28 degrees, with a maximum observed angle of 36 degrees. The average slope angle for keel 1 was approximately 22 degrees with a maximum of 25 degrees. As previously mentioned, it is likely that the morphology for keel 1 was influenced by the keel 2 gouge path, which would explain the much lower than normal slope angles for keel 1. Side slope data prior to, and after, the direction change varied considerably, ranging from 30 to 50 degrees. Compared to previous gouges, the slope angles in Gouge 5 were slightly lower.

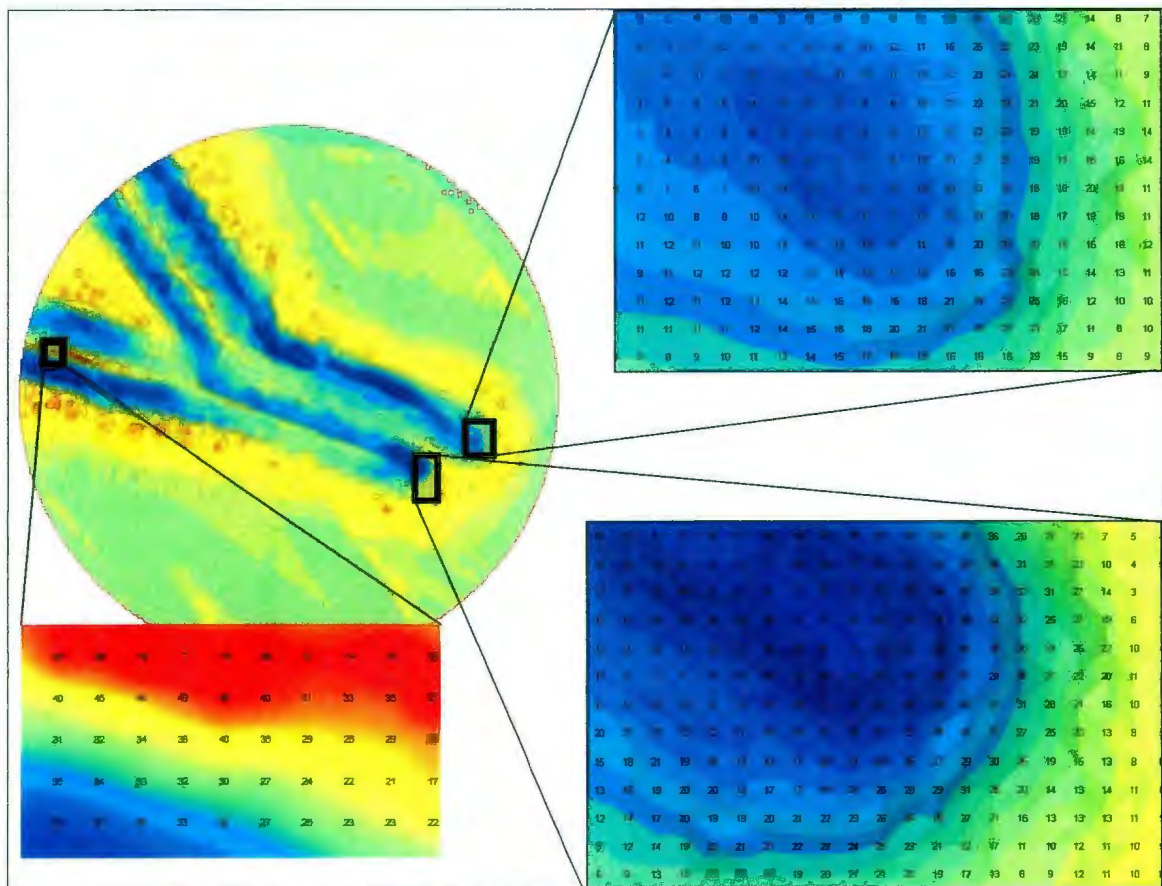


Figure 72: Gouge 5 - Direction Change with Slope Data

3.8 Gouge Study Summary

3.8.1 Gouge Behavior Summary

There were a number of factors that were assessed, relating to ice movement and behavior, in the preceding study. In no particular order the factors that were assessed are:

- a. Indications of sediment strength limiting the gouge depth;
- b. Indications of keel ablation during the gouging process;
- c. Indications of flexure of an ice sheet; and
- d. Indications of weather phenomenon linked to keel movement.

For Gouge 1, near the end of the gouge, there was a significant event in which the main keel abruptly jumped up by 0.5 m while a second keel became instantly deeper by 0.5 m. The larger ice keel finger keel did not appear to shear away, as the morphology appeared to remain consistent. The movement depicted in this event was characteristic of an upward vertical punching of a keel finger, in tandem with a downward drop of the surrounding ice structure. The fact that the elevation profile shows varying degrees of vertical rise in relation to the seabed does support the theory that there is a nonlinear elastic element to the vertical movement. These observations do appear to support the vertical flexure of an ice sheet. Even though the keel did not shear away, the significance of a vertical punch through does indicate that the soil can provide a higher vertical resistance than the strength of the keel, albeit at gouge depths of over 3 m. While not the only factor involved, Gouge 1 clearly demonstrates that gouge depth is a function of soil conditions.

In Gouge 2, the observation of the predominant keel finger being sheared away was an important observation. It was later discovered, through personal communication, that in the area there was a sand layer beneath the first few meters of clay. While it cannot be confirmed, it may be possible that this sand layer may have contributed to the destruction of the keel finger. It is important to note that while the gouge begins as a multi-fingered keel of varying keel elevations, after this event the keel fingers were all at approximately the same elevation. This may explain why some keels have nearly the same elevation in different keel fingers. The observations support both keel ablation, and how the presence of stronger sediments may result in shallower gouges in an area.

Gouge 3 and Gouge 4 both appear to be the result of a broken ridge system. The erratic movement appears more characteristic of a solitary ice structure, than of a massive ice ridge system. The even elevation of ice keels, along with the constant elevation profile, tends to support the theory that a keel system had broken apart and was scouring independently. In both Gouge 3 and Gouge 4, the termination mounds show a vertical drop of approximately 0.6 m. From evidence in Gouge 4, we see that this movement was most likely tidal related. Given that normal tides in the area of Gouge 3 and Gouge 4 are typically around 0.25 m (Huggett et. al., 1975), a drop of approximately 0.6m would strongly suggest that the water level was likely increased due to a strong wind event.

Gouge 5 is nearly a complete contradiction to conventional expectations of gouging. Unlike Gouge 1, which showed a slow build to maximum gouge depth, Gouge 5 achieved

a gouge depth over 4 m (probably around 5 m to 6 m) within a few hundred meters of gouging. Gouge 5 then maintains a constant elevation while gouging into progressively deeper water. This type of behavior contradicts the three-stages of gouging as proposed by Blasco *et al.* (2007), and by the ice sheet flexure proposed in this thesis. How the ice was able to descend in elevation so rapidly is puzzling. A drastic change in sea level may have been possible. For example, if there was a rapid 180 degree change in the wind direction, this would constitute a storm surge followed by a negative surge. It is not known if storm surges in the area of Gouge 5 would be able to create a total sea level change of 4 m.

Gouge 5 shows no obvious signs of keel ablation during the gouging process. Gouge 5 gives the impression that keels are much stronger than the sediment; even though the gouge starts only 10km northeast of Gouge 2, for which there was a clear example of a keel being sheared away. This does not mean that the soil conditions are exactly the same at Gouge site 2 and Gouge site 5, but does highlight the potential for soil variability over short distances. This would indicate the potential difficulty in correlating gouge depth with sediment strength on a larger scale.

An important observation noticed in Gouge 1, and to a greater degree in Gouge 5, was the influence of leading versus lagging keels on gouge morphology. The true depth of a gouge can be hidden. This could present a problem when trying to determine the maximum gouge depth, or even gouge depth probabilistic distribution of a region.

Keel ablation can occur during gouging; this was clearly seen in Gouge 1 and Gouge 2 when prominent keel fingers were either crushed or sheared away. Arguably, in the case of Gouge 3, and Gouge 4, the keels appear to have undergone significant ablation. In the case of Gouge 5, no ablation was noticed when gouging was most intensive; this may be due to sediment strength, the short time frame in which the gouging occurs, or a combination of both.

3.8.2 Gouge Morphology Summary

When evaluating the gouges in the preceding section, two main aspects of morphology were considered: the average attack angle and the general width (W), thickness (T), and depth (D) proportions. The reason for observing the average attack angle was to aid in the future development an idealized prismatic model, while the reason for observing the general proportions was primarily to develop a representative 3D model.

Two sets of observations were generated, one for the overall gouge, and one for the most discernible individual keel in the gouge. The reason for this was to ascertain the extent or existence of any relationship. A summary of the observations for the overall gouge and individual gouge can be seen in Table 4, and Table 5, respectively. The ratios observed in the tables below are approximate, rounded to the nearest whole number. The attack angle is rounded to the nearest degree.

Table 4: Overall Gouge Summary

Gouge	W: D	T: D	W:T	Attack Angle (Degree's)
1	13:1	7:1	2:1	30
2	20:1 - 10:1		-	33
3	22:1	10:1	2:1	36
4	15:1	8:1	2:1	37
5	12:1	10:1	1:1	28

Table 5: Individual Keel Summary

Gouge	W: D	T: D	W:T	Attack Angle (Degree's)
1	10:1	5:1	2:1	30
2	10:1		-	33
3	18:1	10:1	2:1	36
4	8:1	5:1	2:1	37
5	8:1	5:1	2:1	28

It can be noticed in the above tables that the width-to-thickness ratio in almost every observable case was approximately 2:1, not only for the overall gouge but also for the individual keel's.

The width-to-depth and thickness-to-depth ratios for the overall gouges varied considerably; the smallest ratios were observed in Gouge 1 and Gouge 5. The Gouge 2 width-to-depth ratio was approximately 10:1, prior to the deepest keel finger being sheared away and then approximately 20:1 after. The thickness (or possibly width) of Gouge 2 could not be confirmed, because of the unsure movement in the direction change. Gouge 3 was a multi-fingered keel, in which all the fingers were of relatively the same elevation, possibly from a broken ridge system. Gouge 4 was also a multi-fingered keel with two keels of nearly the exact same elevation. Gouge 4 also appeared to be from a broken ridge system. Gouge 5 was the only exception to the 2:1 width-to-thickness ratio; curiously, the individual keel did show an approximate 2:1 ratio. It may be that Gouge 5 was created from two independent keels closely spaced, similar to the W-shaped keels described by (Obert and Brown, 2011).

The width-to-depth and thickness-to-depth ratios of individual keels observed were much smaller and on average were 10:1 and 5:1, respectively. It must be noted that based on the data resolution and the smaller size of the individual keels, the ratios are subject to considerable variation. Smaller ratios have been observed, occasionally 4:1 and in Gouge 1 the smallest ratio was approximately 3:1; however, this occurred close to the point in which the vertical destruction of the keel was noticed.

Curvature in the horizontal direction for individual keels, in this study, did have an outward parabolic appearance. Curvature around the base of keels was observed in each case of the gouge study. After the initial curvature the slope profile did appear to become approximately linear vertically. Profile data of the impressions of the keels, in the direction changes, were reproduced in CAD software, and superimposed, to assess any commonality. The results indicate a reasonable similarity, as can be seen in Figure 73.

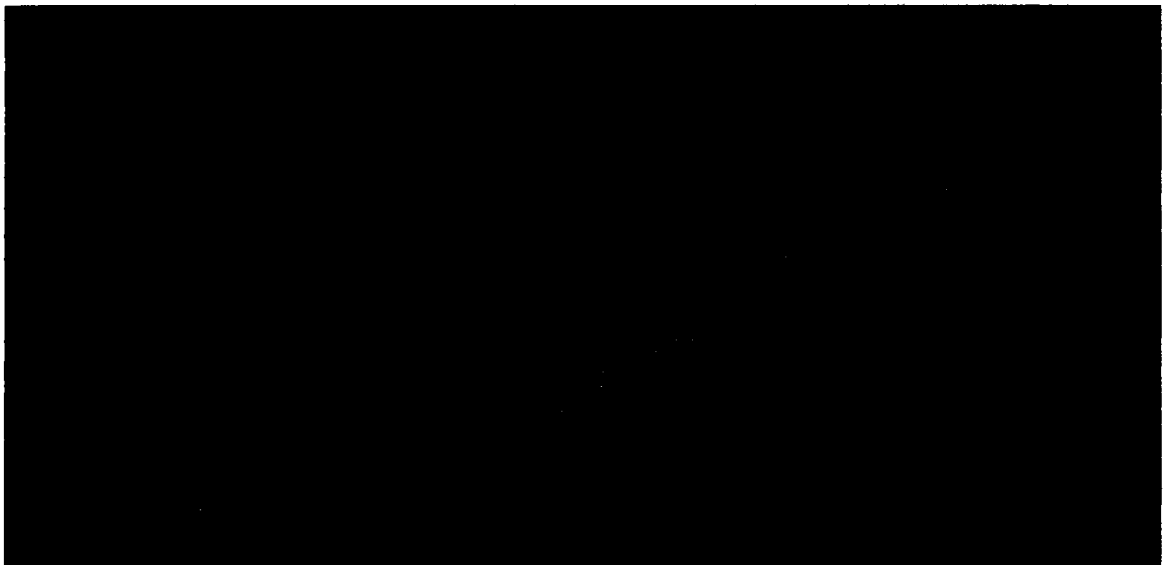


Figure 73: Superimposed Keel Curvature Profiles

From the Gouge morphology study it was observed that there was a general proportion to the gouges, and individual keel fingers. In the case of overall gouges, while there is a strong case for the 2:1 width-to-thickness ratio, the width-to-depth ratio can be affected by the keel ablation and gouge in-fill from keel staggering. The general proportions for individual keels tended to be a 2:1 width-to-thickness ratio, with a corresponding 10:1 and 5:1 width-to-depth and thickness-to-depth ratio, respectively. This is a fairly significant observation, as it indicates that a common 3D shape does appear in pressure ridge ice gouge morphology.

The above observations does support a common proportion theory. However, the observations are based on just five gouges. If this morphology is really that common, then these proportions should also be observable in an extreme gouge database.

4.0 EXTREME GOUGE CATALOGUE REVIEW

4.1 Introduction

To investigate the common morphological trends observed in the preceding gouge study, a study of the Beaufort Sea extreme gouge catalogue compiled by the Geological Survey of Canada, and Canadian Seabed Research Ltd., was undertaken.

The data evaluated comprised 43 extreme gouge entries from 2001, in Volume I of the extreme gouge catalogue (Orlando *et al.*, 2003), and 52 extreme gouge entries from 2004, in Volume II of the extreme gouge catalogue (Oickle *et al.*, 2006). The data consist of sub-bottom profile data and side scan sonar images with an approximate width and depth for each gouge. Each entry was visually inspected for classification as either a multi-keeled event or single-keel/multi-finger gouge. A plot of gouge depth versus gouge width was used to evaluate if there was a trend supporting the morphological observations found in the preceding bathymetric study.

In the preceding section, the common proportion theory was most noticeable in individual keel fingers and individual multi-fingered keels. Multi-keel gouges would not adhere to the common proportion theory as they are created by numerous individual keels spaced laterally within the same ridge system. If a common proportion theory is valid, then it should be easily observed in any plot of individual (multi-fingered) keels. The maximum and minimum observed ratios should serve as boundary lines with the observed Gouge depth to width ratio falling on, or in between the boundary lines.

4.2 Extreme Gouge Plot

A plot of the extreme gouge depth versus width of the extreme gouge catalogue entries can be seen in Figure 74, below. The single keels are highlighted in blue and the multi-keels are highlighted in red. Superimposed on the plot are lines that represent the 10:1 width-to-depth ratio (10 % line) and the 5:1 ratio (20 % line). There are 38 single-keel and 44 multi-keel events. 13 events could not be visually confirmed as either single-keel or multi-keel, and were omitted from the plot. There were six observations of single keel events having the exact same width and gouge depth. For presentation purposes there were 19 observations of multi-keels with widths greater than 100 m which were not included on plot.

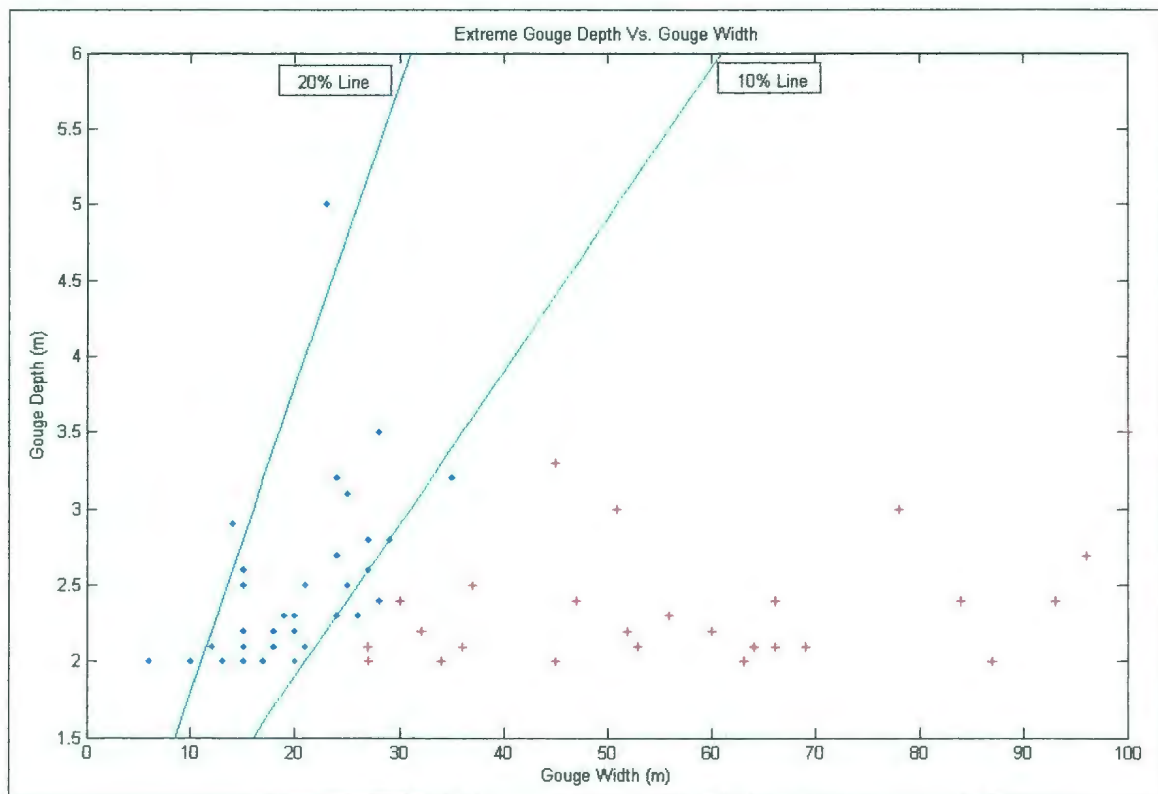


Figure 74: Extreme Gouge Depth versus Width

4.3 Discussion

As can be seen in Figure 74, there is strong correlation to support the morphological observations in the gouge study. The 10:1 ratio line (10 % line) and 5:1 ratio line (20 % line) appears to represent an approximate upper and lower bounds of the single keel events. Although many of the single keel observations fall close to either the 10:1 (10 % line) or 5:1 line (20 % line), there are many observations that fall in between. One explanation of observations in between the two ratios is of keels travelling obliquely. If the width of a keel projects a 10:1 ratio, and the thickness projects a 5:1 ratio, then as the keel begins to obliquely, by geometry, the projected width-to-depth ratio would have to vary between the largest and smallest ratio.

5.0 GOUGE MORPHOLOGY EXPERIMENT

5.1 Introduction

Given the abundance of data supporting the general gouge morphology common proportions theory, a practical experiment was conducted to determine if such an observation would be of any consequence in a gouge model experiment.

A complete gouge experiment was designed and built. This study was done as part of a graduate course requirement, and self-funded. All components of the experiment, including the gouge tank and keel models, were built by hand using commonly available materials. The intent of the experiment was primarily qualitative, and aimed at identifying if there was a significant difference between using a representative 3D keel model, and using an idealized prismatic wedge.

Instead of directly measuring the forces on each keel, a pipeline load cell was created. This was accomplished by attaching strain gauges to a 16 mm (outside diameter) PVC plastic pipe. An arbitrary cover of 2 m of soil (modeled depth) was placed over the pipe and model keels were dragged over the pipeline load cell at different gouge depths. A total of 22 tests were conducted in Beaufort Sea clay using the idealized and representative ice keel models. The following section describes the experiment design, setup, and the results obtained from the experimental gouge program.

5.2 Experiment Design and Setup

5.2.1 Model Ice Keel Design

The controlling factor in the design of the experiment was the scale. Since this experiment was to use commonly available materials the experiment scale was limited in this regard, in particular the size of the model ice keel. The model ice keel based on this thesis study has a 10:5:1 ratio (width/thickness/depth). For a 2 m deep ice keel, a width of 20 m would be required. In order to limit the size of a gouge tank, and soil requirements, a scale factor of 100 was used. The keel models thus have the dimensions of 20 cm: 10 cm: 2 cm (Width: Thickness: Depth). Each model keel was coated in polyurethane to protect it from water damage.

The idealized prismatic model (Figure 75) was made using a simple block of wood and a table saw. The attack angle used for the prismatic model was 30 degrees. This was three degrees less than the average angle suggested by the gouge morphology study, but was chosen due to ease of fabrication.



Figure 75: 30 Degree Prismatic Wedge Experiment Model

The representative 3D keel was fabricated based on the general observations of the gouge morphology study. As noted from the gouge morphology study, the faces of the keels appeared to be rounded in the horizontal plane, and can be described as elliptical. Using the 2:1 proportions, an ellipse was fitted to the overall dimensions of 20 cm to 10 cm. Due to the lack of precision fabrication equipment, the depth of the keel was created by vertically discretizing the elliptical shape into 0.2 cm steps (Figure 77). The model used in the experiments can be seen in Figure 76.



Figure 76: 3D Representative Model Keel

The horizontal curvature of the keel was effectively captured by fitting the elliptical shape to the keel proportions. The curvature of the toe of the keel was less accurate due to the large discretized steps in the keel. The approximation was still a relatively good fit to the keel profiles, as can be seen in Figure 78.

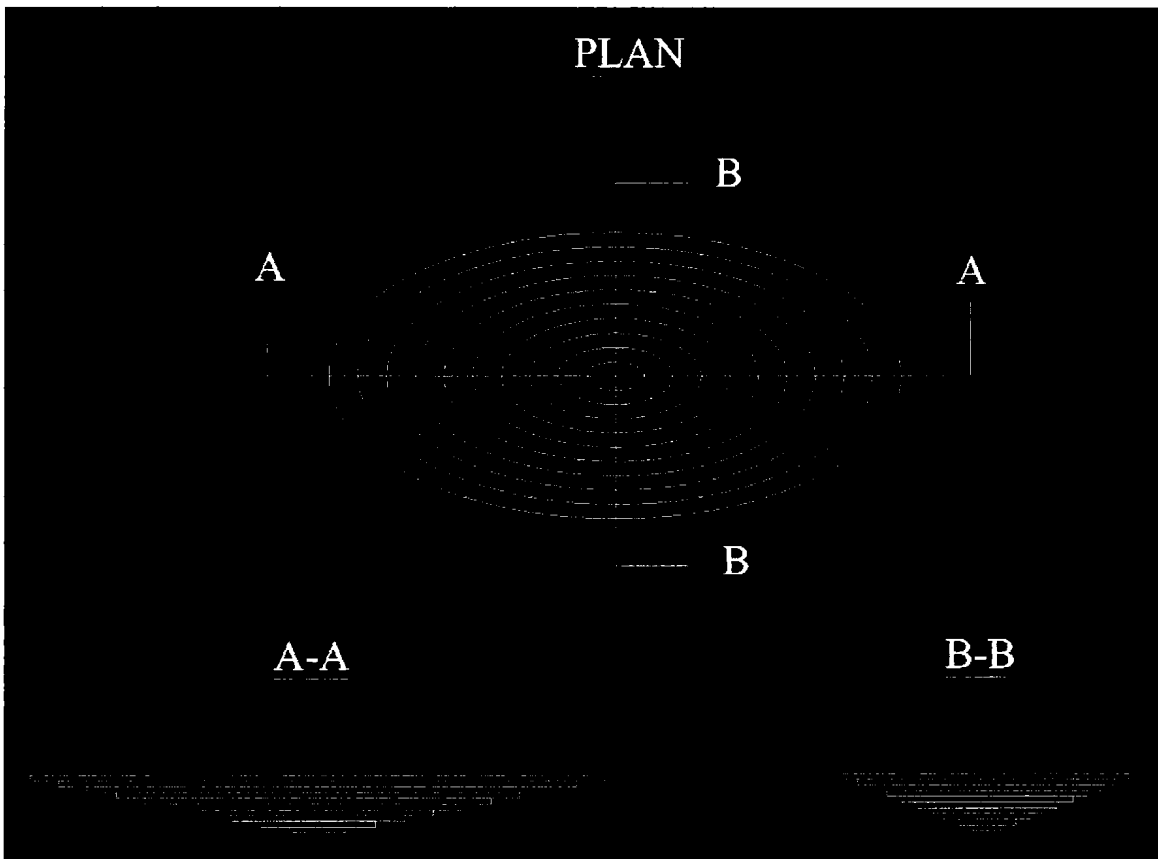


Figure 77: Design of Representative Keel

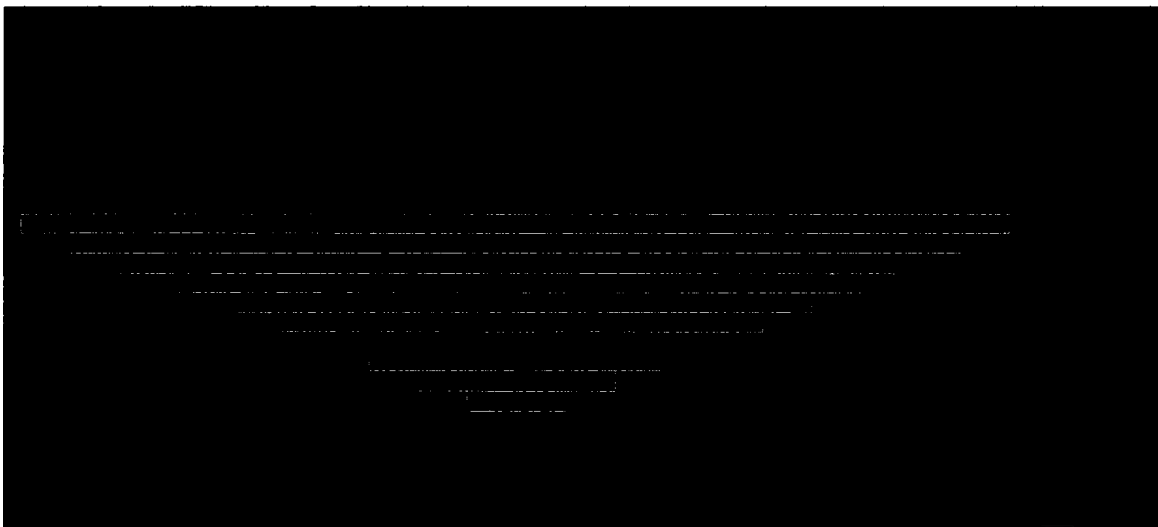


Figure 78: Comparison of Discretization to Gouge Profiles at turning point and termination berms.

5.2.2 The Gouge Tank and Test Bed

The Gouge Tank was designed and constructed from 12.5 mm thick plywood. The box was framed with 4"x4" timber for mechanical support. The overall length of the box was approximately 120 cm long by 62.5 cm wide by 62.5 cm deep. Figure 79, shows the empty gouge tank with pipeline load cell within.

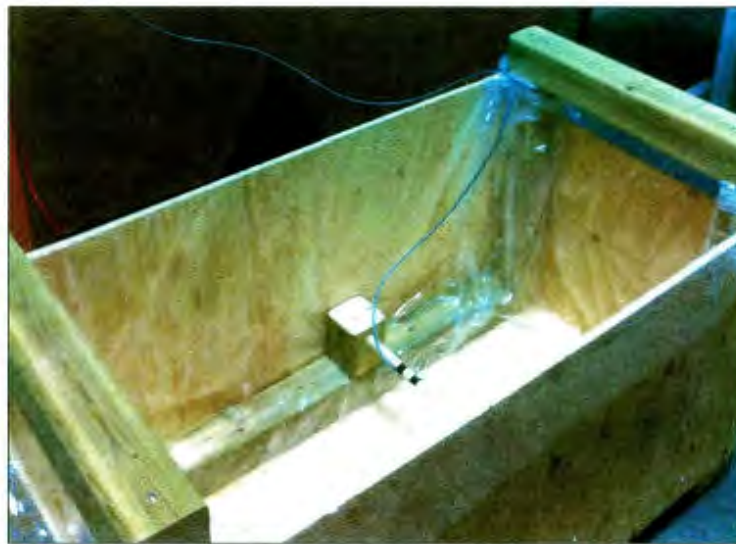


Figure 79: Experimental Tank

The soil test bed that was used in the experiments was Beaufort Sea clay, which was obtained from cores provided by British Petroleum. The clay was taken from various locations on the Beaufort Sea Shelf and upper slope. The sediment had an undrained shear strength of 3-5 kPa, which is representative of Holocene clay that is typically found in the top 1-2 m of seabed sediment. Due to initial very low shear strength, there was not a significant reduction in shear strength due to disturbance. The soil test bed was not consolidated between tests, as the undrained shear strength remained relatively constant between successive tests.

5.2.3 Drive and Drive Assembly

For ease of use, a multi-purpose electrical winch was used to pull the model keels through the test bed of clay. This winch was powered using a 12 V marine battery. The speed of the winch was not adjustable and was approximately 3 cm/s. This speed is not considered to be representative of actual conditions; however, this is of no consequence as the purpose of the experiment was to compare the loads from two model keel shapes.

The components of the movement assembly are: The track, made from simple 4"x4" timber; the guide rails, made from aluminum L-Beams; and the trolley, which was created from a heavy duty steel appliance roller set, fastened to a wood board, with a threaded rod extending down for attachment to the keel model. Lead weights were placed on the wood board to provide the downward force necessary to provide a constant gouge depth. The final design of gouge experiment can be seen in Figure 80.

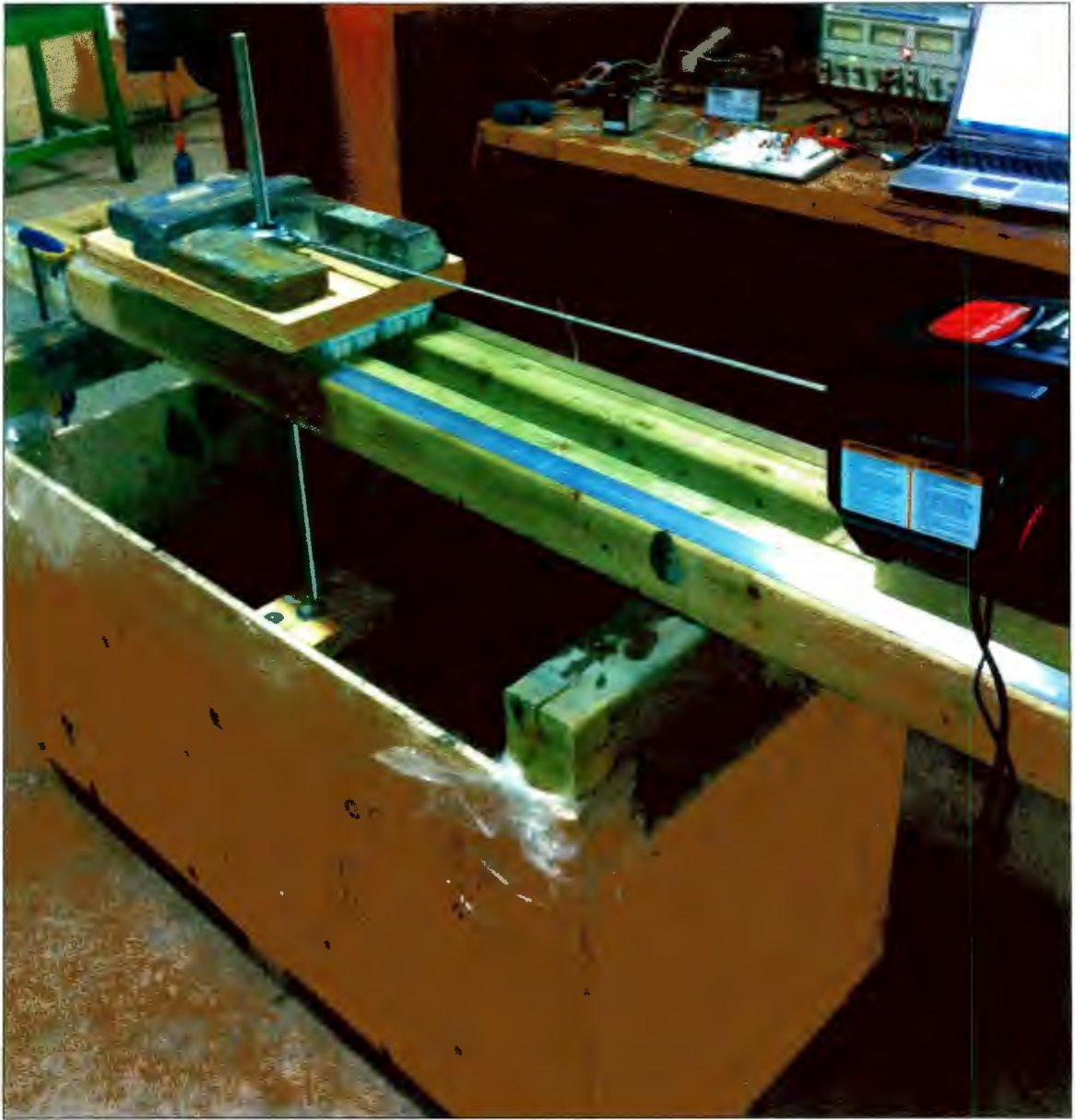


Figure 80: Movement Assembly Attached to Scour Tank

5.2.4 The Model Pipeline Load Cell

A 16mm (outside diameter) PVC pipe was used for the load cell pipeline, this material was chosen to ensure that there was enough deflection in the pipe in order to measure the loads effectively. The pipeline was 60 cm in length, however approximately 9 cm on each end was inserted into a wooden post to emulate the effect of an applied tensile constraint. Figure 81, below shows the pipeline load cell's position in the gouge tank (blue circular weights were used for calibration). The gauges were centered on the pipe; the keel models also gouged over the center of the pipe.



Figure 81: Pipeline Load Cell

The pipeline had two 120 Ohm strain gauges attached at the center of the pipeline, one for measuring deflection in the y-axis, and one for measuring deflection in the x-axis.

Ideally four gauges should have been used to enhance the signal and correct for temperature affects however, due to the desire to limit the invasiveness of additional wires only two gauges were used.

The 120 Ohm load cells had to be incorporated into two separate Wheatstone bridges; this type of configuration is known as a quarter-bridge setup. This allows for strain on the pipeline to be converted to a voltage output. The output of the signals was originally in millivolts and required amplification to volts in order to be read by a data acquisition system. The amplifiers used in the experimental setup were commercially available Omega amplifiers. The Omega amplifiers also provided the Wheatstone bridge with an excitation voltage.

The pipeline load cell was calibrated by placing weights in the center of the pipeline and measuring the corresponding voltage change (as seen in Figure 81). Due to the Poisson effect, and possible inaccuracies in gauge placement, there was a small amount of load that would be observed in the perpendicular axis. No attempt was made to correct the load for this effect. It must be stressed that the load cell was meant to provide a means of simple comparison, extremely accurate measurement of load was not the primary intent.

The first attempt at covering the pipeline in soil resulted in damage to the strain gauges. A second attempt was made after covering the strain gages and wires with a silicon coating.

5.2.5 Data Acquisition System

A data acquisition system was made by using a PIC (peripheral interface controller) chip, and a R232 communication chip. Additional components such as: resistors, capacitors, and a piezo crystal, were required as per manufacturer's recommendation. The components were installed on a "breadboard". A bench top power supply was required to power the data acquisition system. The maximum voltage that could be used by the PIC chip was 5 V; a voltage regulator was used to ensure that the maximum power was not exceeded. Figure 82, shows the setup of the data acquisition system.

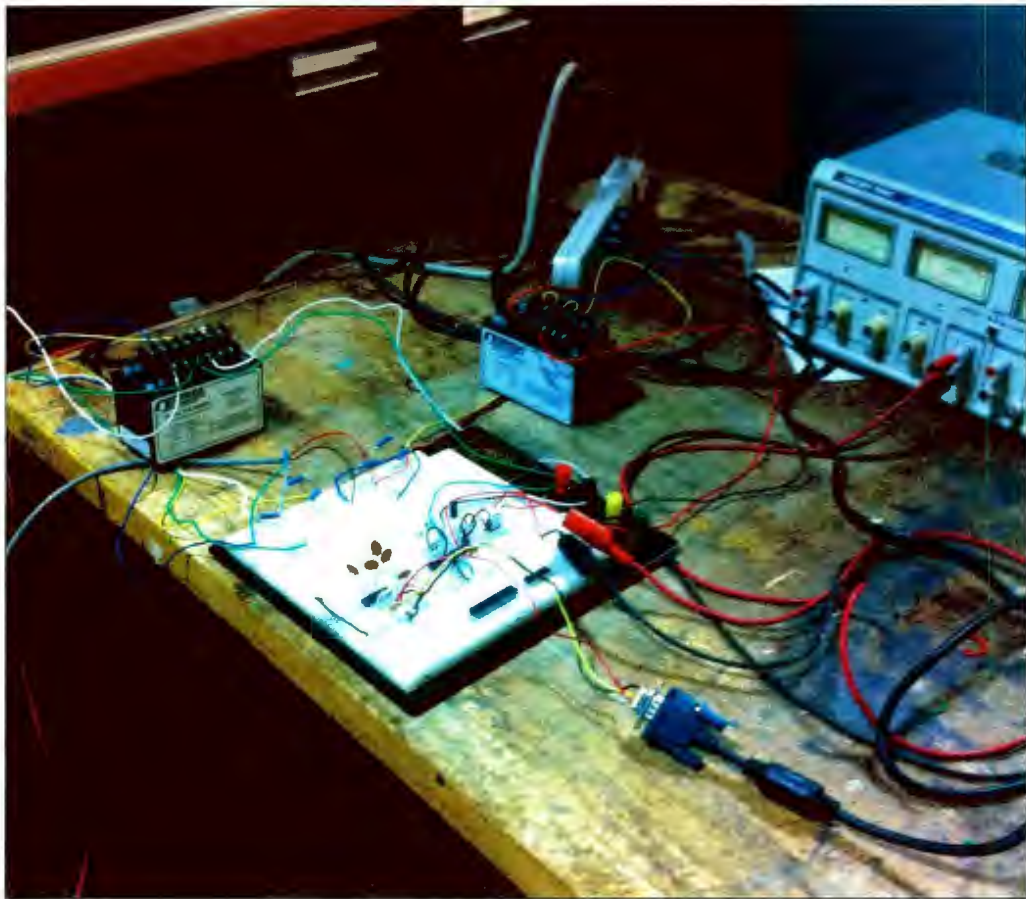


Figure 82: Data Acquisition System

The voltage from the two quarter bridge strain gauge setups were input into the PIC chip. A C++ program was written and downloaded onto the PIC chip using a boot loader. The C++ program commanded the PIC to output the voltages to a R232 communication chip, which in turn sent the voltages in binary code to the hyper terminal on a laptop, via a serial communication cable. The maximum resolution that could be read on the HyperTerminal was 8 bits, so the system resolution was 5v divided by 2^8 bits. This meant that the quantization error was 0.01953125 v/bit divided by two. This resulted in an error of approximately +/- 0.4 N for the lateral load and +/- 0.3 N for the vertical error.

5.2.6 Experiment Methodology

A pipeline load cell was fabricated with two strain gauges, one to measure the strain in the horizontal direction, and one to measure the strain in the vertical direction. The pipeline was 60cm long and was held in place by two wooden posts (each 9cm wide), bolted to the side of the gouge tank. The post would allow axial movement, but restricted lateral movement at the post; this mimicked the ability of the pipe to bend locally while still being subjected to a corrective tensile force.

The strain gauges on the pipeline were calibrated: prior to the commencement of the testing program, after the first series of tests (using the 30 degree wedge keel model), and again at the conclusion of the tests; there was no significant change in the calibration throughout. Soil samples obtained by BP from the Beaufort Sea were emptied into the gouge tank. The soil was compacted by hand into the gouge tank to form a test bed approximately 20 cm deep. Using a handheld lab vane the undrained shear strength of the soil was determined prior to the start of the test, and at the end of the test. In each case the undrained strength ranged from 3 kPa to 5 kPa.

After each test a trowel was used to smooth the test bed. The wooden post holding the model pipeline was used as a guide to ensure the testbed was at the same elevation for each experiment. The gouge depth for the experiments was set by adjusting the nuts on the threaded rod holding the model keel. Depth measurements of the remaining soil on top of the pipeline were made after each experiment to confirm the gouge depth. Four

gouge depths were evaluated: 1.9 m, 1.5 m, 1.0 m, and 0.5 m. A minimum of two tests were conducted at each level, for each model, to observe result variability.

The results from each test were processed in Microsoft Excel. The loads are expressed in model terms, as the exact scaling relationship for the applied loads are undefined. The parametric study focused on if there was a significant difference from using the two model keels to warrant further study. The gouge depth is referred to in scale terms due to the simple scaling relationship of length.

5.3 Experimental Results

The results of the experiments can be seen in Table 6, and Table 7, below. The results evaluate the maximum lateral, vertical, and maximum resultant load on the pipeline load cell.

Table 6: 30 Degree Idealized Wedge Experimental Results

TEST	Gouge Depth (m) (Scale)	Maximum Lateral Load (N)	Maximum Vertical Load (N)	Maximum Resultant Load (N)
3	0.5	10.2	7.23	11.8
4	0.5	11.1	7.23	12.6
1	1	11.9	7.9	12.6
2	1	12.8	9.2	15.1
5	1.5	26.4	22.3	32.2
6	1.5	26.4	23.0	31.6
7	1.9	31.5	28.9	38.0
8	1.9	29.8	29.5	35.1

Table 7: 3D Representative Model Keel Experiment Results

TEST	Gouge Depth (m) (Scale)	Maximum Lateral Load (N)	Maximum Vertical Load (N)	Maximum Resultant Load (N)
7	0.5	9.4	8.6	10.4
8	0.5	9.4	7.2	10.8
9	0.5	11.9	10.5	13.0
10	0.5	8.5	7.2	9.0
5	1	13.6	9.2	15.1
6	1	13.6	9.9	14.2
11	1.5	16.2	15.8	20.6
12	1.5	17.9	15.8	21.3
3	1.5	12.8	10.5	15.0
4	1.5	12.8	11.8	15.0
1	1.9	19.6	17.8	21.9
2	1.9	18.7	15.8	20.4
13	1.9	20.4	19.1	25.8
14	1.9	19.6	18.4	25.2

A plot of the resultant loads can be seen in Figure 83; the gouge depth is dimensionless and expressed as a ratio of gouge depth to pipeline cover (2m). In comparison, as gouge depths increase (ratio approaching 1:1) the 3D representative keel transmits less of a load onto the pipeline than the prismatic wedge. At a gouge depth of 1.9m the average resultant force on the pipeline from the 30 degree wedge is 36.6N, while the average for the theoretical keel is 23.3 N, a difference of 36%. As the gouge depth to gouge cover ratio decreases (gouges become shallower) it can be observed that the resultant loads become approximately equal.

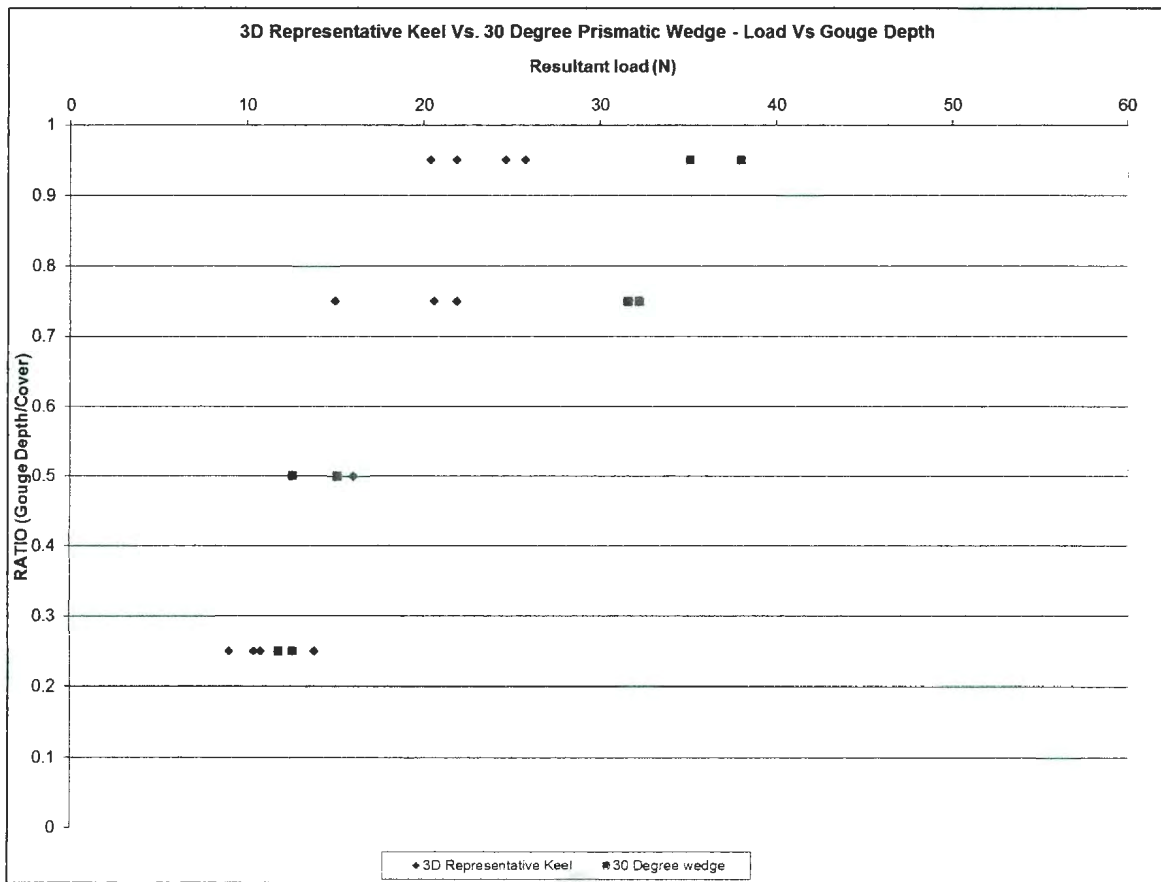


Figure 83: Representative Keel Vs. 30 Degree Prismatic Wedge - Resultant Loads

Another aspect of the keel morphology that is of interest is the soil pressure that is transferred by each model shape into the soil. The projected pressure from each test can be seen in Table 8 and Table 9. A comparison of the pressures between the 30 degree prismatic wedge, and the 3D representative keel can be seen in Table 10.

Table 8: 30 Degree Wedge - Projected Pressure

Test	Gouge Depth (m) (scale)	Vertical Projected Area (m ²)	Lateral Projected Area (m ²)	Maximum Vertical Force (N)	Maximum Lateral Force (N)	Vertical Projected Pressure (N/m ²)	Lateral Projected Pressure (N/m ²)
3	0.5	0.01481	0.001	7.23	10.2	488	10200
4	0.5	0.01481	0.001	7.23	11.1	488	11100
1	1	0.01654	0.002	7.9	11.9	478	5950
2	1	0.01654	0.002	9.2	12.8	556	6400
5	1.5	0.01828	0.003	22.3	26.4	1220	8800
6	1.5	0.01828	0.003	23.0	26.4	1258	8800
7	1.9	0.01986	0.0038	28.9	31.5	1455	8289
8	1.9	0.01986	0.0038	29.5	29.8	1485	7842

Table 9: 3D Representative Keel - Projected Pressure

Test	Gouge Depth (m) (scale)	Vertical Projected Area (m ²)	Lateral Projected Area (m ²)	Maximum Vertical Force (N)	Maximum Lateral Force (N)	Vertical Projected Pressure (N/m ²)	Lateral Projected Pressure (N/m ²)
7	0.5	0.00141	0.00018	8.6	9.4	6086	52222
8	0.5	0.00141	0.00018	7.2	9.4	5096	52222
9	0.5	0.00141	0.00018	10.5	11.9	7431	66111
10	0.5	0.00141	0.00018	7.2	8.5	5096	47222
5	1	0.00393	0.0006	9.2	13.6	2344	22667
6	1	0.00393	0.0006	9.9	13.6	2522	22667
11	1.5	0.01005	0.00128	15.8	16.2	1572	12656
12	1.5	0.01005	0.00128	15.8	17.9	1572	13984
3	1.5	0.01005	0.00128	10.5	12.8	1045	10000
4	1.5	0.01005	0.00128	11.8	12.8	1174	10000
1	1.9	0.0157	0.002	17.8	19.6	1134	9800
2	1.9	0.0157	0.002	15.8	18.7	1006	9350
13	1.9	0.0157	0.002	19.1	20.4	1217	10200
14	1.9	0.0157	0.002	18.4	19.6	1172	9800

Table 10: Projected Pressure Comparison

Gouge Depth (m) (<i>scale</i>)	30 Degree Wedge – Avg. Vertical Projected Pressure (N/m ²)	30 Degree Wedge – Avg. Lateral Projected Pressure (N/m ²)	3D Rep. Keel – Avg. Vertical Projected Pressure (N/m ²)	3D Rep. Keel – Avg. Lateral Projected Pressure (N/m ²)
0.5	488	10650	5927	54444
1	517	6175	2433	22667
1.5	1239	8800	1341	11660
1.9	1470	8066	1132	9788

It can be seen from the above tables that the projected pressure on the 3D representative keel is higher than that of the traditional prismatic wedge for shallower gouges. However, at a gouge depth of 1.9m, the projected vertical pressure is higher for the prismatic wedge model, while the lateral projected pressure is still higher for the representative keel. The variation in pressure based on depth is possibly due to a function of: shape, bearing area, and proximity to the model pipe. Further study of the sub-gouge deformation of soils of the 3D representative keel model is required to further explain this phenomenon.

It must be noted that the projected pressure of the 3D representative keel, for shallow gouging, is uncharacteristically high. This is likely due to influence caused by the build-up of the frontal mound material.

One characteristic that was noticed was that the maximum vertical and lateral loads increased rapidly, but peaked at different times during the experiments; this occurred in every experiment, regardless of the keel model type. An example of this can be seen in Figure 82. The results for all experiments conducted can be found in Appendix A. This is believed to be due to the pipe flexing in the lateral direction from horizontal forces transferred through the soil, ahead of the keel.

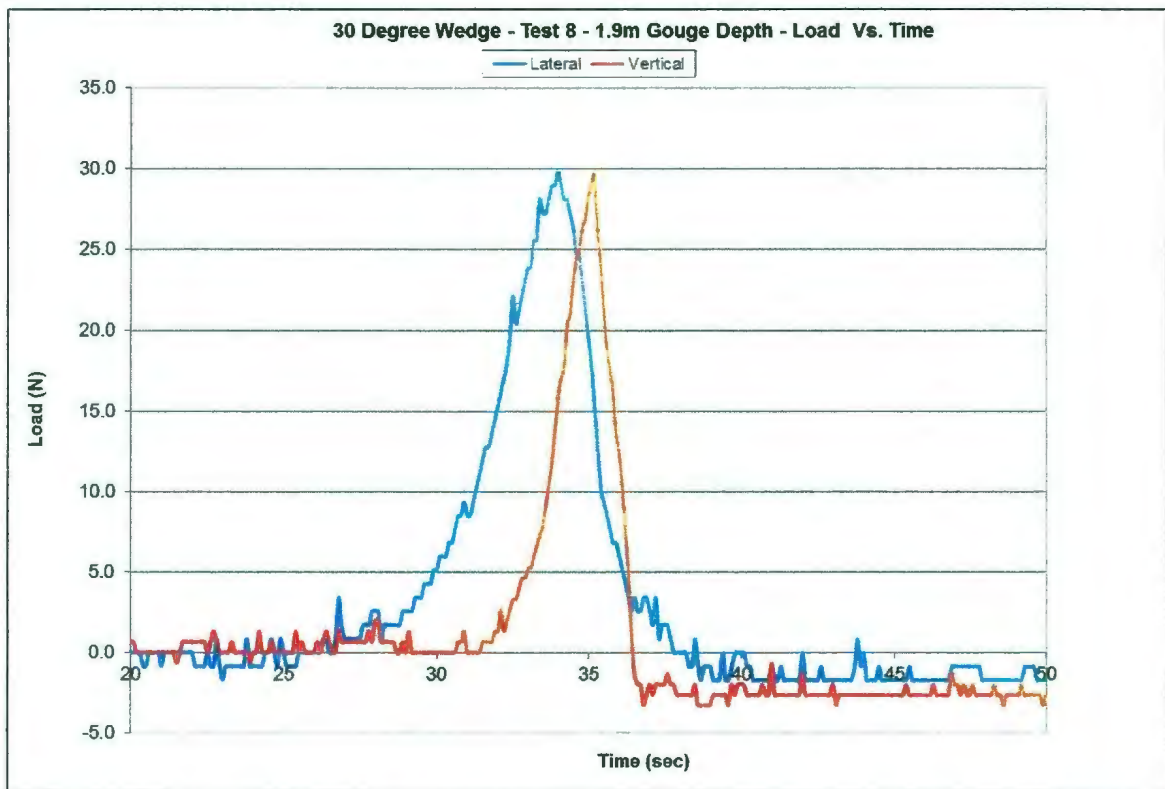


Figure 84: Difference is peak load times for lateral and vertical load on the 30° wedge keel model

From interpretation of the experiment in Figure 84, the pipeline begins to first experience purely lateral movement followed by downward vertical movement 1-2 seconds later (after 3 m to 6 m of keel movement). As the keel passes over the pipeline, the pipeline

continues to be pushed vertically while laterally the pipe begins to rebound. As the keel moves past the pipeline the vertical force component drops at a faster rate than the lateral force.

5.4 Discussion of Results

From the simple experiment program conducted, it can be observed that there is a significant difference in loads on a model pipeline from a 3D representative model compared to a traditional idealized prismatic model. The difference, however, was only observed in very deep gouges, in which the ratio of gouge depth to pipeline cover was 0.75 or greater. Ratios of 0.5, or lower, showed no difference in the resultant loads between the representative 3D keel model and an idealized traditional keel model.

In each experiment the lateral forces in were higher than the vertical forces, however as the gouge depth increased the difference between lateral and vertical forces decreased. One explanation for this result is that there are two separate mechanisms at work, a lateral component possibly due to soil movement ahead of the keel, and a vertical component from downward soil movement beneath the base of the keel.

6.0 SUMMARY, CONCLUSIONS, AND RECOMMENDATIONS

6.1 Summary

The purpose of this thesis was to study gouge morphology in order to develop a representative physical ice keel model. A review of the factors involved in gouging was conducted to provide guidance to the gouge morphology study and place the scour problem into context. An in-depth study of five extreme gouges that displayed marked direction changes was conducted in order to assess pressure ridge ice keel morphology. After conducting the gouge study, a common morphology was recognized and equated to a common leading edge keel geometry. The recognition of a common leading edge keel geometry was further confirmed after a review of the extreme gouge catalogue compiled by the GSC and CSR. In order to assess the significance of common keel geometry, a 1g scale model experiment was designed and built in order to compare the results of a representative ice keel model, to a traditionally used prismatic wedge model.

6.2 Conclusions

6.2.1 *Conclusions on Keel Morphology and Experimental Results*

After studying five sets of extreme gouge bathymetric data, a common morphological shape was found, for individual pressure ridge keels and individual keel fingers of keels. The shape of the keel/keel finger, was observed to have a slight curvature about the toe of the keel, but the slope of the keel/keel finger appeared to be relatively linear. A 3D common ratio of 10:5:1 for keel width: keel thickness: gouge depth was also observed in the five sets of extreme gouge bathymetric data. Further study into an extreme gouge database, compiled by the GSC and CSR, further supported the observation of a common 3D proportion theory. These conclusions are based on multi-beam bathymetric data, with 1m resolution.

When comparing the 3D representative keel to that of the traditionally used prismatic wedge keel, in a simple scale model experiment, it was found that the results varied significantly. Comparative plots showed that, when gouging over a model pipeline, as the ratio of gouge depth to gouge cover increased, the traditional wedge shape model resulted in up to 36% higher resultant loads. For gouge depth to cover depth ratios less than 0.5, the resultant loads were approximately the same. When considering the difference in projected pressures from the 3D representative keel and the traditional prismatic wedge keel, it can be found that the projected pressures are generally higher for the 3D representative keel, however as the gouge depth to gouge cover ratio increases, the projected pressures become almost equal.

6.2.2 Conclusions on Factors Affecting Gouge Morphology

It was initially proposed that there is a general uncertainty of comparing the morphology of a pressure keel that has not been involved in the gouging process to one that has. The work of Timco and Burden (1997) had found a common keel width to height of keel ratio of 3.9:1. The ratio proposed by the common proportion theory in this thesis proposes that the smallest ratio was approximately 5:1, however this ratio is fairly sensitive to variations in gouge depth. It has been observed, in a number of gouges, that there have been significant morphological changes that have occurred during the gouging process. Based on the limitations of vertical resolution of the multi-beam system, it cannot be proven from the observed data that the keel does, or does not, undergo some immediate restructuring during the gouging process.

The theory of the ice sheet of a pressure ridge keel system flexing, and allowing elastic like vertical movement of the keel, has been strongly supported by observation of bathymetric data. Observations of keel fingers being sheared or destroyed, combined with observation of vertical flexure of the ice sheet also supports the argument that gouge depth is controlled by sediment strength. However, in the deepest gouge (Gouge 5) observed the behavior contradicted the previous four gouges, and gave the impression that the soil strength was significantly less than the vertical force of the ice keel.

It is known that wind is the primary driving force of ice. The theory that extreme wind events are responsible for creating extreme gouges is very much plausible. It is also

known that with extreme wind events, particularly in the winter season, storm surges and negative surges does occur. The characteristic behavior of tidal surges does appear to explain some of the movement in the termination mounds of some of the gouges observed. While it still remains a valid theory, there is no way to prove undoubtedly that tidal surges were responsible for strange vertical movements observed in the gouge study.

All keels observed in this study were multi-fingered keels and in some cases possibly multi-keels. An important observation regarding multi-fingered keels is that the order of the keel fingers does appear to greatly affect the characteristics of the gouge. It has been observed that when the larger keel is leading, smaller keels following behind does cause the larger keel to be partially in-filled. This is of great concern to statistical studies and gouge depth prediction, as the actual gouge depth of a keel may have been deeper than what the gouge morphology indicates.

The notion that the soil in gouges may have a common shape due to material slumping was explored by comparing the side slope angles to end berm angles. It was found that in the majority of cases there was a significant difference between the side slope angles to angles found in termination berms, and also by difference in side slopes based on the orientation of the keel, and differences between one side of the gouge to the other. By virtue of this fact, it can be ruled out that the shapes observed are due to material slumping, as all angles in the gouge would have to be approximately equal for the slumping theory to be correct.

6.3 Recommendations

6.3.1 Recommendations Regarding Keel Morphology and Experimentation

It must be stressed that the experiment conducted as part of this thesis was a very simple and crude parametric study. The results of the experiment does provide the justification for a more robust experimental program to be conducted in order to better study the effect of using a representative keel model in scale model programs. A more robust program should consist of centrifuge scale model test and, where possible, validation using full scale test.

The identification of a common 3D shape adds a new level of complexity to the ice gouge problem. It is recommended that a scale model program using the representative keel shape would have to study the effects of not only gouging in the primary axis, but also oblique movements, to better understand the full capabilities of the keel.

In every gouge it was noticed that the keel was multi-fingered. It is recommended that further development of a multi-keeled representative model should be explored to ascertain the effects.

6.3.2 Recommendations Regarding the Study of Gouge Factors

The ability to distinguish the vertical flexure of an ice sheet, and the discrete destruction of keel fingers, is proof that sediment strength can be a limiting factor on gouge depth. These phenomenon were observed by studying individual gouges through to their termination. The process of studying gouges in this manner has been long and laborious, but provided much more insight into the behavior and capabilities of ice gouging. It is recommended that morphological studies, similar to the one conducted in this thesis, be undertaken as part of research into any heavily gouged region. A geotechnical investigation conducted in tandem with an intense survey of one extreme gouge can provide a wealth of information for advancing the field of ice gouge engineering.

Two factors of particular importance that could not be addressed in this study were: the possibility of storm surges with extreme wind events causing extreme gouges, and the possibility of ice zonation affecting ice gouging. Future study through field observation or satellite monitoring, in tandem with weather observation, could provide great insight into the ice gouge phenomenon. This type of study is highly recommended as part of any serious program to address development in the Beaufort Sea region.

7.0 BIBLIOGRAPHY

- B. Wright & Associates Ltd. (2005). Ice-Related R&D Requirements for Beaufort Sea Production Systems PERD/CHC Report 35-60.
- Barrette, P. (2011). Offshore Pipeline Protection Against Seabed Gouging By Ice: An Overview. *Cold Reg. Sci. Technol.*,69, pp. 3-20.
- Been, K., Kosar, K., Hachey, J., Rogers, B.T., and Palmer, A.C. (1990). Ice Gouge Models, proceedings, 9th International Conference, Offshore Mechanics and Arctic Engineering, OMAE, Volume V, Houston, TX, USA, pp. 179-188.
- Blasco, S., Benette, R., and Mackillop, K. (2007). Seabed Ice Scour Research In the Beaufort Sea. Presentation to PERD/CCTII Workshop on Engineering Issues for Offshore Beaufort Sea Development, Calgary, Alberta, November 2007.
ftp://ftp2.chc.nrc.ca/CRTreports/PERD_CCTII_workshop_07_session_2.pdf.
- Bowen, R.G., and Topham, D.R. (1994). A study of the morphology of a discontinuous section of a first year arctic pressure ridge. *Cold Regions Science and Technology* 24 (1996) pp. 83-100.
- Chari, T.R. (1975). Some geotechnical aspects of iceberg grounding. PhD thesis to the Faculty of Engineering and Applied Science, Memorial University of Newfoundland.
- C-CORE. (1996). PRISE Phase 3c: Extreme Ice Gouge Event – Modeling and Interpretation C-CORE Report 96-C32.
- C-CORE. (1999). Preliminary Report Pipeline Assessment for Ice Damage To Subsea Pipelines. Submitted to Minerals Management Service, U.S department of the Interior.
- C-CORE. (2000). Risk Assessment of Ice Damage to Buried Marine Pipelines. Draft Final Report. Publication 00-C31.
- EBA Engineering Consultants Ltd. (1992). Correlation of Ice Gouge Depth with Seabed Sediment Properties Canadian Beaufort Sea. 0306-34825.
- Fisheries and Oceans Canada. (1999). Canadian Coast Guard: Ice Navigation in Canadian Waters. Cat. No. T31-73/199E ISBN 0-660-17873-7. Copyright: Department of Public Works and Government Services Canada.

- Government of Canada. (2009). Foundation for a Sustainable Northern Future Report of the Joint Review Panel for the Mackenzie Gas Project Volume I Chapters 1 to 10. December, 2009.
- Green, H. P. (1984). Geotechnical Modelling of Iceberg-Seabed Interaction. Master's Thesis to the Faculty of Engineering and Applied Science, Memorial University of Newfoundland.
- Henry, R. F. (1975). Storm Surges. The Beaufort Sea Project, Technical Report #19.
- Hachey, J., and Been, K. (1990). Geotechnical Summary for North Point Amauligak Pipeline Corridor Volume 1.
- Hequette, A., Desrosiers, M., and Barnes, P. (1995). Sea ice gouging on the inner shelf of the southeastern Canadian Beaufort Sea. *International Journal of Marine Geology, Geochemistry, and Geophysics*. 128, pp. 201-219
- Huggett, W.S., Woodward, M.J., Stephenson, F., Hermiston, F.V., and Douglas A. (1975). Near Bottom Currents and Offshore Tides. The Beaufort Sea Project, Technical Report #16.
- Ivanovic, A., Neilson, R.D., Giuliani G., and Bransby, B.F. (2011). Influence of object geometry on penetration into the seabed. *Frontiers in Offshore Geotechnics II – Gourvenec & White (eds) © 2011 Taylor & Francis Group, London, ISBN 978-0-415-58480-7*.
- Kovacs, A., Weeks, W.F., Ackley, S.F., and Hibler III, W.D. (1973). Structure of a multiyear pressure ridge. *Arctic Jnl. Arctic Institute of N. America*. 26 1 (1973), pp. 23–31.
- King, A.(2002). Iceberg Scour Risk Analysis for Pipelines On The Labrador Shelf. Master's Thesis to the Faculty of Engineering and Applied Science, Memorial University of Newfoundland.
- National Energy Board (Canada). (2011). News Release: “National Energy Board issues Certificate of Public Convenience and Necessity for Mackenzie Valley Pipeline”. <http://www.neb-one.gc.ca/clf-nsi/rthnb/nwsrls/2011/nwsrls07-eng.html>.
- Obert, K.M., and Brown, T.G. (2011). Ice ridge keel characteristics and distribution in the Northumberland Strait. *Cold Regions Science and Technology* 66, pp. 53–64.
- O'Connor, M.J., and Blasco, S.M. (1980). Development of a Proposed Model to Account for Surficial Geology of the Southern Beaufort Sea.

- Oickle, E., Campbell, P., and Blasco S. (2006). The Beaufort Sea Extreme Ice Scour Catalogue (Volume II).
- Orlando, L., Kendell, K., Cambell, P., and Blasco S. (2003). The Beaufort Sea Extreme Ice Scour Catalogue.
- Palmer, A. (2011). *Journal of Pipeline Engineering* Vol. 10, No. 2, second quarter, 2011.
- Palmer, A. (1997). Geotechnical evidence of ice gouge as a guide to pipeline burial depth. *Canadian Geotechnical Journal*, 34, pp. 1002-1003.
- Paulin, M. (1992). Physical Model Analysis of Iceberg Scour in Dry and Submerged Sand. Master's Thesis to the Faculty of Engineering and Applied Science, Memorial University of Newfoundland.
- Prasad, K.S.R. (1985). Analytical and Experimental Modelling of Iceberg Gouges. Master's Thesis to the Faculty of Engineering and Applied Science, Memorial University of Newfoundland.
- Reimnitz, E., Toimil, L., and Barnes, P. (1978). Arctic Continental Shelf Morphology Related to Sea-Ice Zonation, Beaufort Sea, Alaska. *International Journal of Marine Geology, Geochemistry, and Geophysics*, 28, pp. 179-210
- Reimnitz, E., and Maurer, D.K. (1979). Effects of Storm Surges on the Beaufort Sea Coast, Northern Alaska. *Arctic Journal* Vol 32, No. 4, pp. 329-344.
- Thorndike, A.S., and Colony, R.L. (1982). Sea ice motion in response to geostrophic Winds. *J. Geophys. Res.* 89, 5845–5852.
- Timco, G.W., and Burden, R.P. (1997). An analysis of the shapes of sea ice ridges, *Cold Regions Science and Technology*, Volume 25, Issue 1, January 1997, Pages 65-77, ISSN 0165-232X, 10.1016/S0165-232X(96)00017-1.
- Timco, G.W., and Frederking, R. (2009). Overview of Historical Canadian Beaufort Sea Information. Technical Report CHC-TR-057.
- Wikipedia, The Free Encyclopedia. Wikimedia Foundation, Inc. July 22, 2004. Web. January 5, 2004. < http://en.wikipedia.org/wiki/Mackenzie_Valley_Pipeline>.
- Woodworth-Lynas, C.M.T., Phillips, R., Clark, J.I., Paulin, M., Hynes, F., and Xiao, X. (1995). Verification of centrifuge model results against field data: Results of Pressure Ridge Ice Gouge Experiment (PRISE). Second International Conference on Development of the Russian Arctic Offshore, St Petersburg, Russia, September 1995.

Younan, A.H., Hamilton, J.M., Weaver, J., (2007). Ice Gouge Reliability of Offshore Arctic Pipelines. The American Society of Mechanical Engineers (ASME), San Diego, pp.1 -7.

APPENDIX A – EXPERIMENTAL RESULTS

